Neutron Star Mergers

EMMI PHYSICS DAY, 28. NOVEMBER 2017
AM HELMHOLTZZENTRUM FÜR SCHWERIONENFORSCHUNG
GSI, DARMSTADT

MATTHIAS HANAUSKE, KENTARO TAKAMI, LUKE BOVARD, JOSE FONT, FILIPPO GALEAZZI, JENS PAPENFORT, LUKAS WEIH, ELIAS MOST, COSIMA BREU, FEDERICO GUERCILENA, NATASCHA WECHSELBERGER, ZEKIYE SIMAY YILMAZ, CHRISTINA MITROPOULOS, JAN STEINHEIMER, STEFAN SCHRAMM, DAVID BLASCHKE, MARK ALFORD, KAI SCHWENZER, ANTONIOS NATHANAIL, ROMAN GOLD, ALEJANDRO CRUZ OSORIO, ANDREAS ZACCHI, JÜRGEN SCHAFFNER-BIELICH, LAURA TOLOS, SVEN KÖPPEL, GLORIA MONTAÑA, MICHAEL RATTAY, HORST STÖCKER AND LUCIANO REZZOLLA

FRANKFURT INSTITUTE FOR ADVANCED STUDIES
JOHANN WOLFGANG GOETHE UNIVERSITÄT
INSTITUT FÜR THEORETISCHE PHYSIK
ARBEITSGRUPPE RELATIVISTISCHE ASTROPHYSIK
D-60438 FRANKFURT AM MAIN

Content

- Introduction:
  Neutron stars, neutron star merger product, Einstein equation, gravitational waves, gravitational wave detectors
- GW170817 - the long-awaited event
- Computersimulation of neutron star mergers in full general relativity
  (3+1)-Split of spacetime, the equation of state (EOS), the merger product –> creation of a hypermassive neutron star, temperature-density-rotation profiles, post-merger phase, constraining the EOS with gravitational wave data
- Detecting the hadron-quark phase transition with gravitational waves
- r-process nucleosynthesis in binary neutron star mergers

Properties of Neutron Stars

radius ~ 10 km, mass ~ 1-2 sun masses, large magnetic fields ~ 10^{11} Tesla, high rotation (up to 716 Hz)

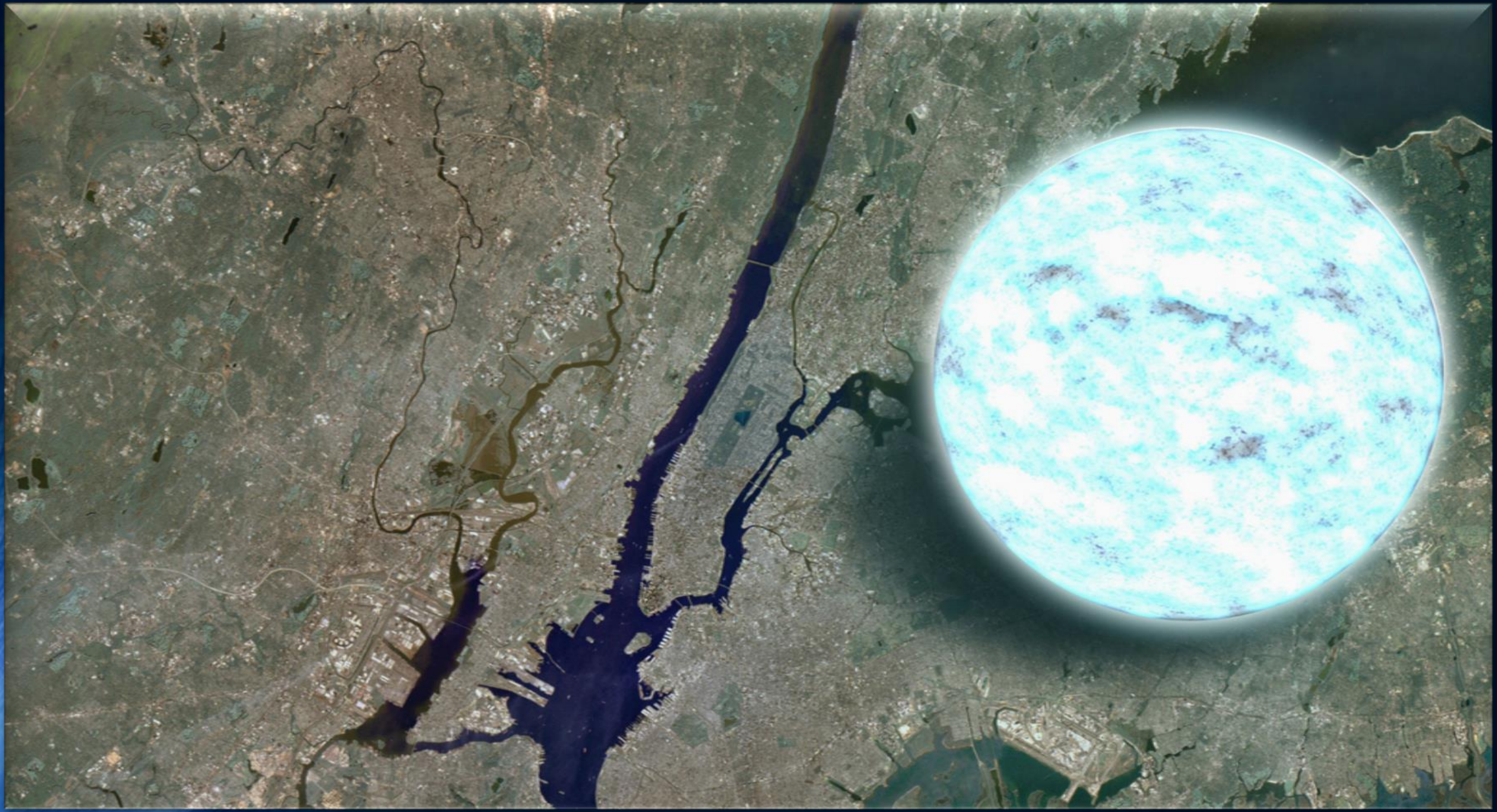

NASA/Goddard Space Flight Center

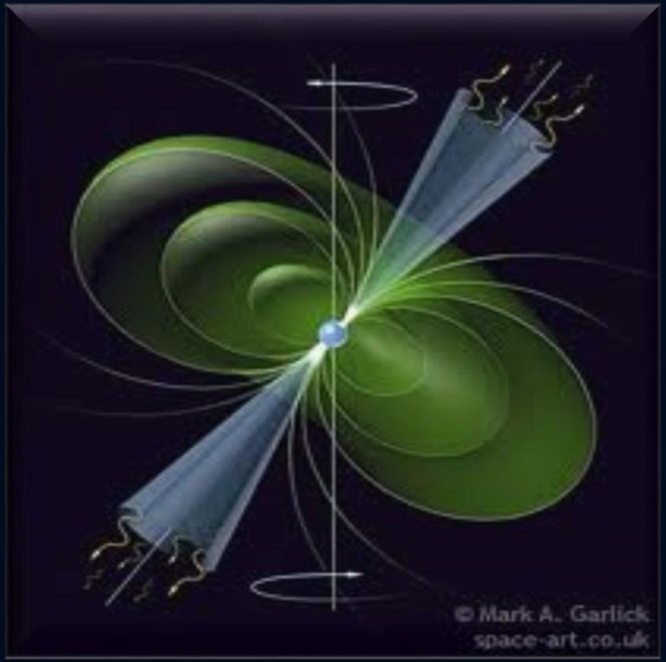

Pulsars are Rotating Neutron Stars

Currently we know about 2500 neutron stars

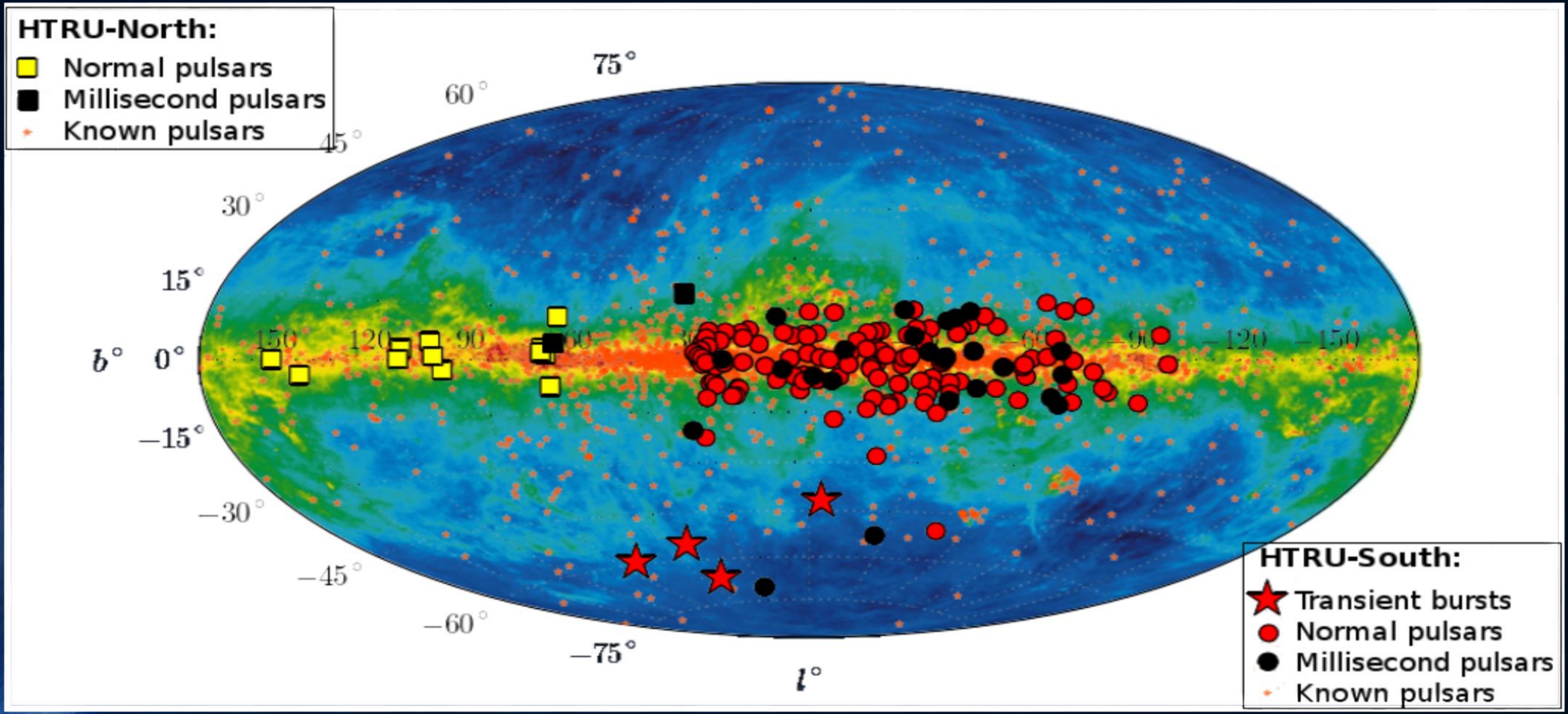

Binary Neutron Star Systems

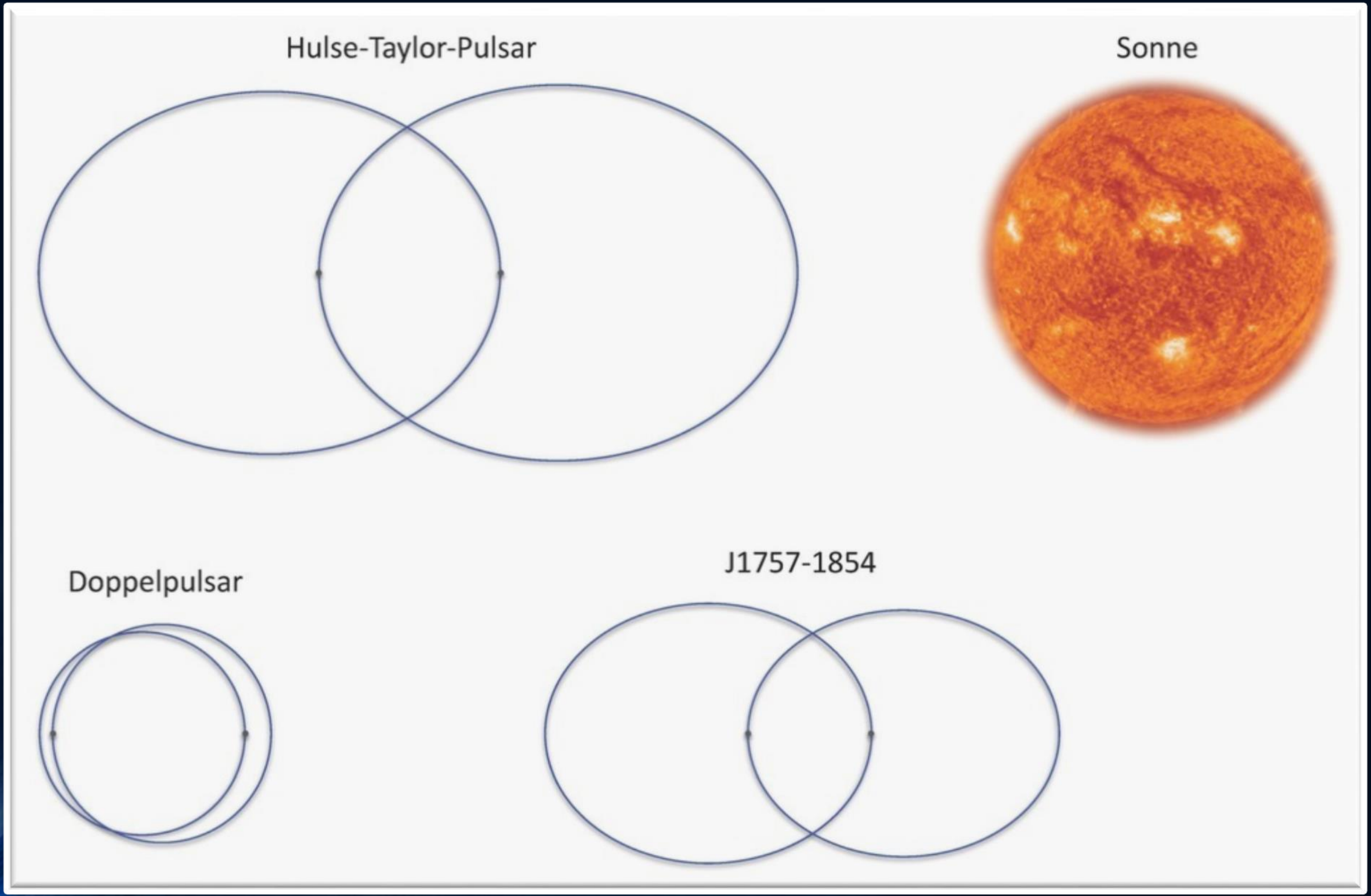

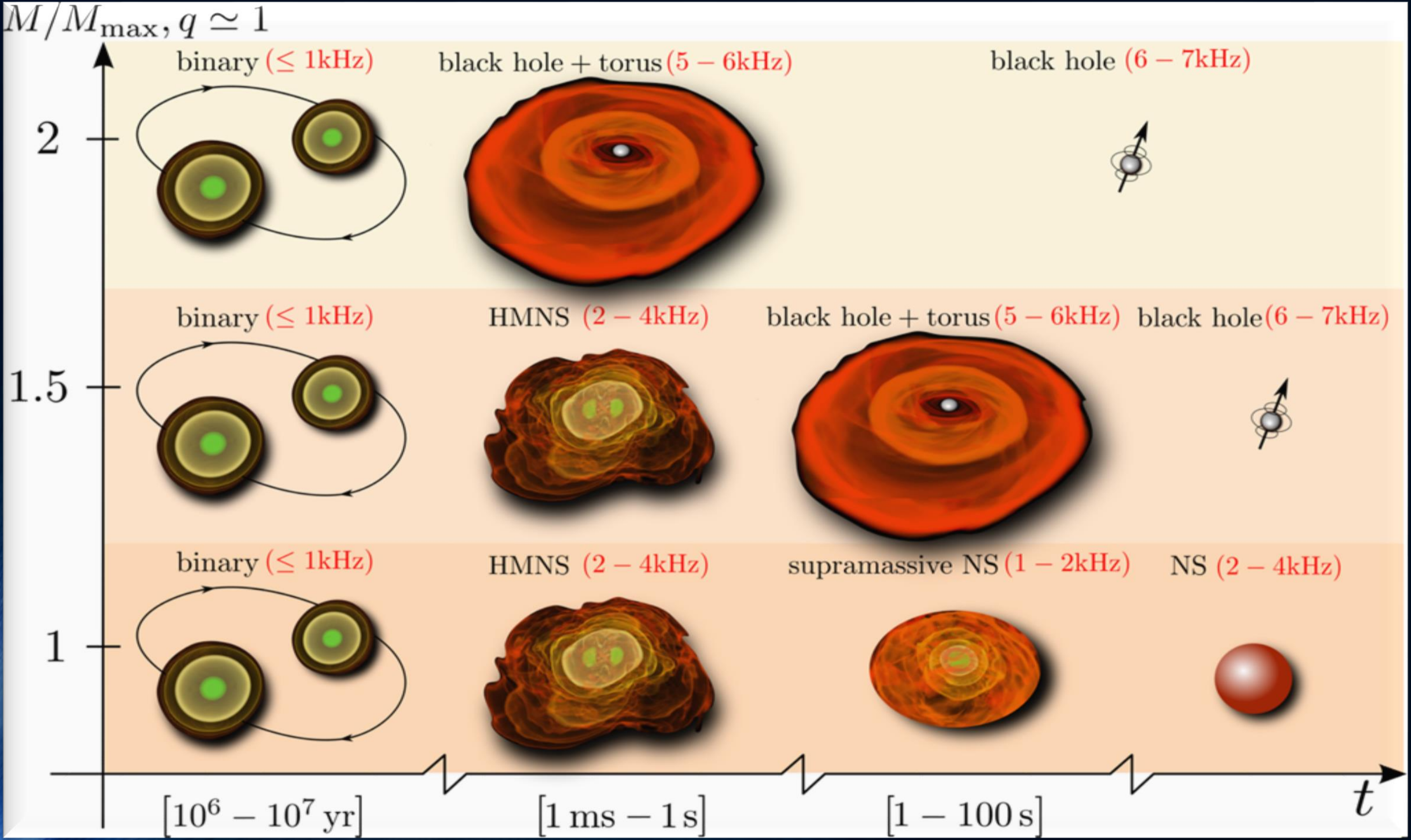
$M/M_{\rm max}, q \simeq 1$
binary ($\leq$ 1kHz)
black hole + torus (5 – 6kHz)
black hole (6 – 7kHz)
2
binary ($\leq$ 1kHz)
HMNS (2 – 4kHz)
black hole + torus (5 – 6kHz)
black hole (6 – 7kHz)
1.5
binary ($\leq$ 1kHz)
HMNS (2 – 4kHz)
supramassive NS (1 – 2kHz)
NS (2 – 4kHz)
1
$[10^6 - 10^7\,{\rm yr}]$
$[1\,{\rm ms} - 1\,{\rm s}]$
$[1 - 100\,{\rm s}]$
t

General Relativity

The Einstein Equation

100 years ago, Albert Einstein presented the main equation of general relativity: **The Einstein-Equation**

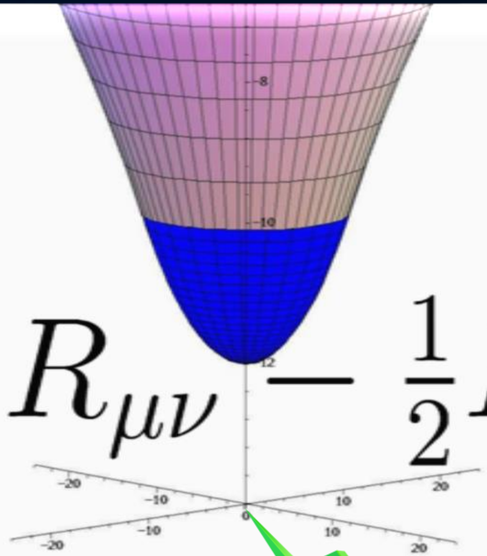

$$R_{\mu\nu} - \frac{1}{2} R\, g_{\mu\nu} = \frac{8\pi G}{c^4} T_{\mu\nu}$$

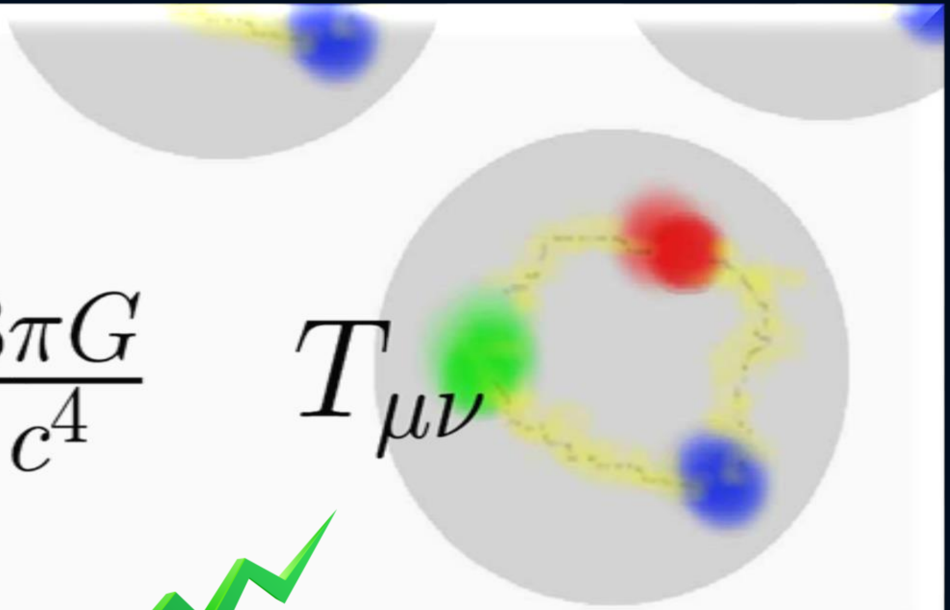

<u>Spacetime curvature</u>

Properties of the spacetime metric

<u>Mass, Energy and Momentum of the System</u>

Equation of state of elementary matter
(density, temperature)

Gravitational Waves (A.Einstein, 1916)

Gravitational Waves detected!!!

Collision of two Black Holes GW150914

Masses: 36 & 29 Sun masses

Distance to the earth 410 Mpc (1.34 Billion Light Years)

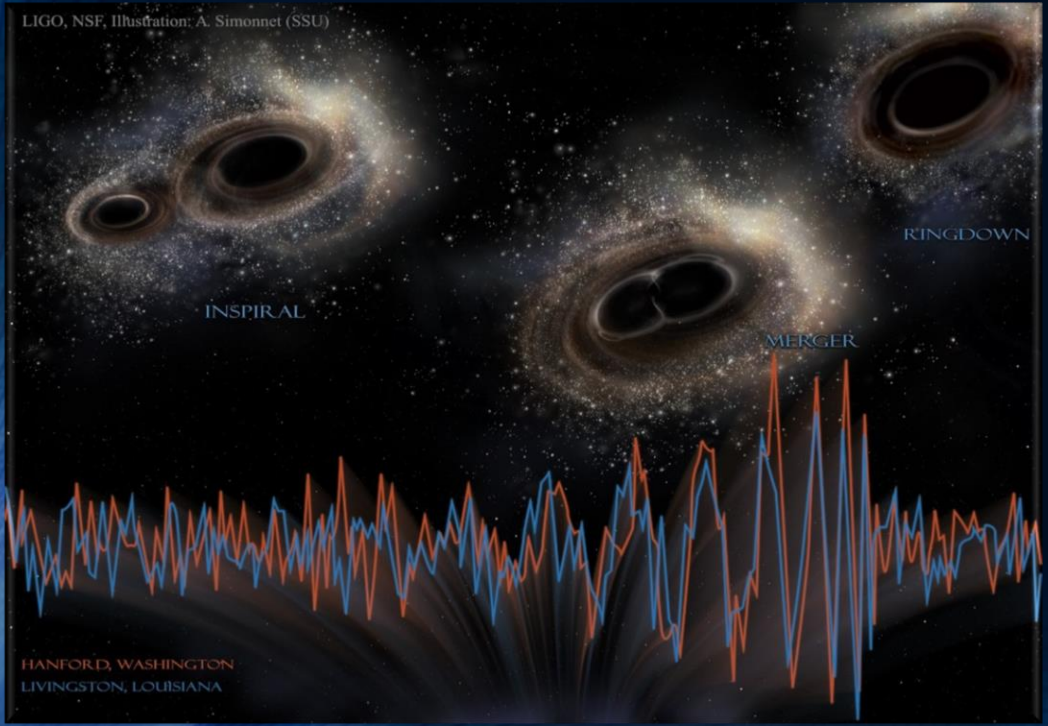

Längen – Differenz < 10^{-18} m

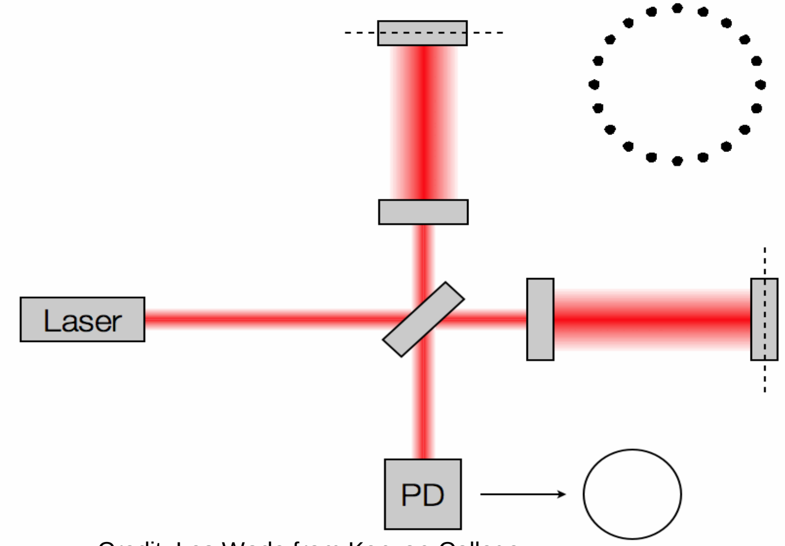

Credit: Les Wade from Kenyon College

Gravitational Waves from Neutron Star Mergers

Neutron Star Collision (Simulation)

Collision of two Black Holes

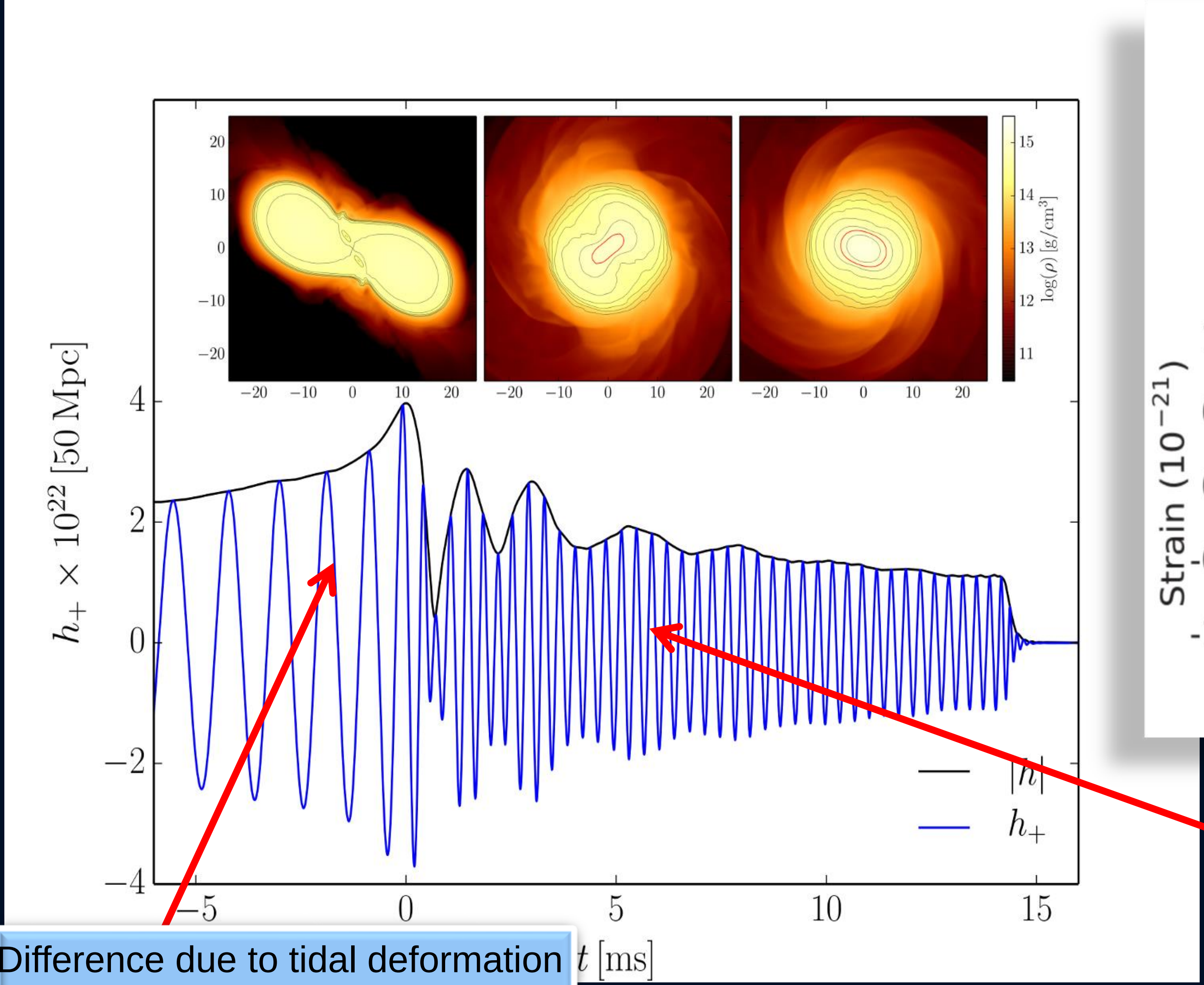

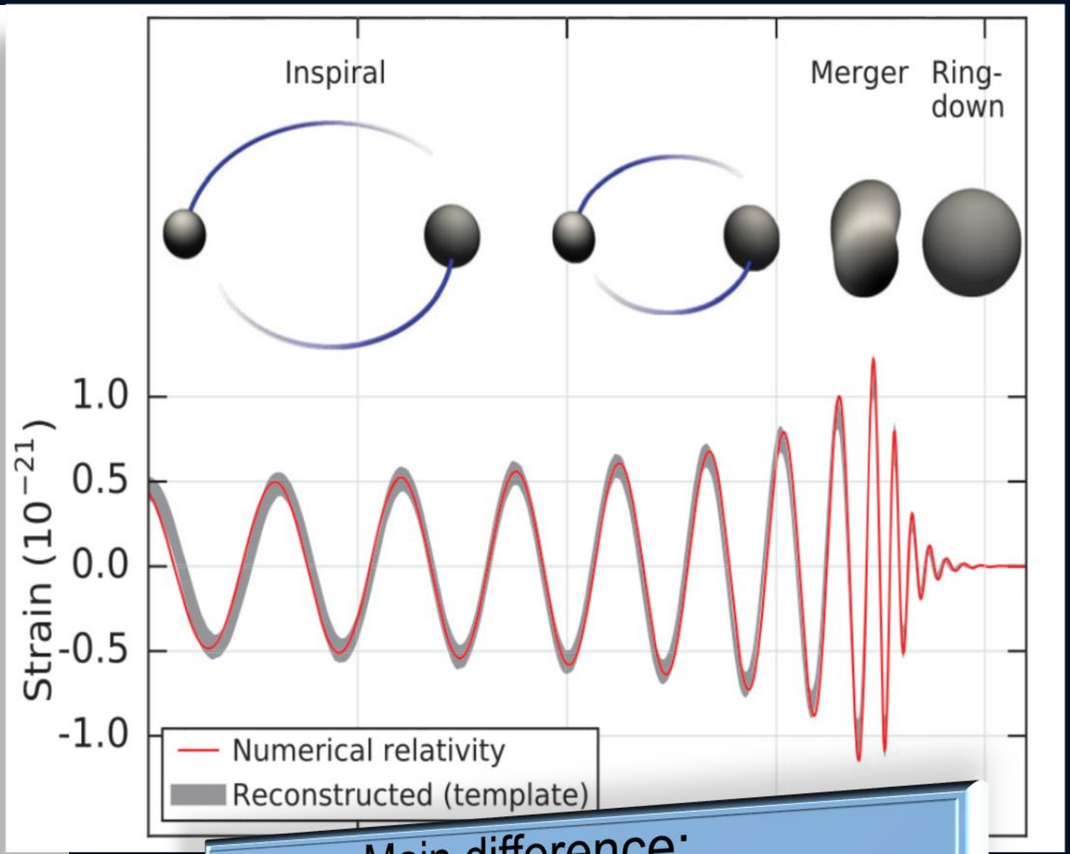

Difference due to tidal deformation in the late Inspiral phase

Main difference:
In binary neutron star mergers a **Post-Merger Phase** often exists

The long-awaited event GW170817

	Low-spin priors ($\|\chi\| \leq 0.05$)	High-spin priors ($\|\chi\| \leq 0.89$)
Primary mass m_1	1.36–1.60 $M_\odot$	1.36–2.26 $M_\odot$
Secondary mass m_2	1.17–1.36 $M_\odot$	0.86–1.36 $M_\odot$
Chirp mass $\mathcal{M}$	$1.188^{+0.004}_{-0.002} M_\odot$	$1.188^{+0.004}_{-0.002} M_\odot$
Mass ratio m_2/m_1	0.7–1.0	0.4–1.0
Total mass $m_{\rm tot}$	$2.74^{+0.04}_{-0.01} M_\odot$	$2.82^{+0.47}_{-0.09} M_\odot$
Radiated energy $E_{\rm rad}$	$> 0.025 M_\odot c^2$	$> 0.025 M_\odot c^2$
Luminosity distance $D_{\rm L}$	40^{+8}_{-14} Mpc	40^{+8}_{-14} Mpc
Viewing angle Θ	$\leq 55°$	$\leq 56°$
Using NGC 4993 location	$\leq 28°$	$\leq 28°$
Combined dimensionless tidal deformability $\tilde{\Lambda}$	≤ 800	≤ 700
Dimensionless tidal deformability $\Lambda(1.4 M_\odot)$	≤ 800	≤ 1400

Gravitational Wave GW170817 and Gamma-Ray Emission GRB170817A

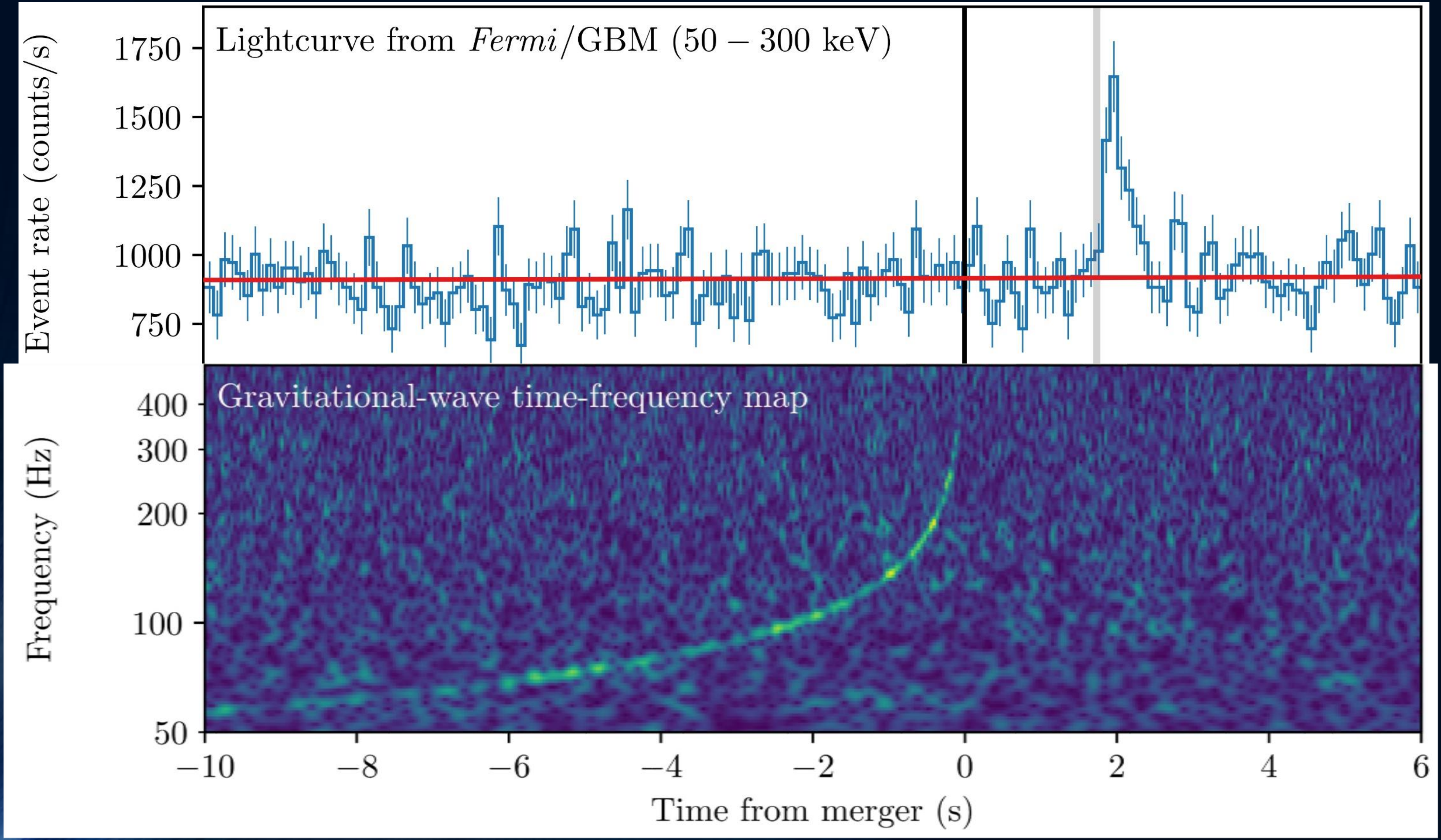

Measured Mass Ratio of GW170817 (for high and low spin assumption)

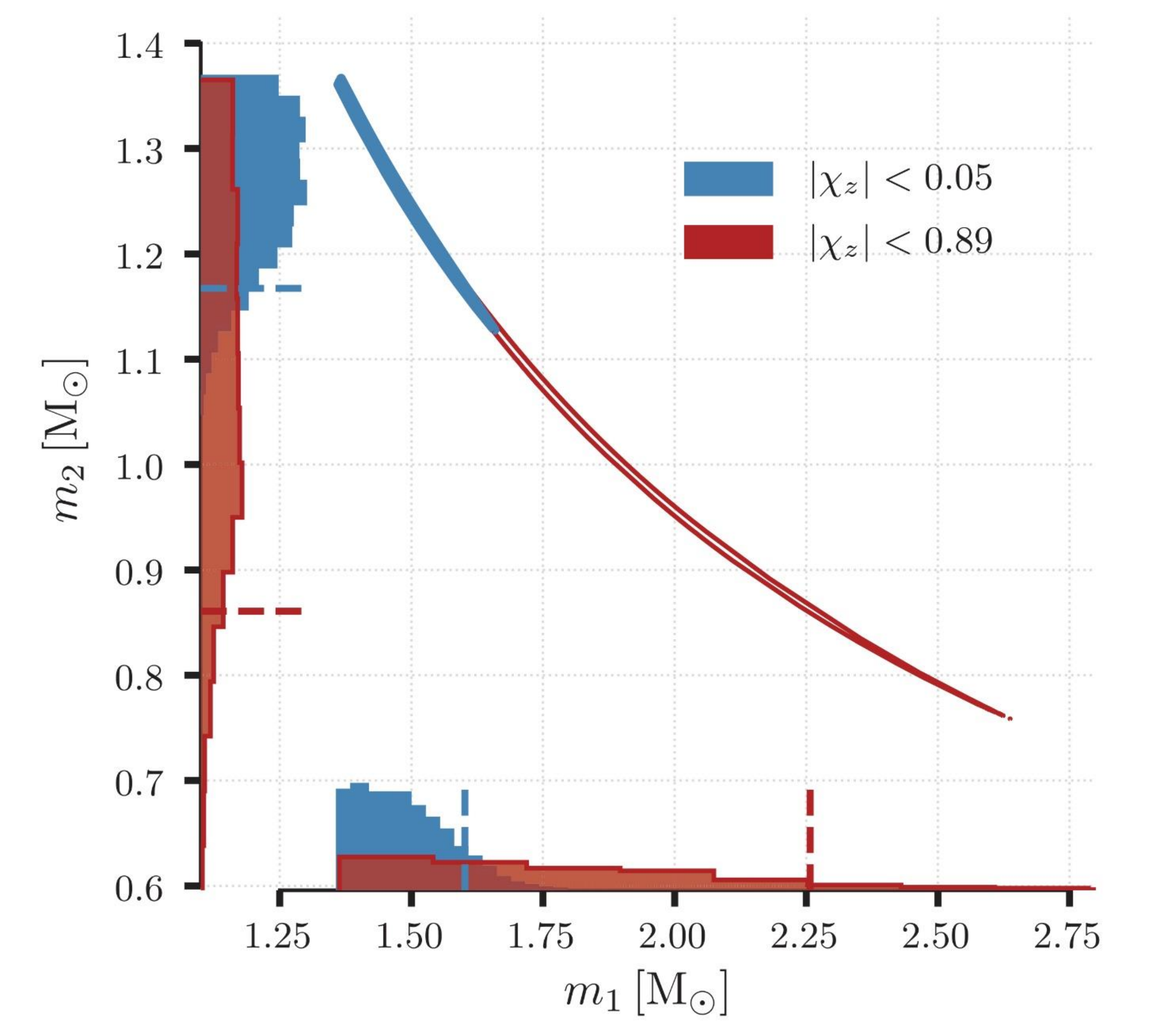

GW170817: Tidal Deformability Restrictions on the Equation of State (EOS) (for high and low spin assumption)

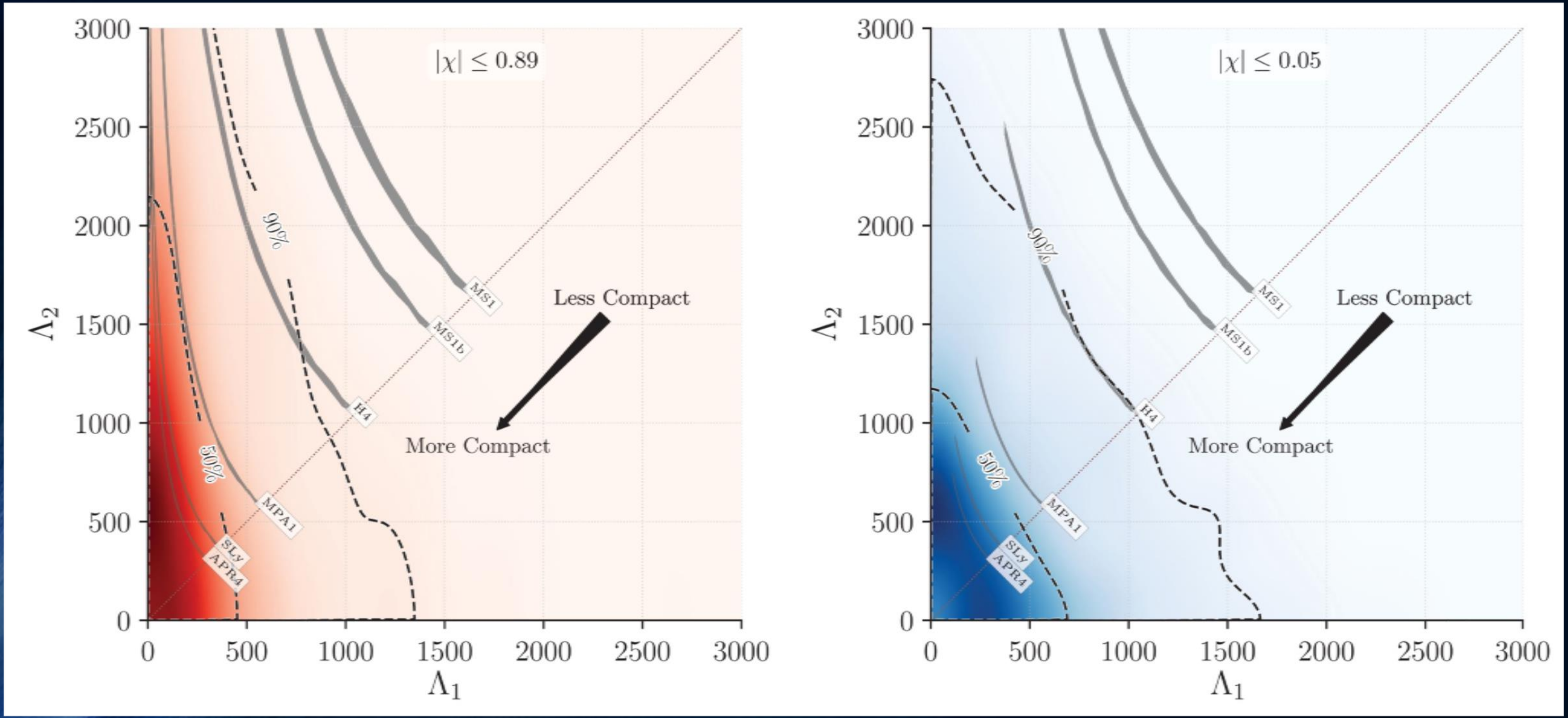

Numerical Relativity and Relativistic Hydrodynamics of Binary Neutron Star Mergers

Numerical simulations of a merger of two compact stars are based on a (3+1) decomposition of spacetime of the Einstein and hydrodynamic equations.

$$R_{\mu\nu} - \frac{1}{2} g_{\mu\nu} R = 8\pi T_{\mu\nu}$$

$$\nabla_\mu (\rho u^\mu) = 0\,, \qquad \nabla_\nu T^{\mu\nu} = 0\,.$$

(3+1) decomposition of spacetime

$$g_{\mu\nu} = \begin{pmatrix} -\alpha^2 + \beta_i \beta^i & \beta_i \\ \beta_i & \gamma_{ij} \end{pmatrix}$$

$$d\tau^2 = \alpha^2(t, x^j) dt^2 \qquad x^i_{t+dt} = x^i_t - \beta^i(t, x^j) dt$$

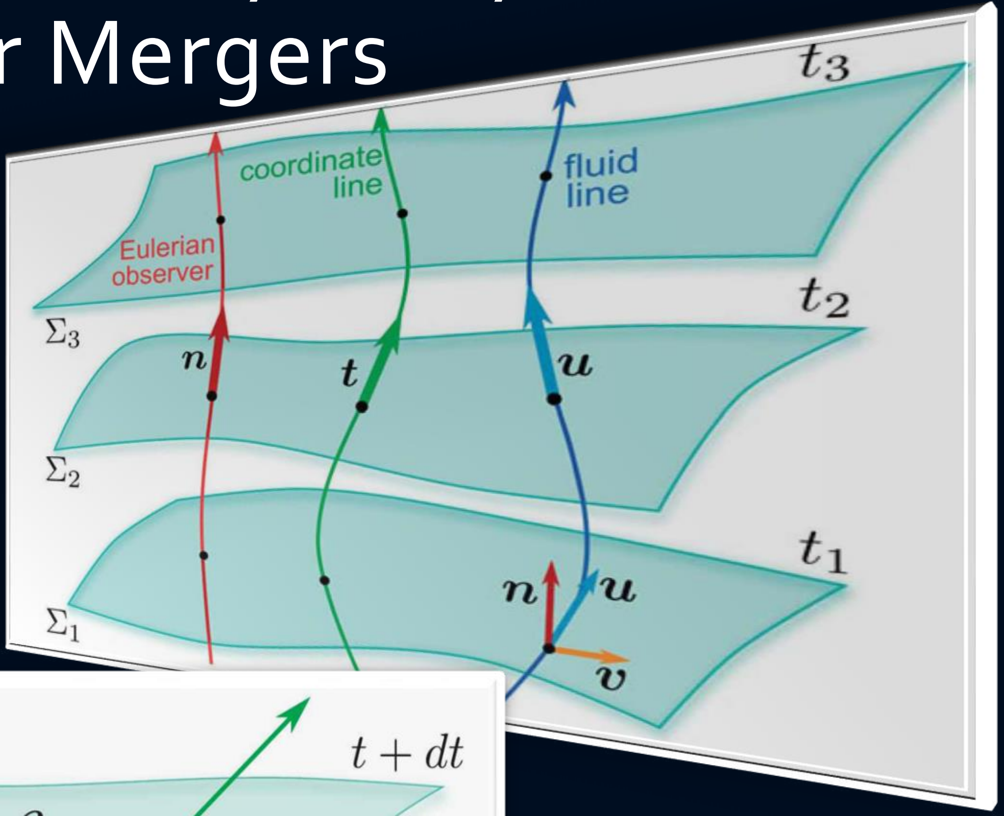

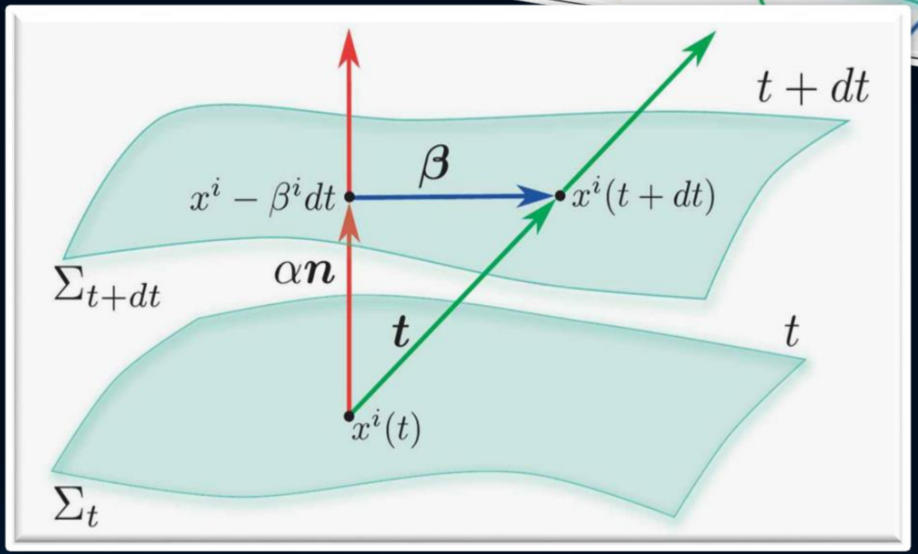

All figures and equations from: Luciano Rezzolla, Olindo Zanotti: Relativistic Hydrodynamics, Oxford Univ. Press, Oxford (2013)

Computersimulation of a Neutron Star Merger in full General Relativity

Credits: Cosima Breu, David Radice and Luciano Rezzolla

Density

8.5 14

lg(rho) [g/cm^3]

Temperature

0 50

T [MeV]

HMNS Evolution for different EoSs

High mass simulations (M=1.35 Msolar)

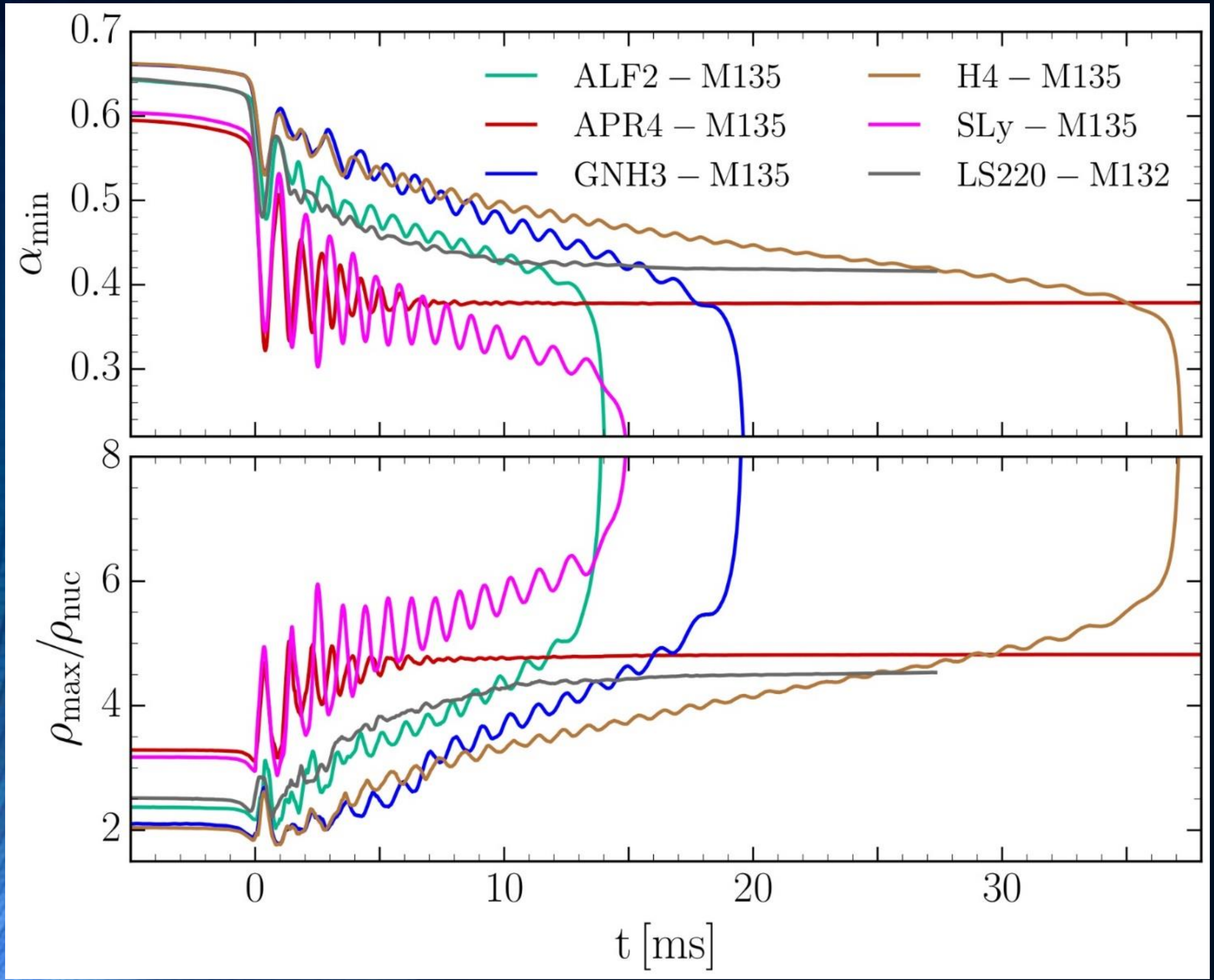

Central value of the lapse function α_c (upper panel) and maximum of the rest mass density ρ_{max} in units of ρ_0 (lower panel) versus time for the high mass simulations.

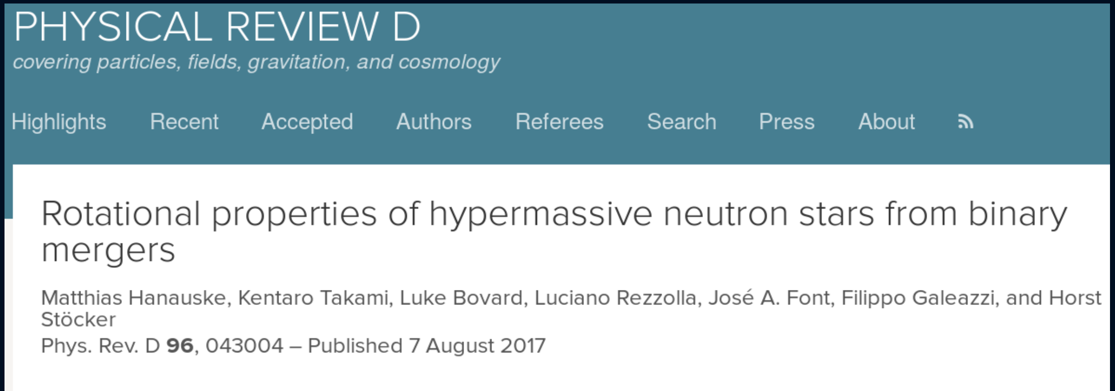
PHYSICAL REVIEW D
covering particles, fields, gravitation, and cosmology

Highlights Recent Accepted Authors Referees Search Press About

Rotational properties of hypermassive neutron stars from binary mergers

Matthias Hanauske, Kentaro Takami, Luke Bovard, Luciano Rezzolla, José A. Font, Filippo Galeazzi, and Horst Stöcker

Phys. Rev. D **96**, 043004 – Published 7 August 2017

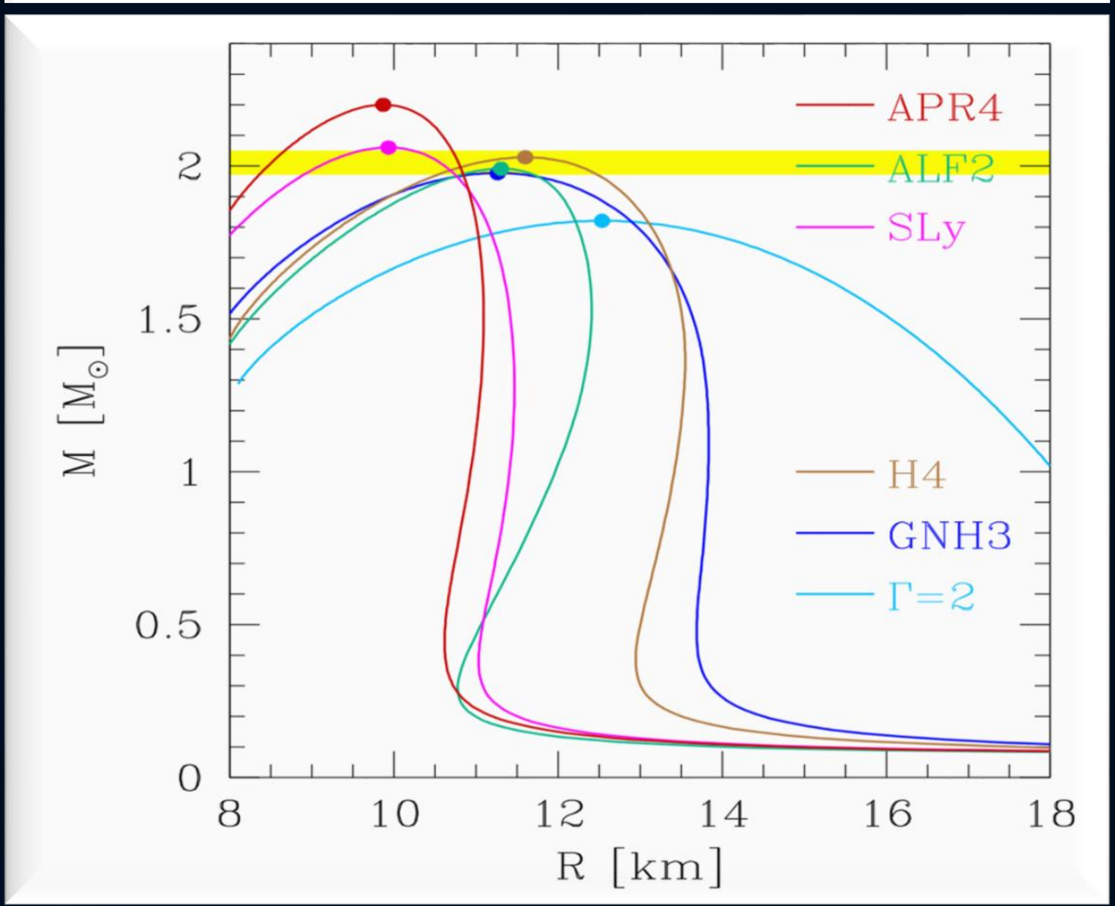

Mass-Radius relation for different EOSs

Logarithm of the density Temperature

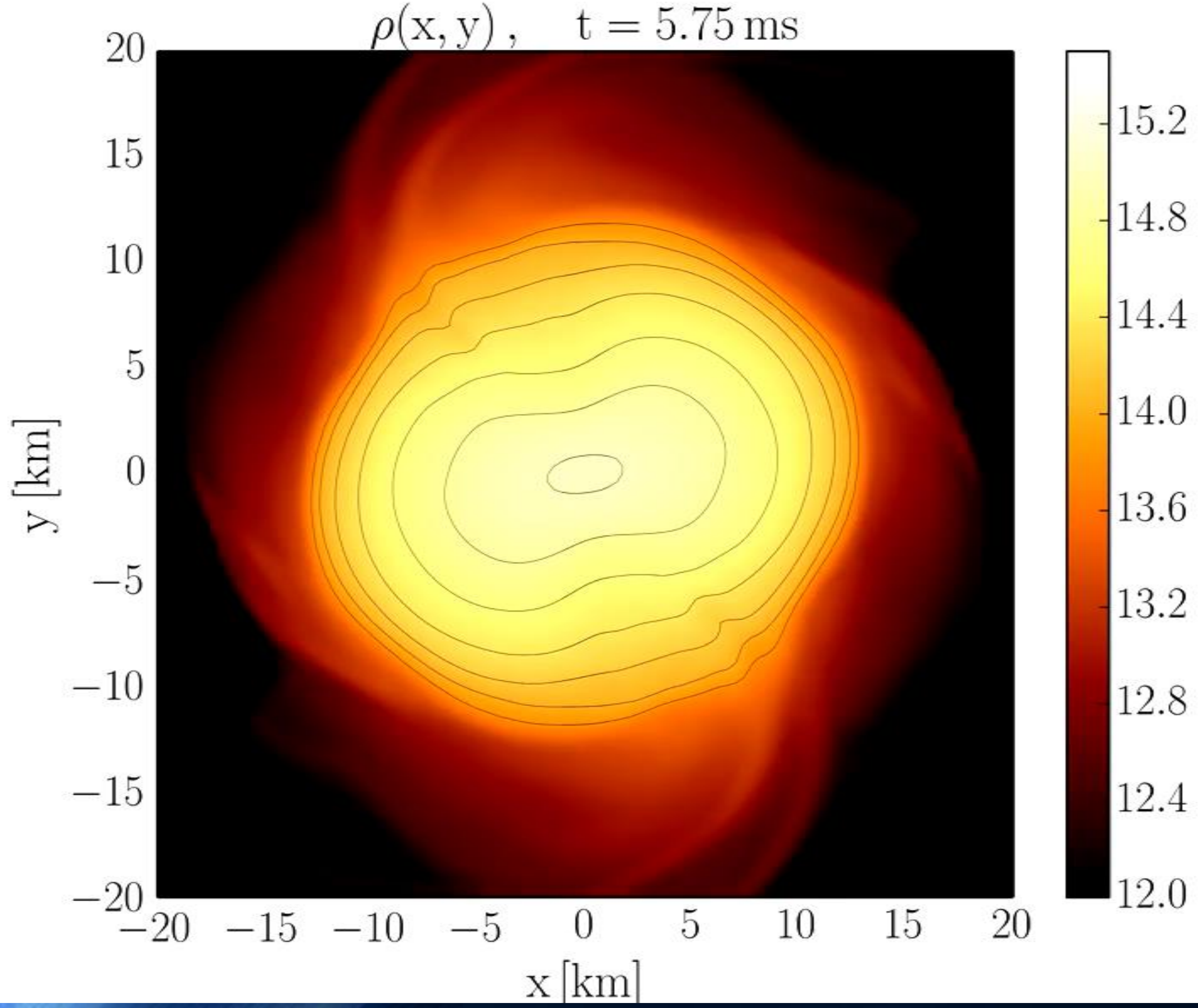

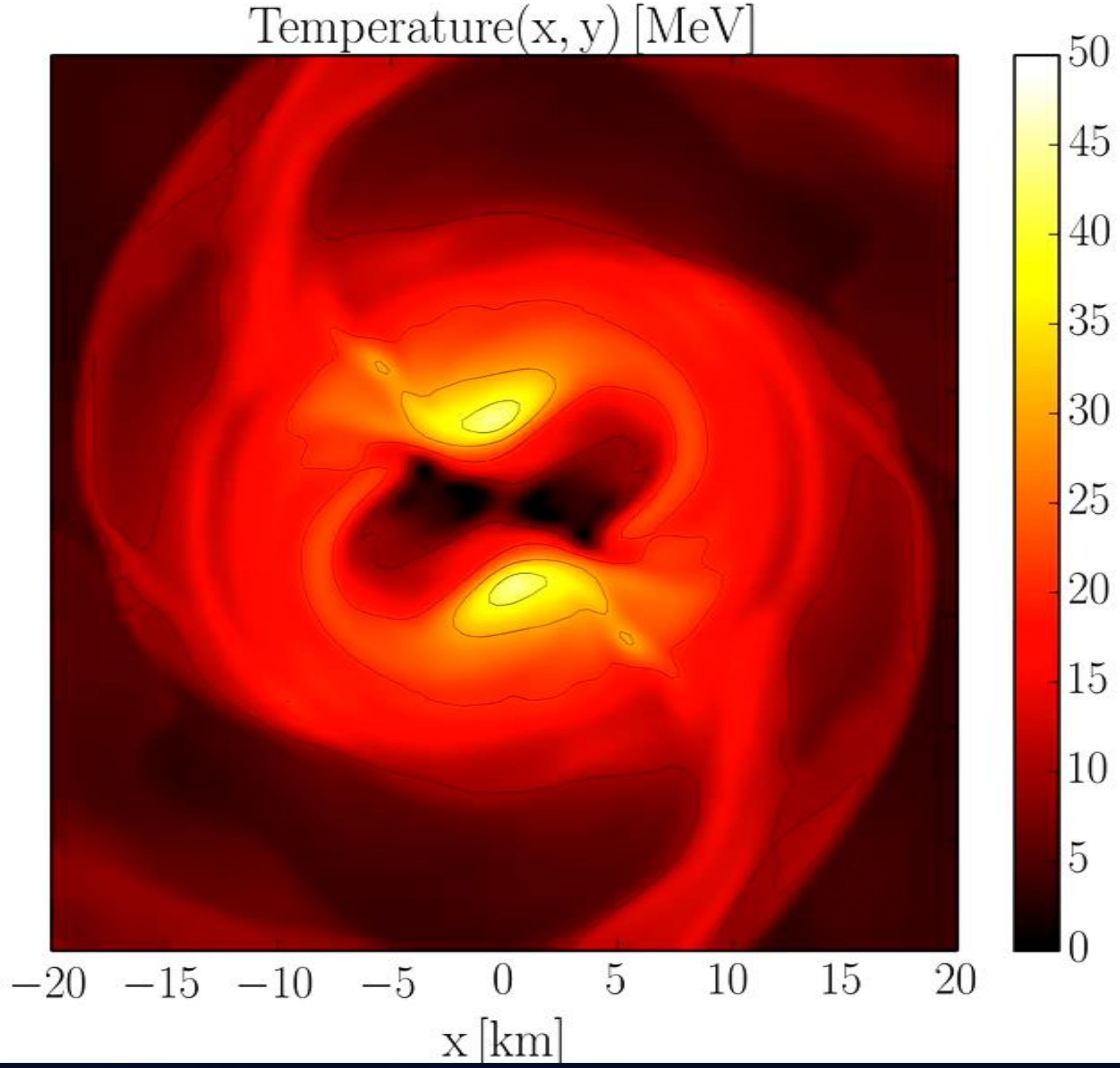

M. Hanauske, J. Steinheimer, L. Bovard, A. Mukherjee, S.Schramm, K. Takami, J.Papenfort, N.Wechselberger, L.Rezzolla, Luciano and H.Stöcker; "Concluding Remarks: Connecting Relativistic Heavy Ion Collisions and Neutron Star Mergers by the Equation of State of Dense Hadron-and Quark Matter as signalled by Gravitational Waves"; Journal of Physics: Conference Series, 878(1), p.012031 (2017)

The Co-Rotating Frame

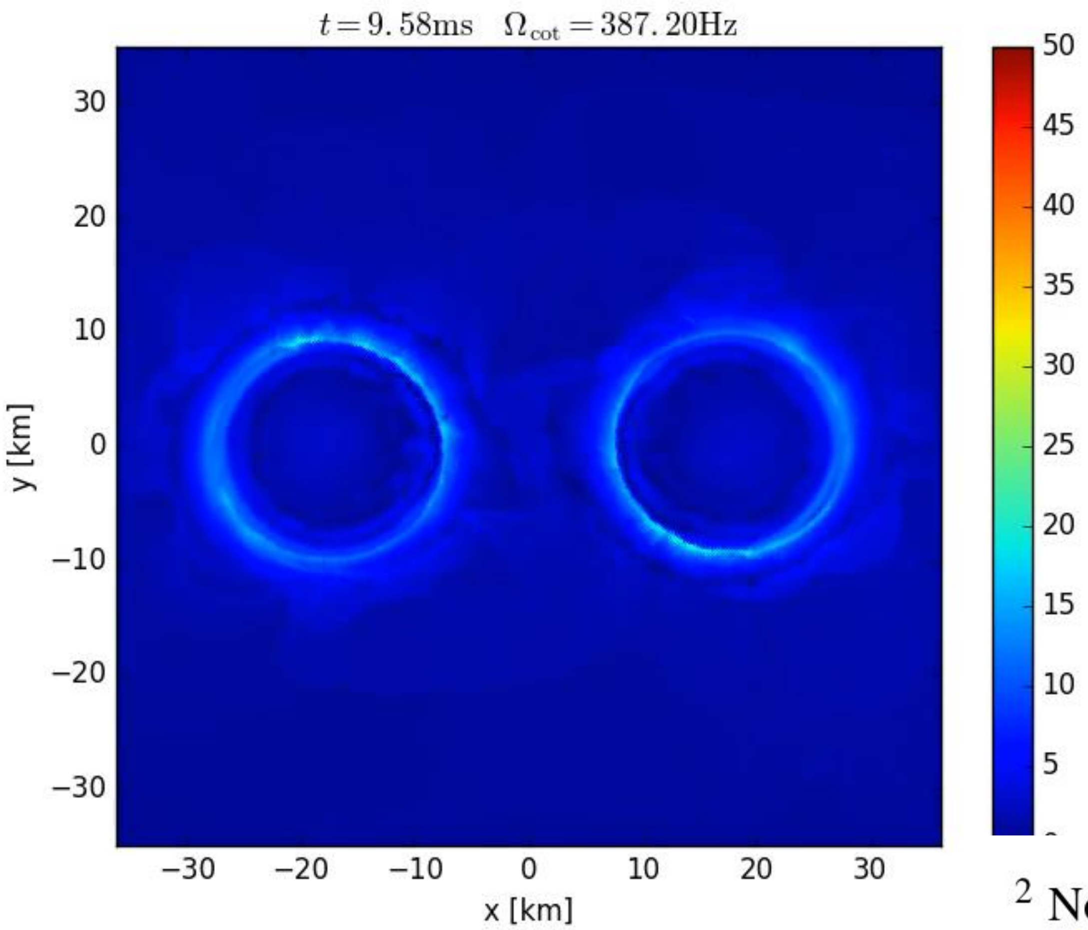

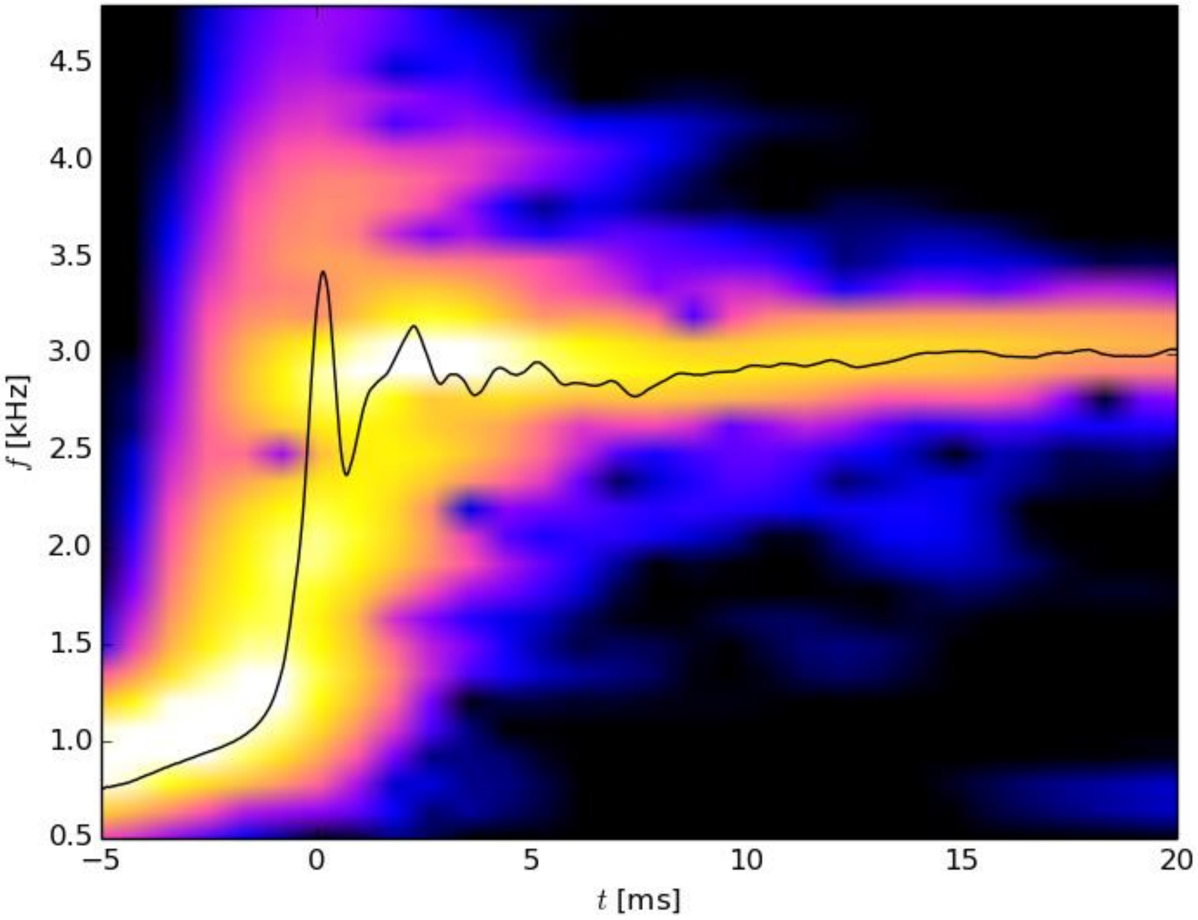

[2] Note that the angular-velocity distribution in the lower central panel of Fig. 10 refers to the corotating frame and that this frame is rotating at half the angular frequency of the emitted gravitational waves, Ω_{GW}. Because the maximum of the angular velocity Ω_{max} is of the order of $\Omega_{GW}/2$ (cf. left panel of Fig. 12), the ring structure in this panel is approximately at zero angular velocity.

Simulation and movie has been produced by Luke Bovard

Evolution of Tracer-particles tracking individual fluid elements in the equatorial plane of the HMNS at post-merger times

M.G. Alford, L. Bovard, M. Hanauske, L. Rezzolla and K. Schwenzer
"On the importance of viscous dissipation and heat conduction in binary neutron-star mergers" (submitted to PRL, see arxiv)

Different rotational behaviour of the quark-gluon-plasma produced in non-central ultra-relativistic heavy ion collisions
L. Adamczyk et.al., "Global Lambda-hyperon polarization in nuclear collisions: evidence for the most vortical fluid", Nature 548, 2017

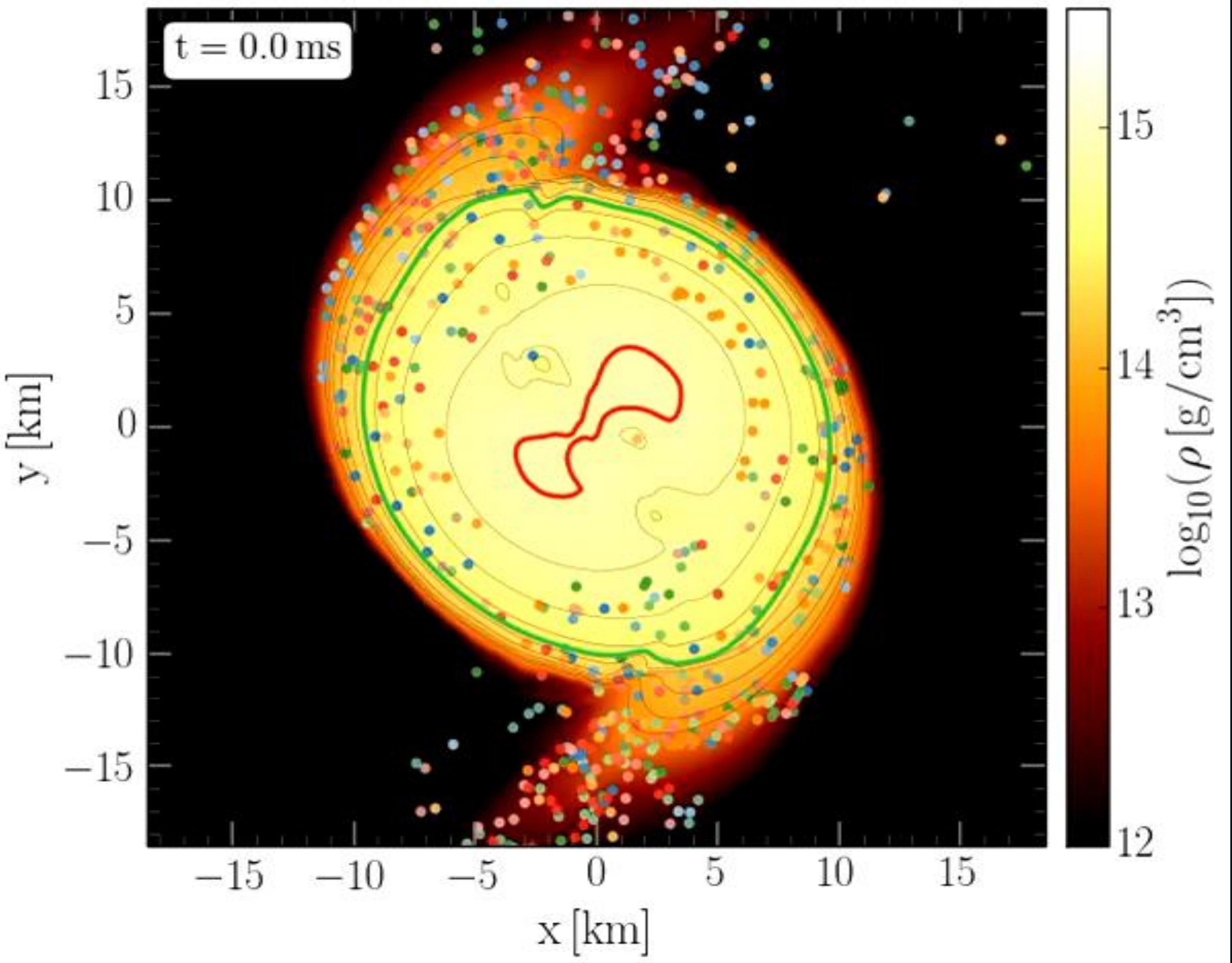

Temperature

Angular Velocity

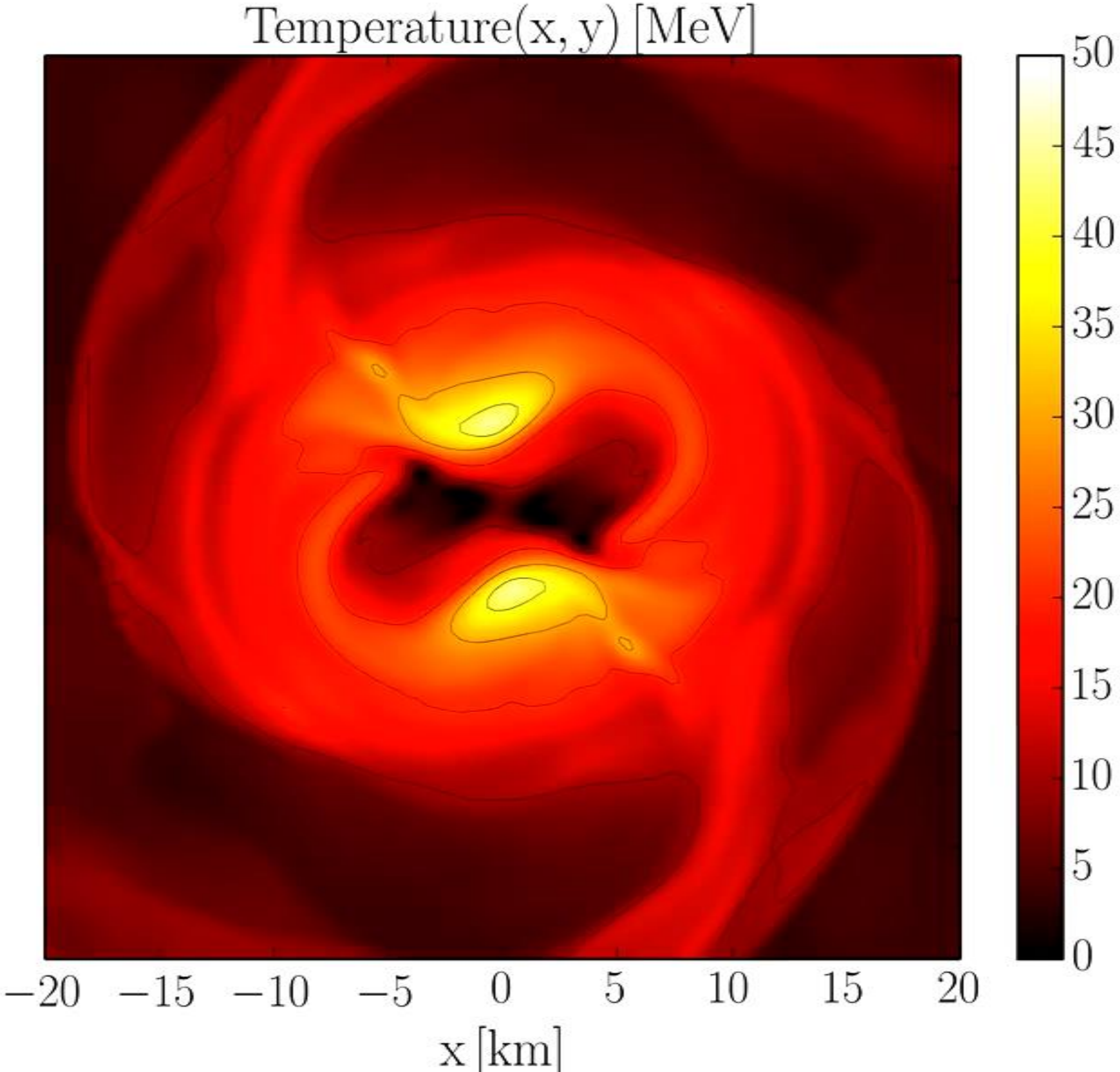

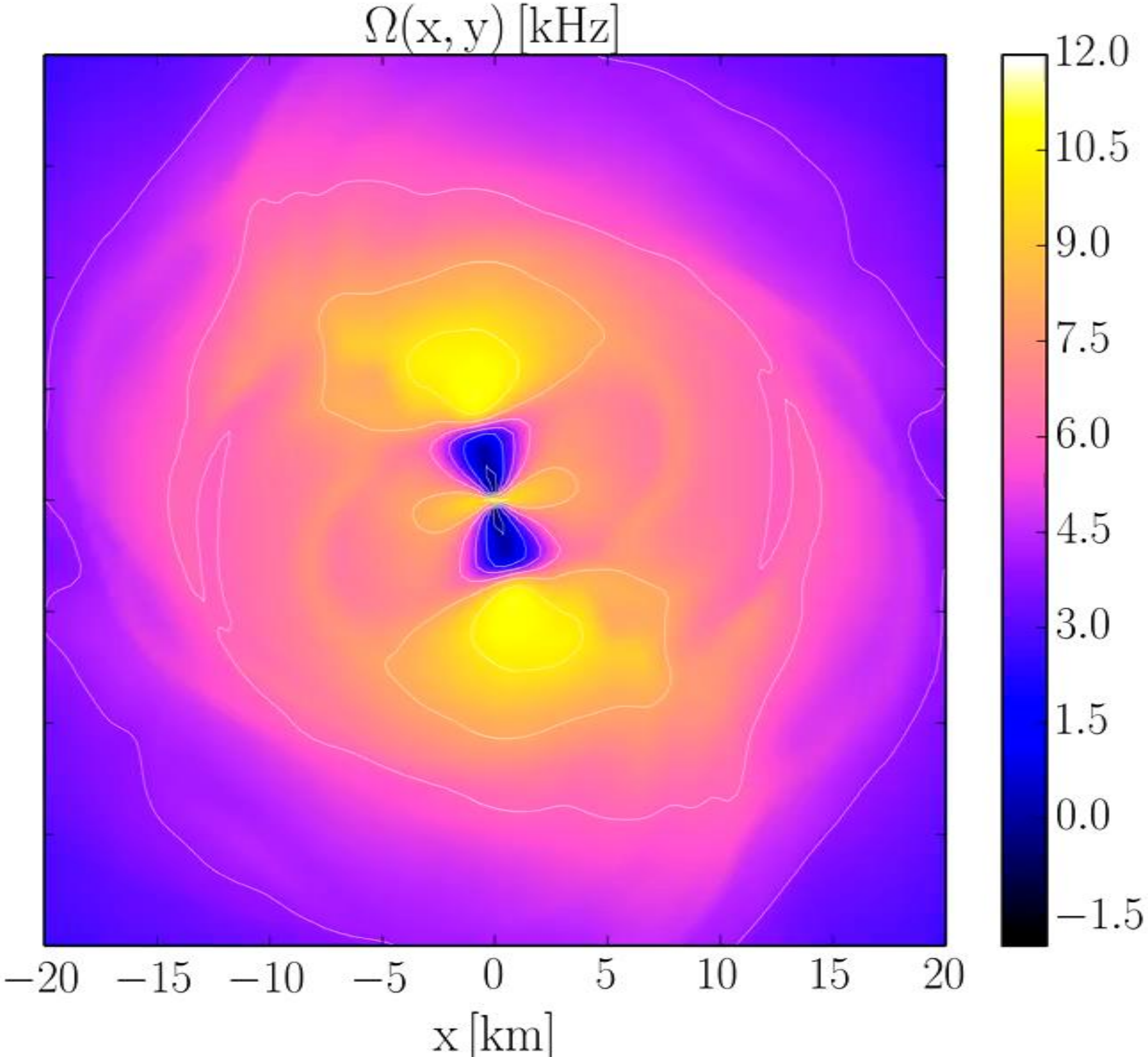

Time-averaged Rotation Profiles of the HMNSs

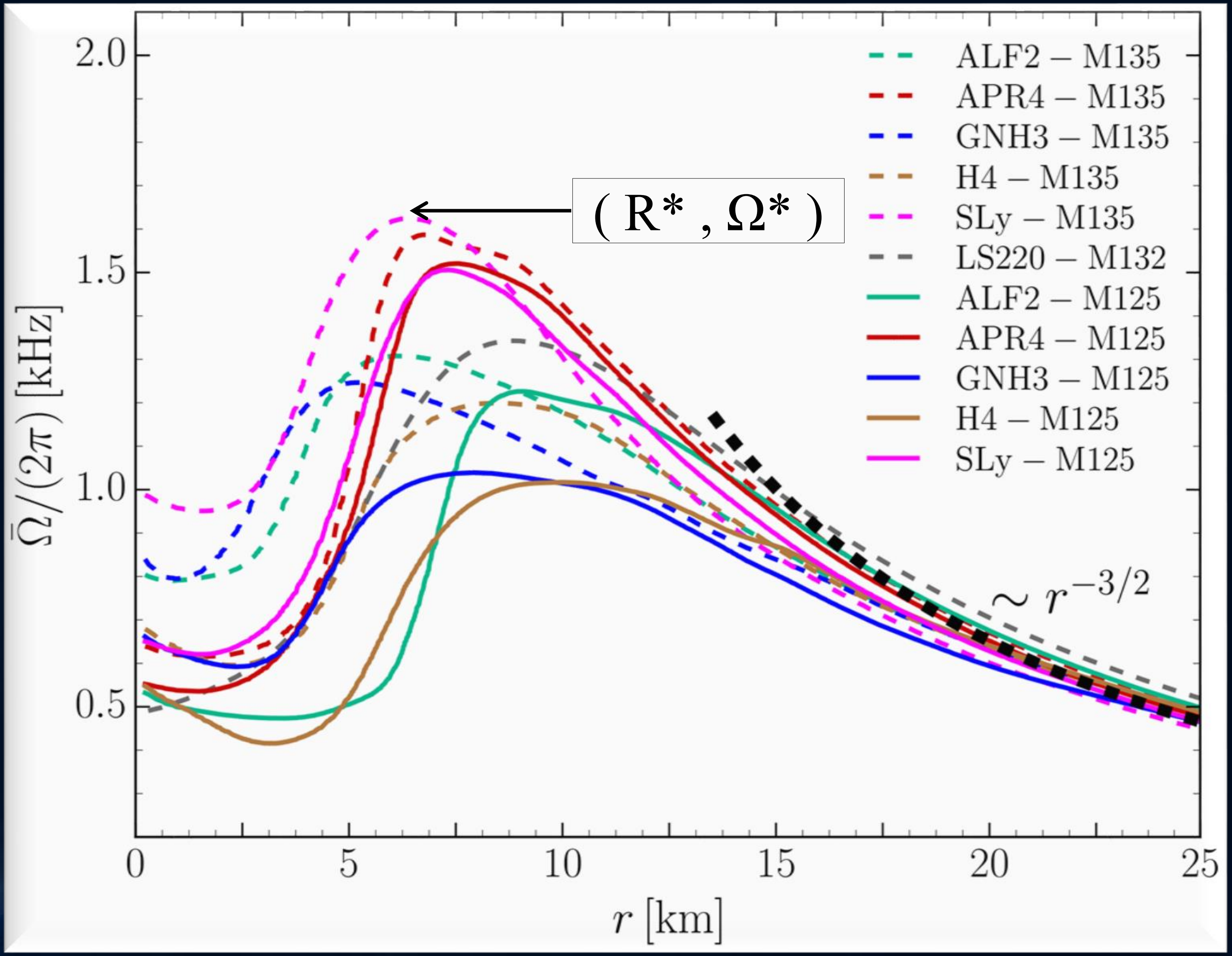

Time-averaged rotation profiles for different EoS
Low mass runs (solid curves), high mass runs (dashed curves).

<u>Soft EoSs</u>:
Sly
APR4

<u>Stiff EoSs</u>:
GNH3
H4

Maximum of the rotation profile Ω*(t) (blue) and ist radial position R*(t) (orange) for the non-collapsing simulation (ALF2, M=1.25)

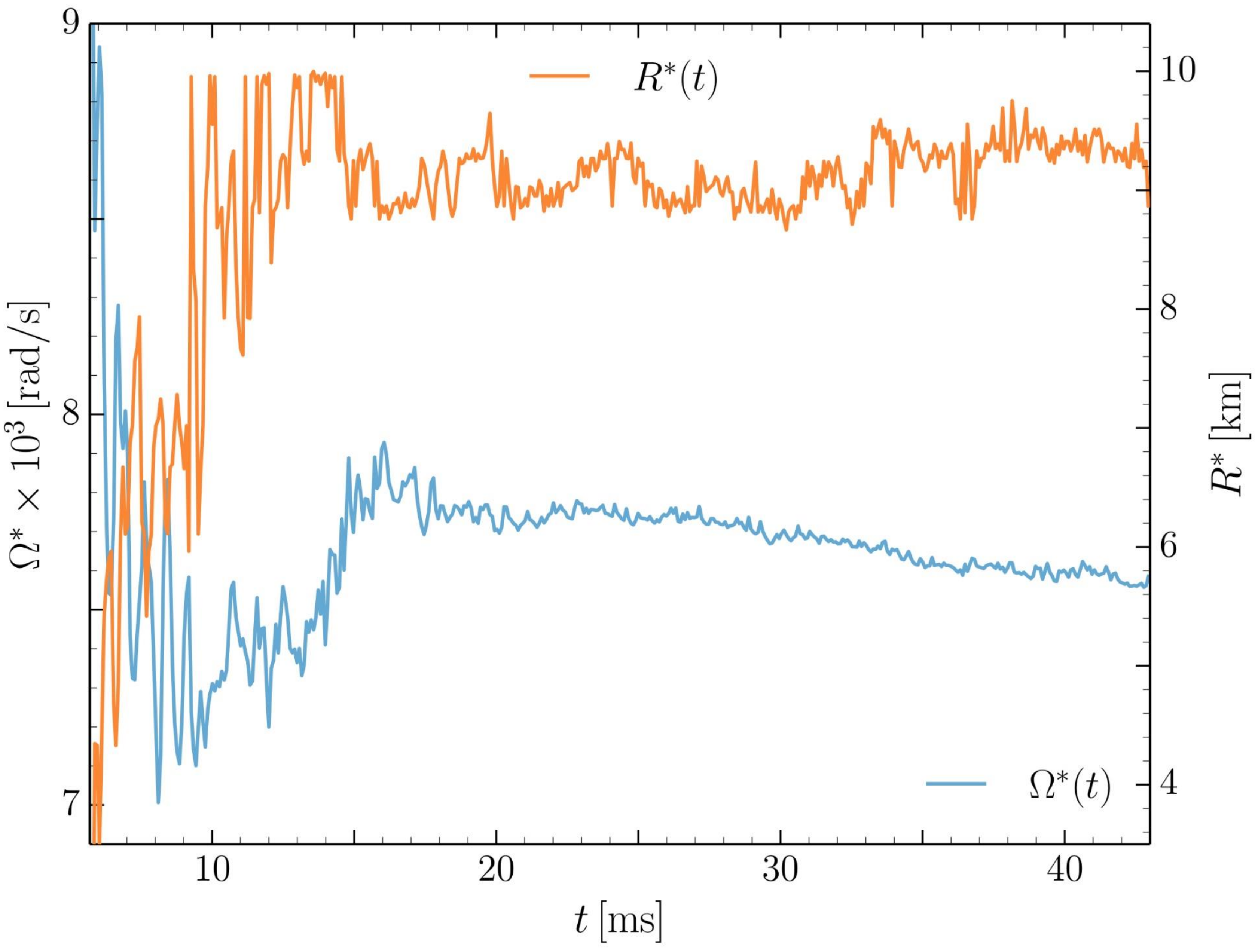

GW170817: Evolution of the HMNS until BH formation

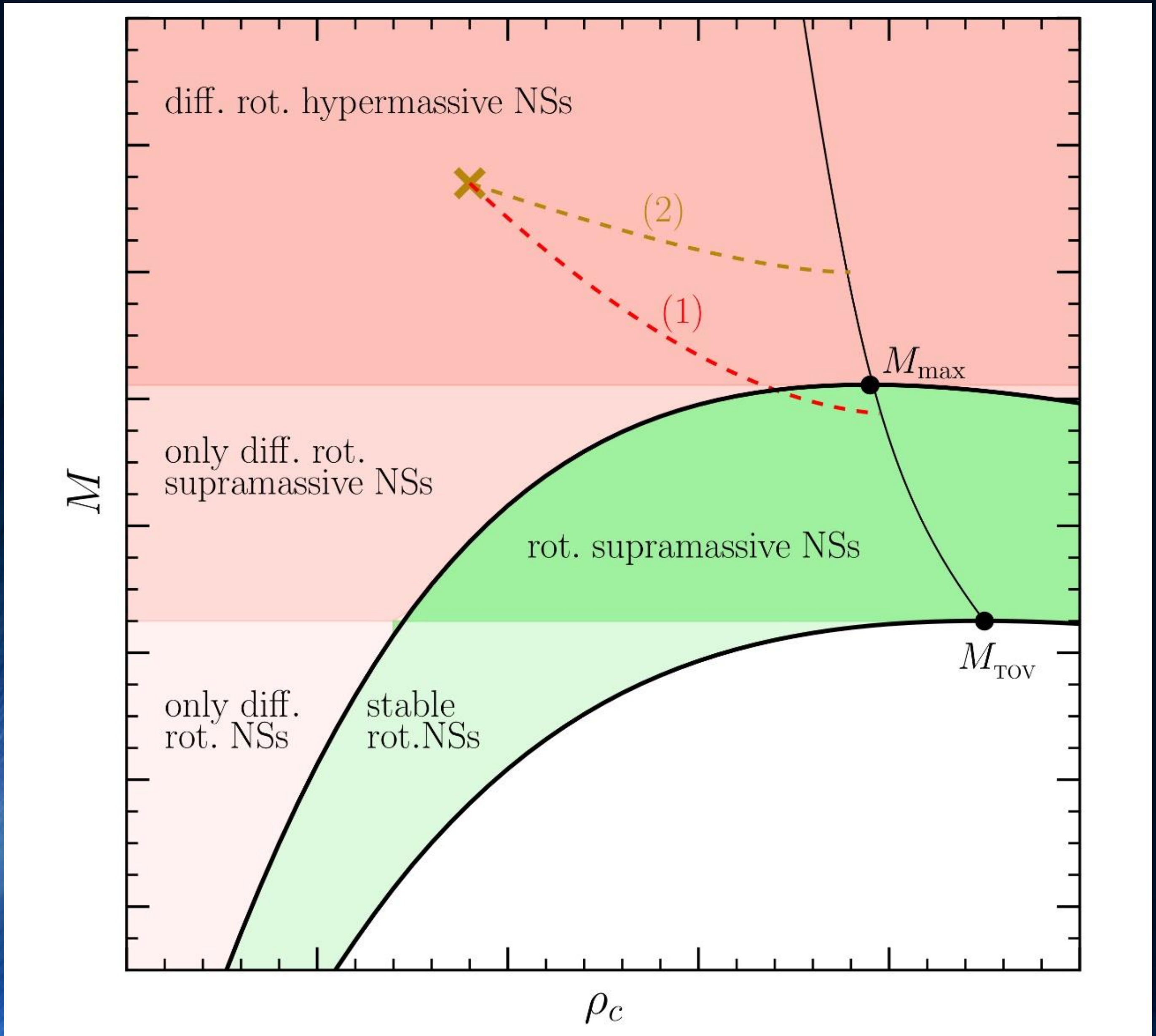

The highly differentially rotating hypermassive/supramassive neutron star will spin down and redistribute its angular momentum (e.g. due to magnetic braking). After ~1 second it will cross the stability line as a uniformly rotating supramassive neutron star (close to Mmax) and collapse to a black hole. Parts of the ejected matter will fall back into the black hole producing the gamma-ray burst.

GW170817: Constraining the Maximum Mass and the EOS

USING GRAVITATIONAL-WAVE OBSERVATIONS AND QUASI-UNIVERSAL RELATIONS TO CONSTRAIN THE MAXIMUM MASS OF NEUTRON STARS

LUCIANO REZZOLLA[1,2], ELIAS R. MOST[1], AND LUKAS R. WEIH[1]

Draft version November 2, 2017

ABSTRACT

Combining the gravitational-wave observations of merging systems of binary neutron stars and quasi-universal relations we set constraints on the maximum mass that can be attained by nonrotating stellar models of neutron stars. More specifically, exploiting the recent observation of the gravitational-wave event GW170817 (Abbott et al. 2017b) and the quasi-universal relation between the maximum mass of nonrotating stellar models $M_{\rm TOV}$ and the maximum mass that can be supported through uniform rotation $M_{\rm max} = (1.203 \pm 0.022)\, M_{\rm TOV}$ (Breu & Rezzolla 2016), we set limits for the maximum mass to be $2.01 \pm 0.04 \leq M_{\rm TOV}/M_{\odot} \lesssim 2.16 \pm 0.03$, where the lower limit in this range comes from pulsar observations (Antoniadis et al. 2013). Our estimate, which follows a very simple line of arguments and does not rely on the interpretation of the electromagnetic signal, can be further refined as new detections become available. We also briefly discuss the impact that our conclusions have on the equation of state of nuclear matter.

See arXiv:1711.00314v1 [astro-ph.HE] 1 Nov 2017

GW-Spectrum for different EOSs

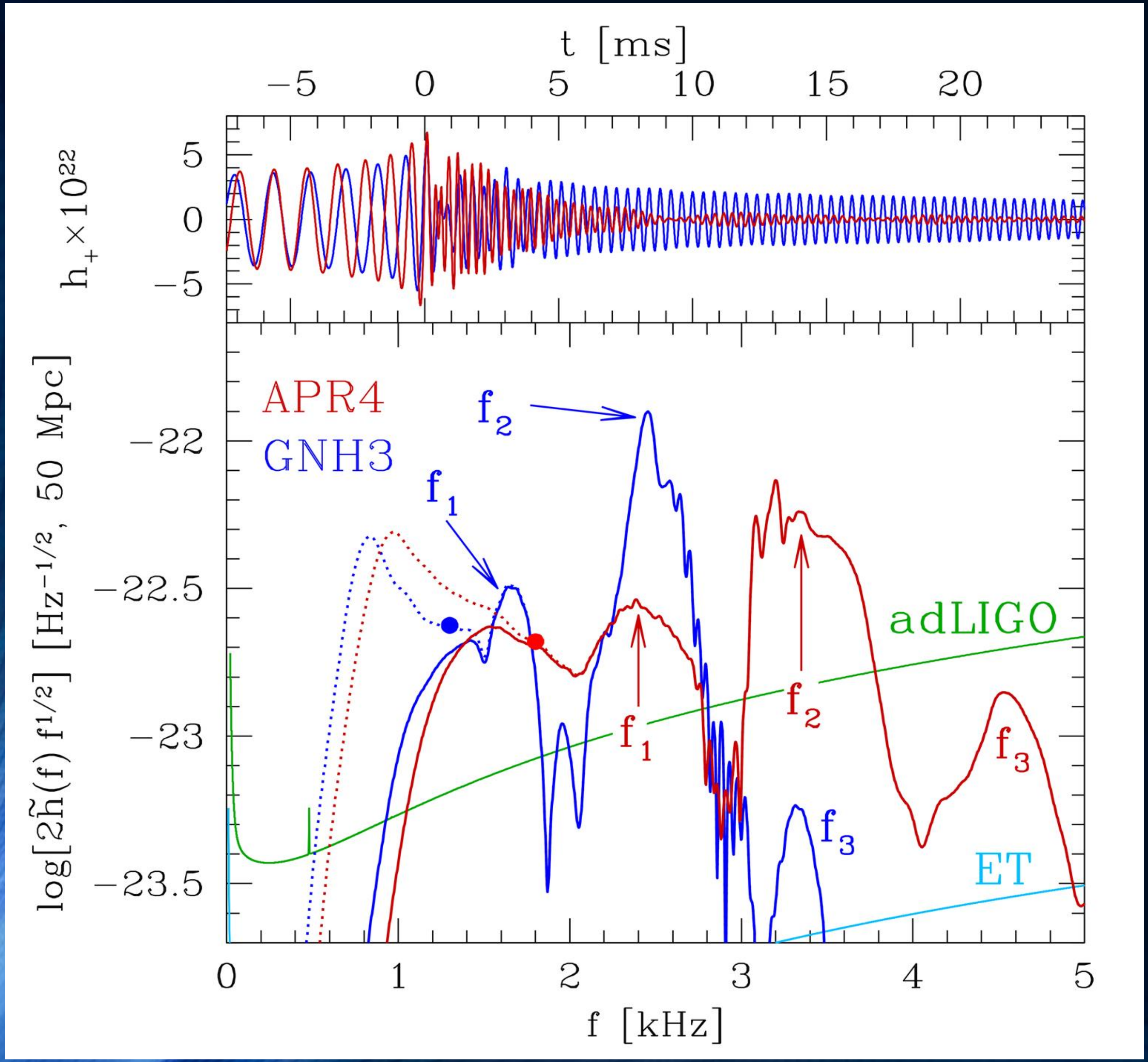

See:

Kentaro Takami, Luciano Rezzolla, and Luca Baiotti, Physical Review D 91, 064001 (2015)

Hotokezaka, K., Kiuchi, K., Kyutoku, K., Muranushi, T., Sekiguchi, Y. I., Shibata, M., & Taniguchi, K. (2013). Physical Review D, 88(4), 044026.

Bauswein, A., & Janka, H. T. (2012). Physical review letters, 108(1), 011101.

Clark, J. A., Bauswein, A., Stergioulas, N., & Shoemaker, D. (2015). arXiv:1509.08522.

Bernuzzi, S., Dietrich, T., & Nagar, A. (2015). Physical review letters, 115(9), 091101.

Time Evolution of the GW-Spectrum

The power spectral density profile of the post-merger emission is characterized by several distinct frequencies f_{max}, f_1, f_2, f_3 and f_{2-0} . After approximately 5 ms after merger, the only remaining dominant frequency is the f_2-frequency (See L.Rezzolla and K.Takami, arXiv:1604.00246)

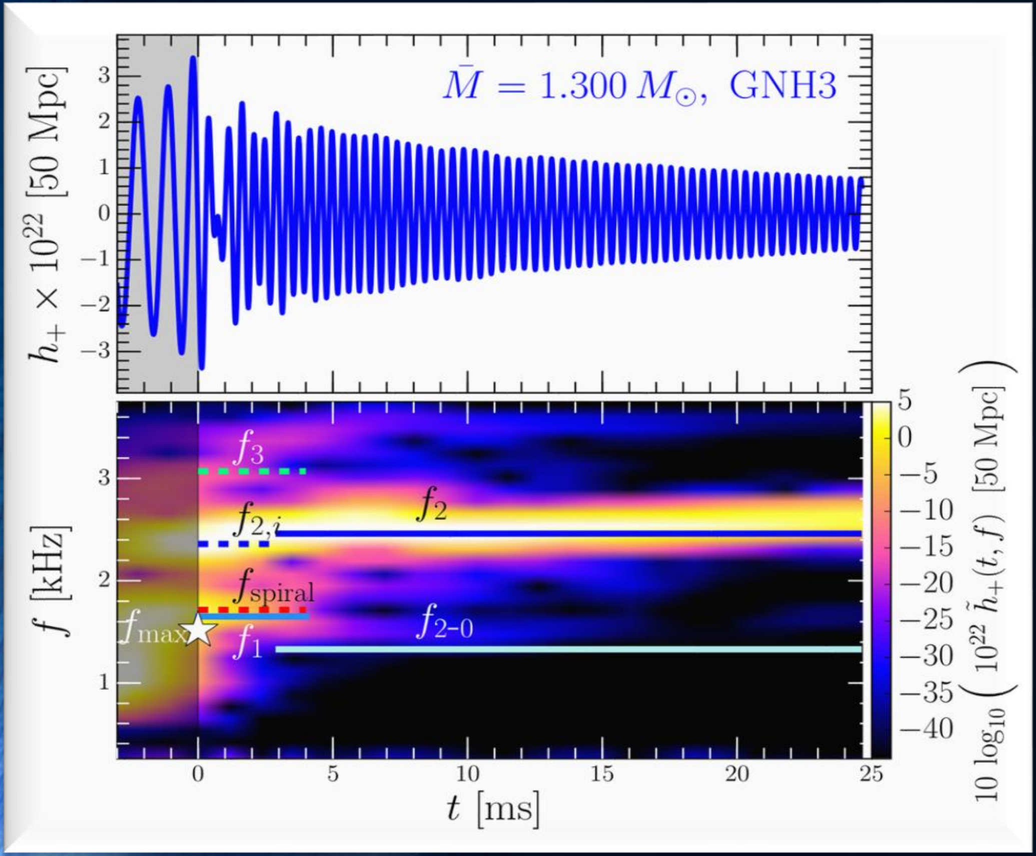

Stiff EOS

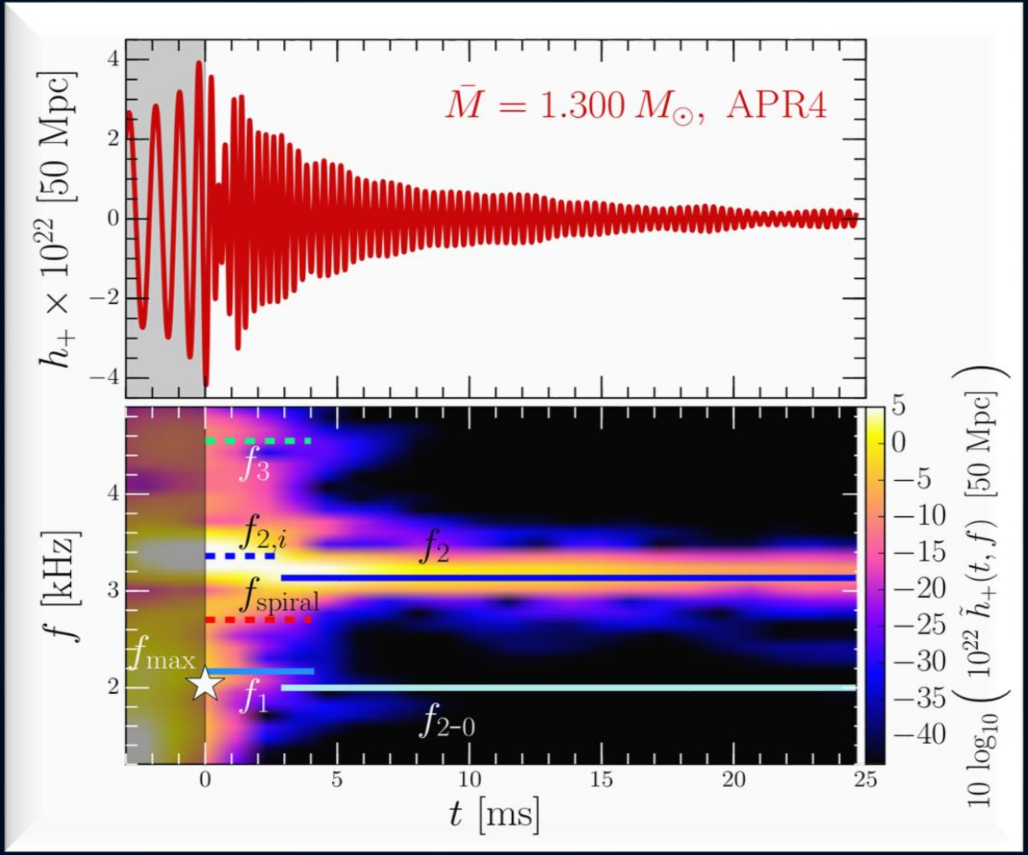

Soft EOS

Unfortunately, due to the low sensitivity at high gravitational wave frequencies, no post-merger signal has been found in GW170817.

But advanced detectors / next-generation detectors will be able to detect!

Evolution of the frequency spectrum of the emitted gravitational waves for the stiff GNH3 (left) and soft APR4 (right) EOS.

The QCD – Phase Transition and the Interior of a Hybrid Star

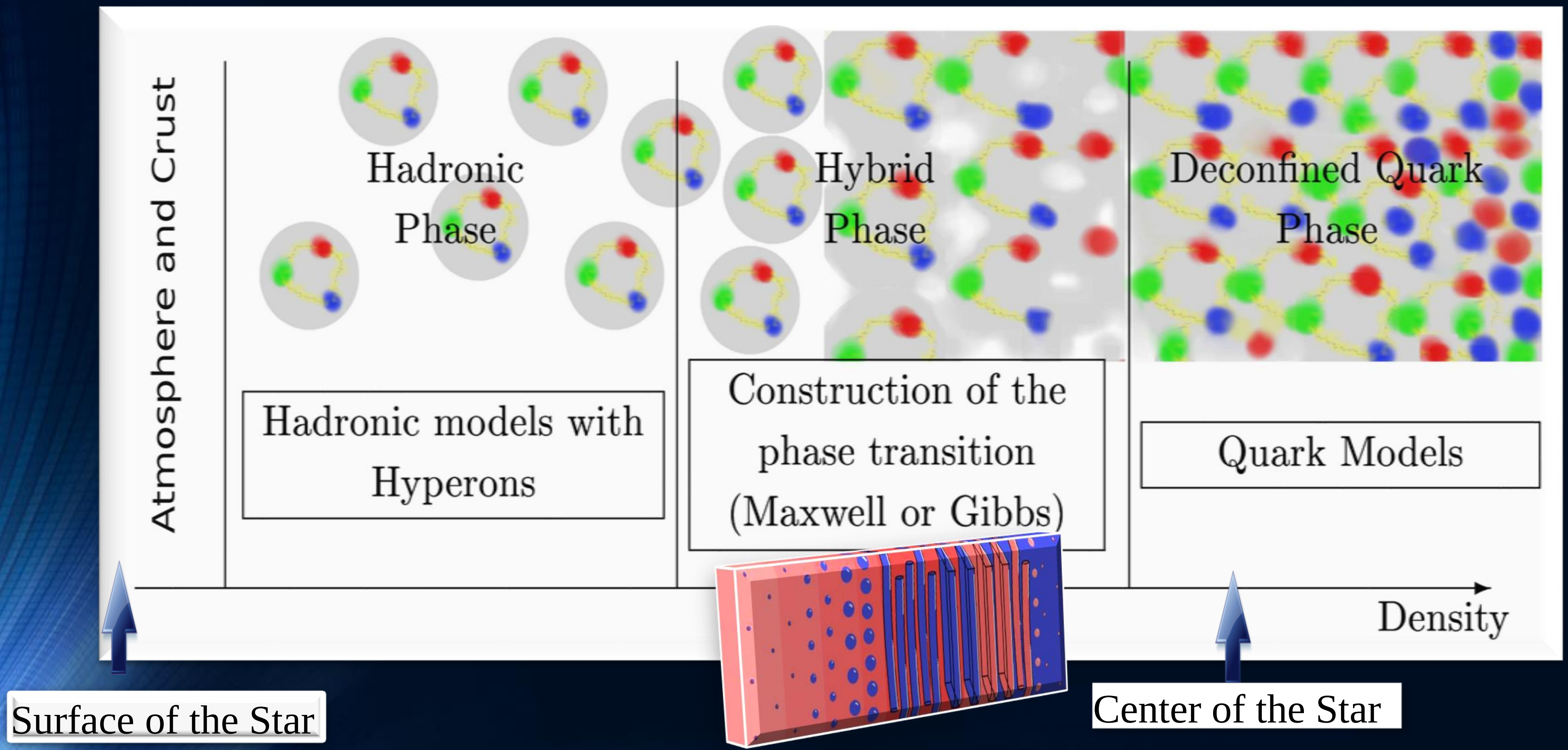

See: *Stable hybrid stars within a SU(3) Quark-Meson-Model*,
A.Zacchi, M.Hanauske, J.Schaffner-Bielich, PRD 93, 065011 (2016)

The Twin Star collapse

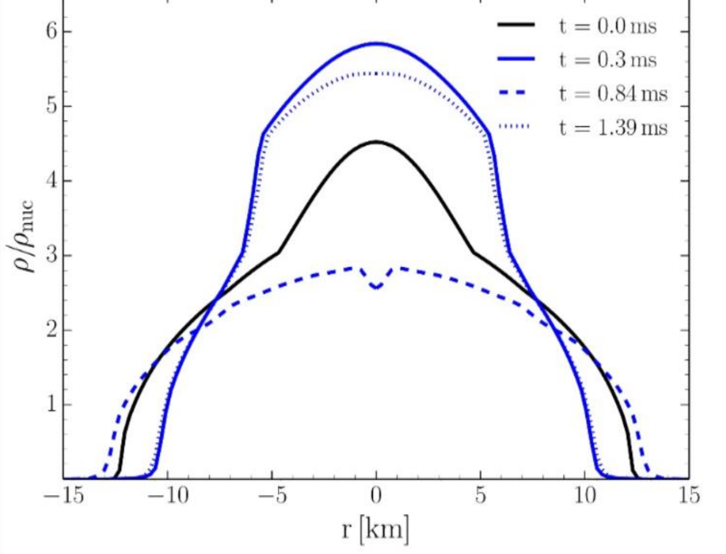

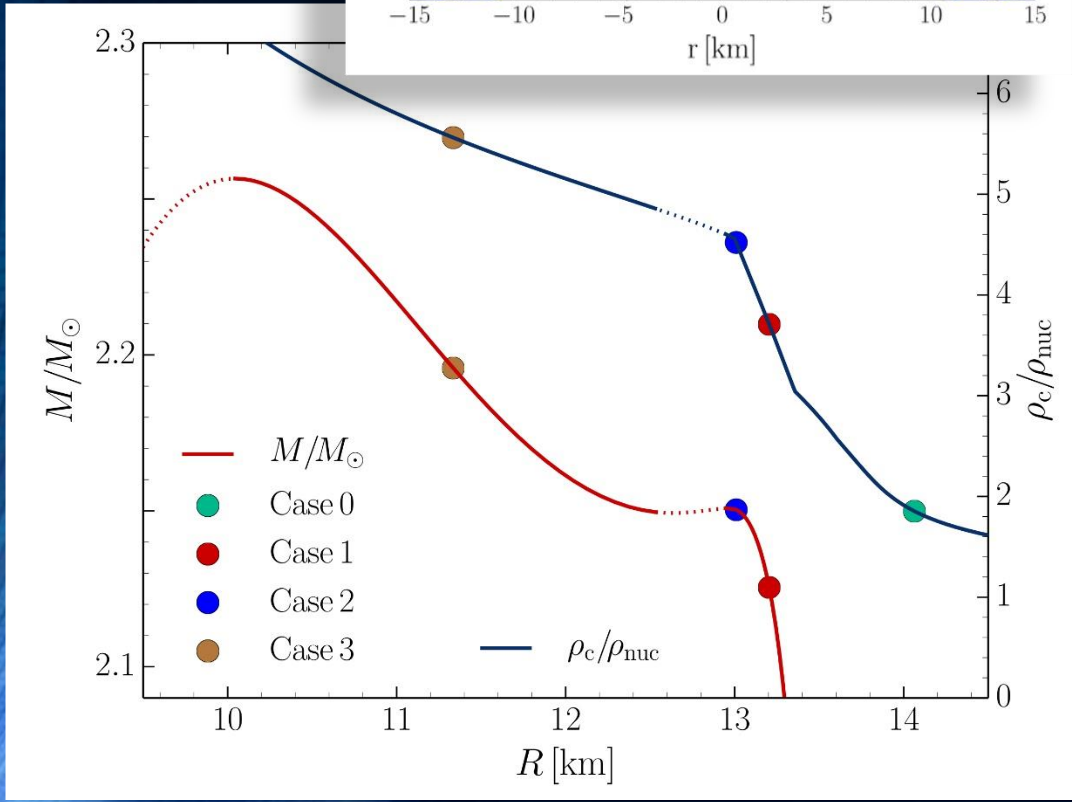

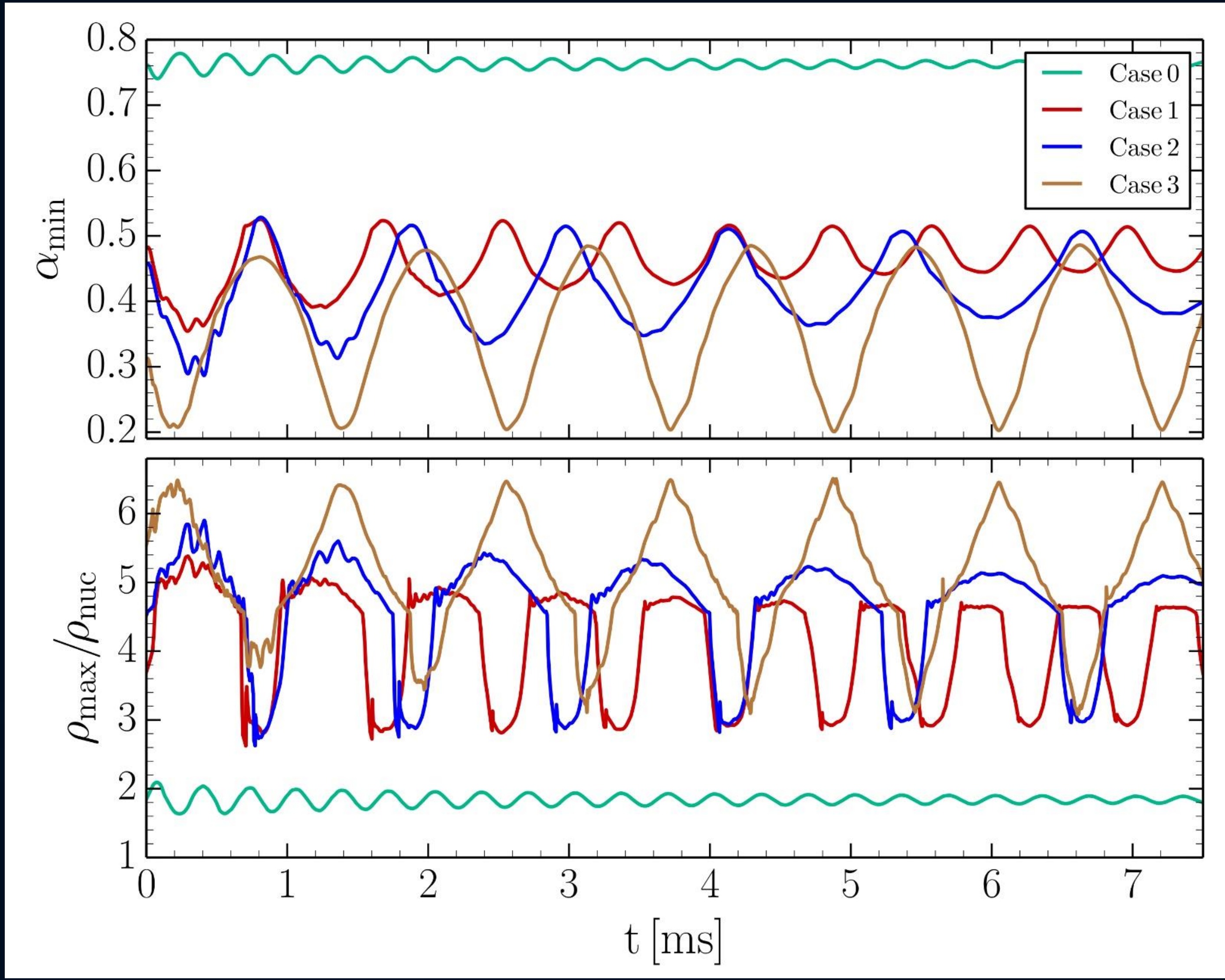

Radial oscillations of twin star configurations

M. Hanauske, Z.S. Yilmaz, C. Mitropoulos, L. Rezzolla and H. Stöcker
"Gravitational waves from binary compact star mergers in the context of strange matter", in Proceedings SQM2017

How to observe the QGP with gravitational waves from NS mergers?

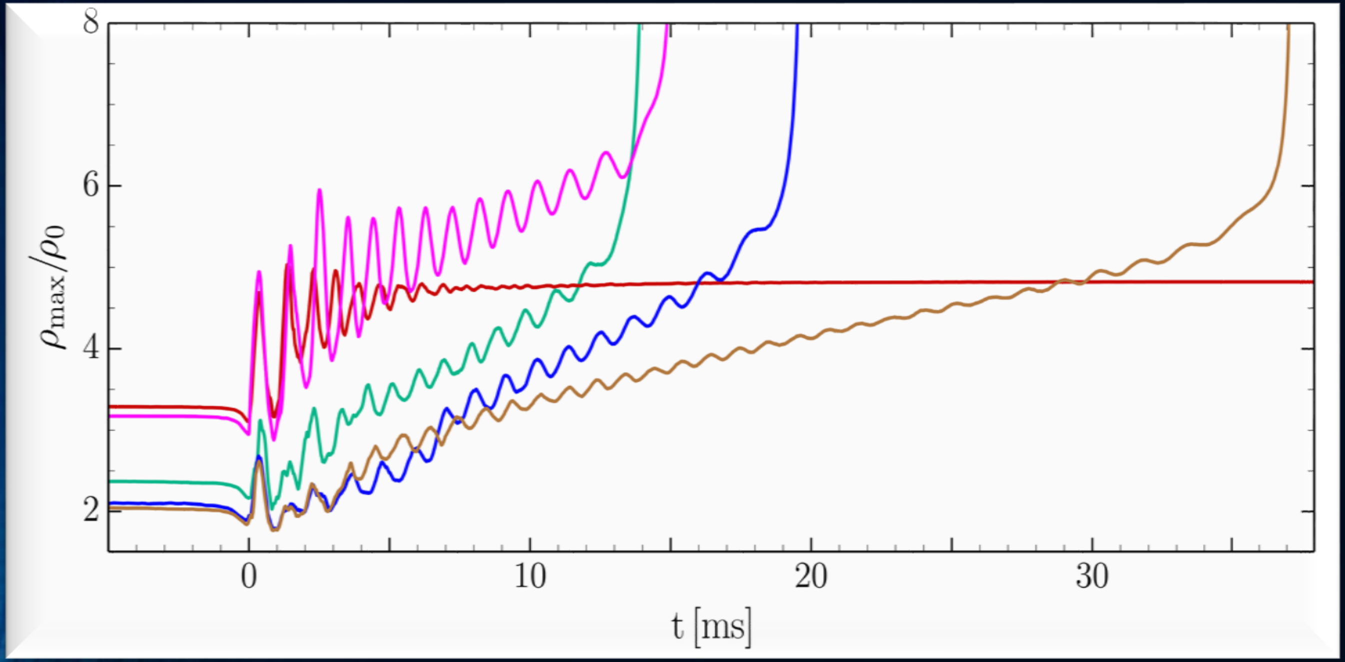

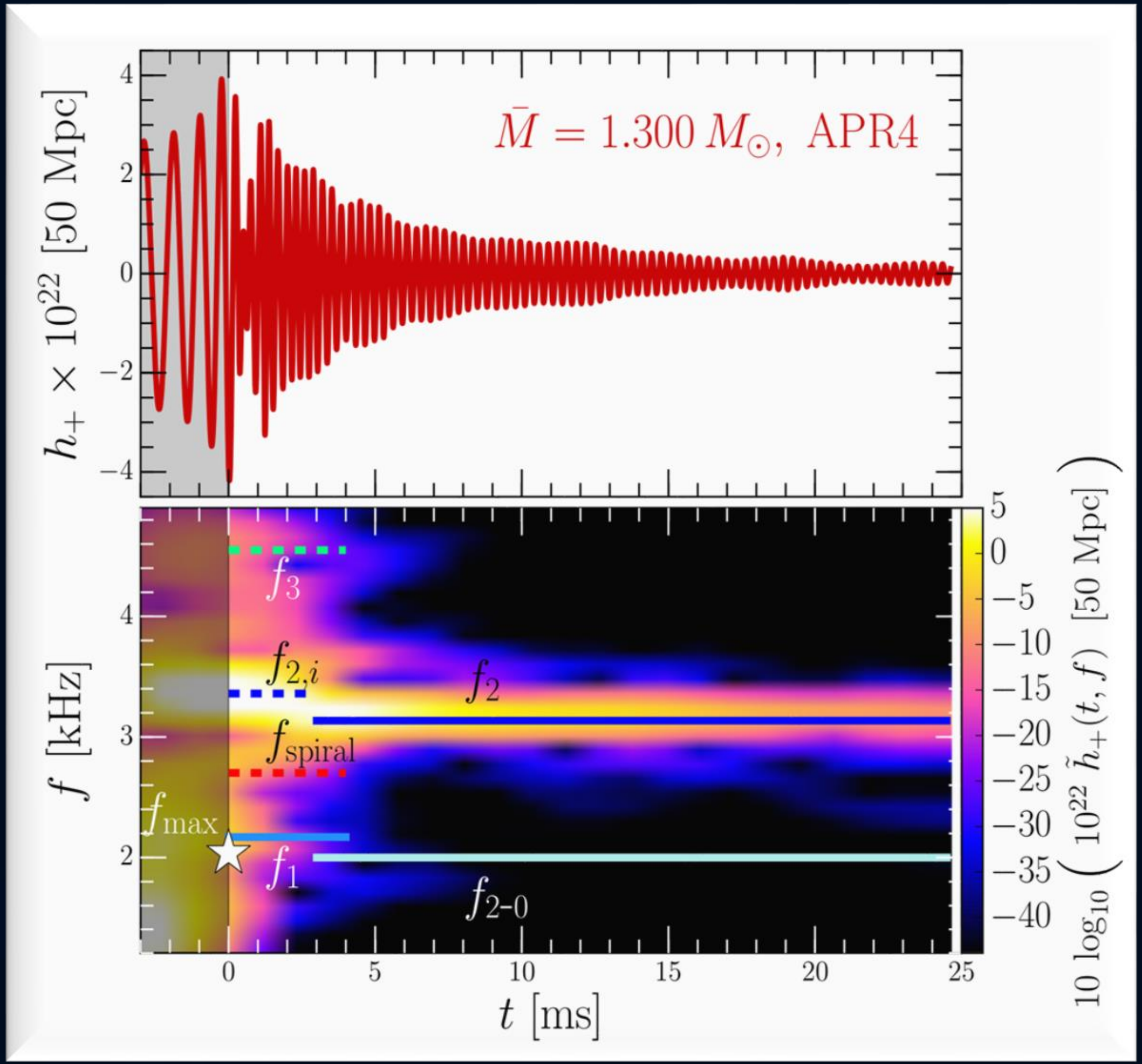

The appearance of the hadron-quark phase transition in the interior region of the HMNS will change the spectral properties of the emitted GW if it is strong enough. If the unstable twin star region will be reached during the "post-transient" phase, the f2-frequency peak of the GW signal will change rapidly due to the sudden speed up of the differentially rotating HMNS.

Hybrid star mergers represent optimal astrophysical laboratories to investigate the QCD phase structure and in addition with the observations from heavy ion collisions it will be possibly reach a conclusive picture on the QCD phase structure at high density and temperature.

On r-process nucleosynthesis from matter ejected in binary neutron star mergers

Luke Bovard,[1] Dirk Martin,[2] Federico Guercilena,[1] Almudena Arcones,[2] Luciano Rezzolla,[1,3] and Oleg Korobkin[4]

[1] *Institut für Theoretische Physik, Johann Wolfgang Goethe-Universität, Max-von-Laue-Straße 1, 60438 Frankfurt, Germany*
[2] *Institut für Kernphysik, Technische Universität Darmstadt, Schlossgartenstraße 9, 64289 Darmstadt, Germany*
[3] *Frankfurt Institute for Advanced Studies, Ruth-Moufang-Straße 1, 60438 Frankfurt, Germany*
[4] *Center for Theoretical Astrophysics, Los Alamos National Laboratory, Los Alamos, NM 87545, USA*

When binary systems of neutron stars merge, a very small fraction of their rest mass is ejected, either dynamically or secularly. This material is neutron-rich and its nucleosynthesis could provide the astrophysical site for the production of heavy elements in the universe, together with a kilonova signal confirming neutron-star mergers as the origin of short gamma-ray bursts. We perform full general-relativistic simulations of binary neutron-star mergers employing three different nuclear-physics EOSs, considering both equal- and unequal-mass configurations, and adopting a leakage scheme to account for neutrino radiative losses. Using a combination of techniques, we carry out an extensive and systematic study of the hydrodynamical, thermodynamical, and geometrical properties of the matter ejected dynamically, employing the `WinNet` nuclear-reaction network to recover the relative abundances of heavy elements produced by each configurations. Among the results obtained, three are particularly important. First, we find that both the properties of the dynamical ejecta and the nucleosynthesis yields are robust against variations of the EOS and masses, and match very well the observed chemical abundances. Second, using a conservative but robust criterion for unbound matter, we find that the amount of ejected mass is $\lesssim 10^{-3}\,M_{\odot}$, hence at least one order of magnitude smaller than what normally assumed in modelling kilonova signals. Finally, using a simplified and gray-opacity model we assess the observability of the infrared kilonova emission finding, that for all binaries the luminosity peaks around $\sim 1/2$ day in the H-band, reaching a maximum magnitude of -13, and decreasing rapidly after one day. These rather low luminosities make the prospects for detecting kilonovae less promising than what assumed so far.

r-process nucleosynthesis in binary neutron star mergers

Luke Bovard, Dirk Martin, Federico Guercilena, Almudena Arcones, Luciano Rezzolla and Oleg Korobkin

arXiv:1709.09630v1 [gr-qc] 27 Sep 2017

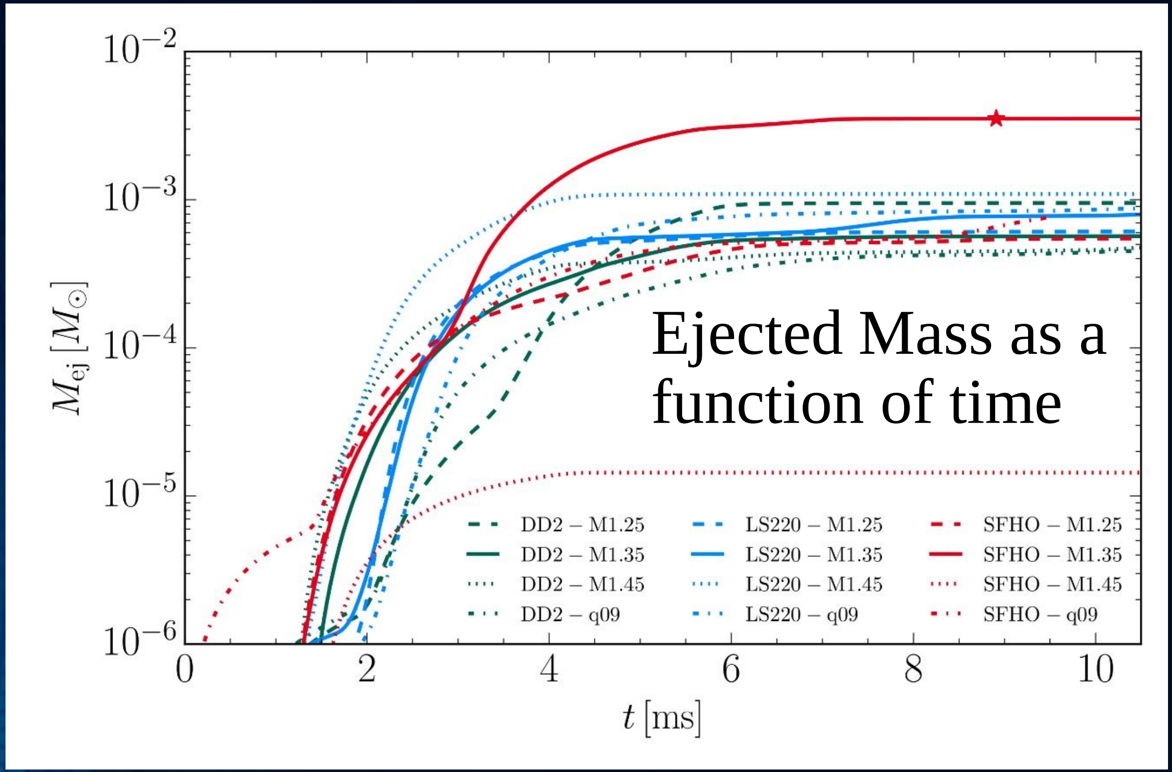

Simulation of the relative abundances of heavy elements produced in a binary neutron star merger.

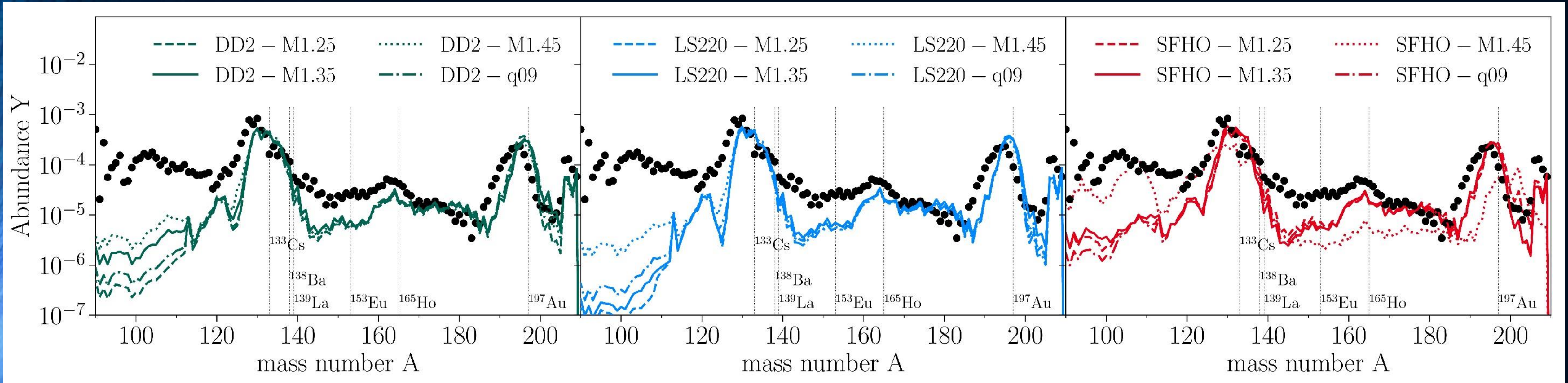

The Origin of the Solar System Elements

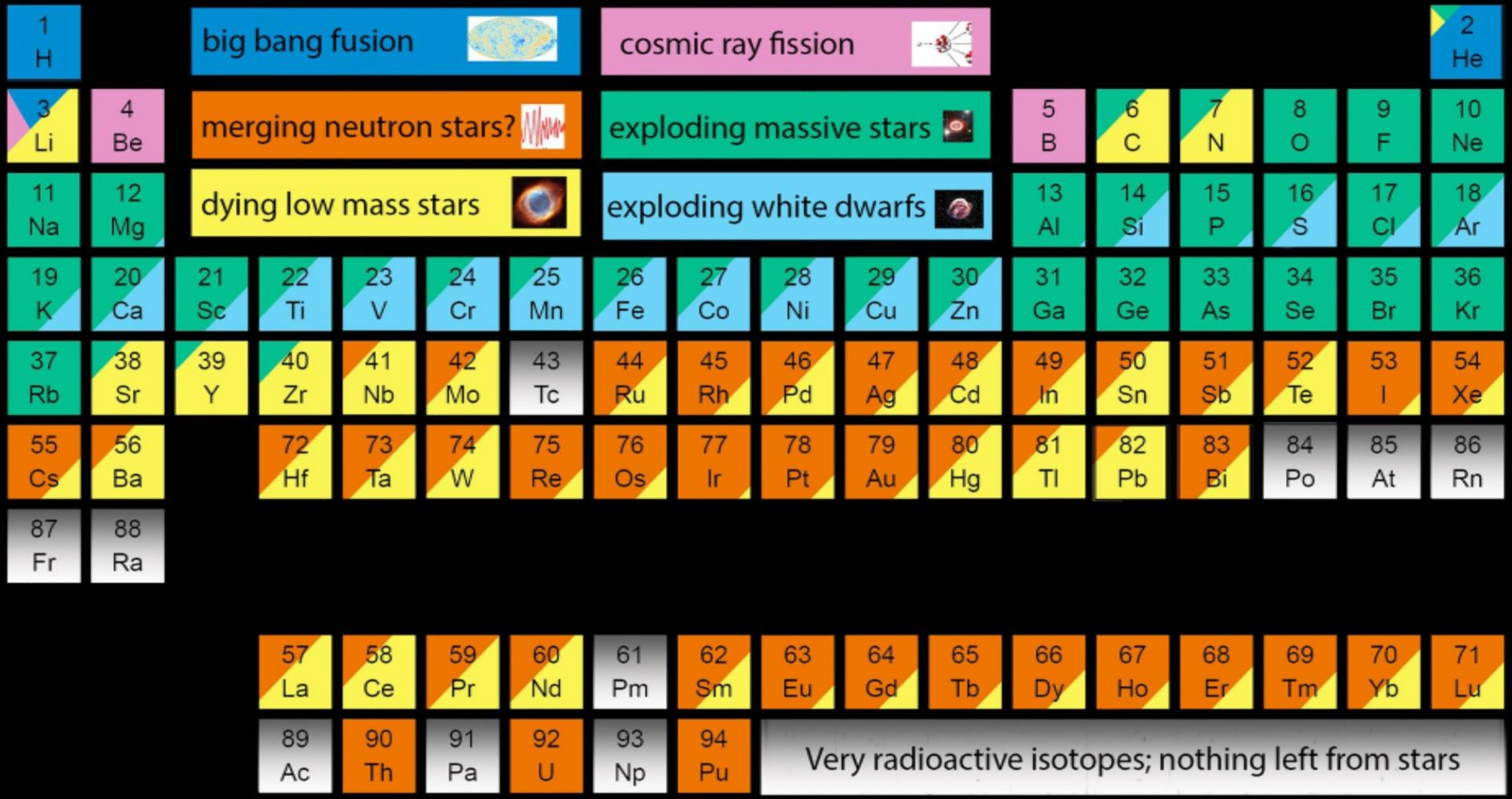

Graphic created by Jennifer Johnson
http://www.astronomy.ohio-state.edu/~jaj/nucleo/

Astronomical Image Credits:
ESA/NASA/AASNova

Summary

- On August 17, 2017, a long-awaited event has taken place: the Advanced LIGO and Virgo gravitational-wave detectors have recorded the signal from the inspiral and merger of a binary neutron-star system.
- The analysis of the gravitational wave data in combination with the independently detected gamma-ray burst and electromagnetic counterpart results in a neutron star merger scenario which is in good agreement with numerical simulations of binary neutron star mergers performed in full general relativity.
- During the late post-merger simulation, the value of central rest-mass density will reach extreme values and it is expected that a hadron-quark phase transition will be present in the interior region of the HMNS.
- Astrophysical observables of the hadron-quark phase transition may be detectable when advanced gravitational wave detectors reach design sensitivity or with next-generation detectors.

Additional Slides

Head-On Collision of Neutron Stars

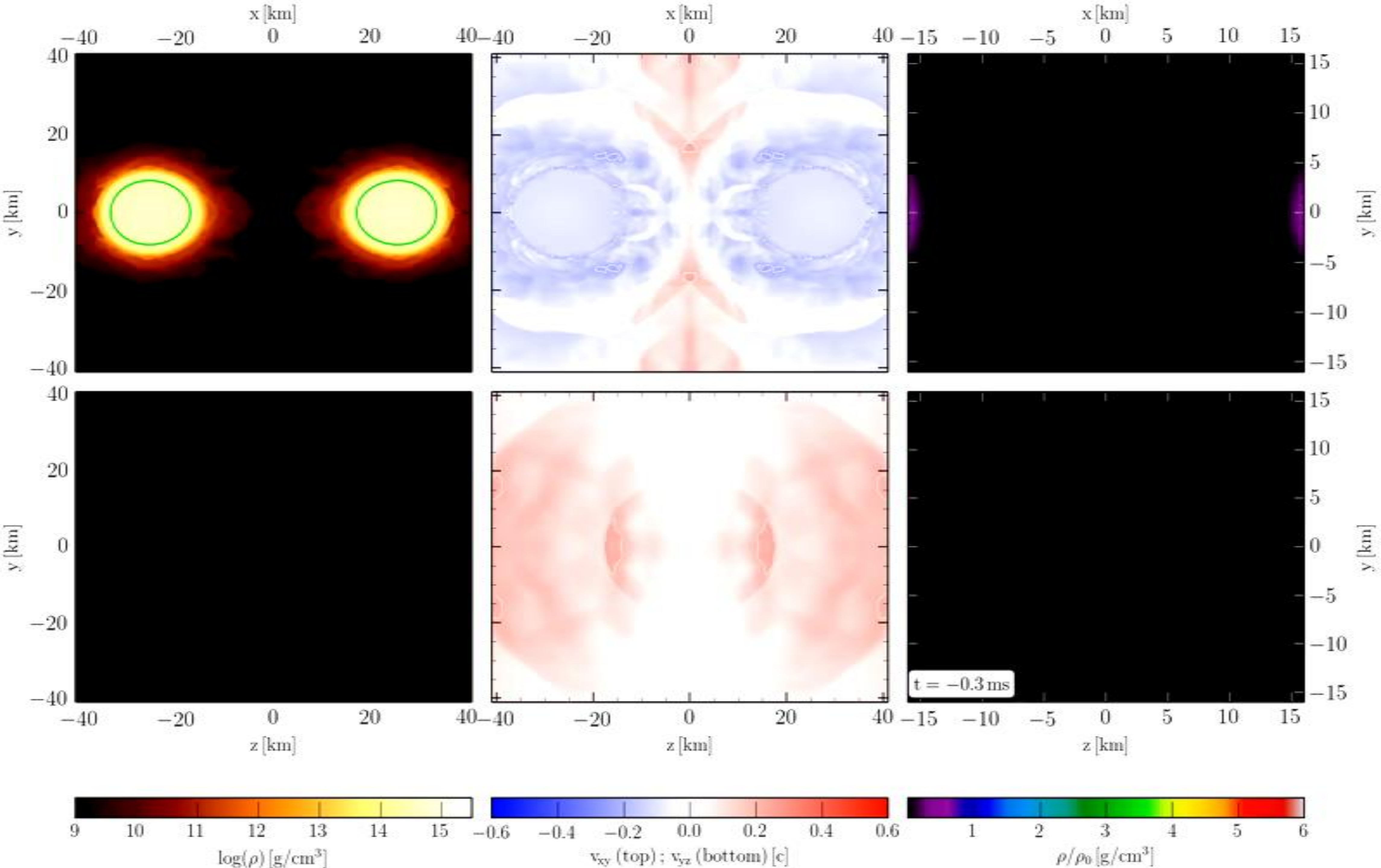

Head-On Collision of Hybrid Stars

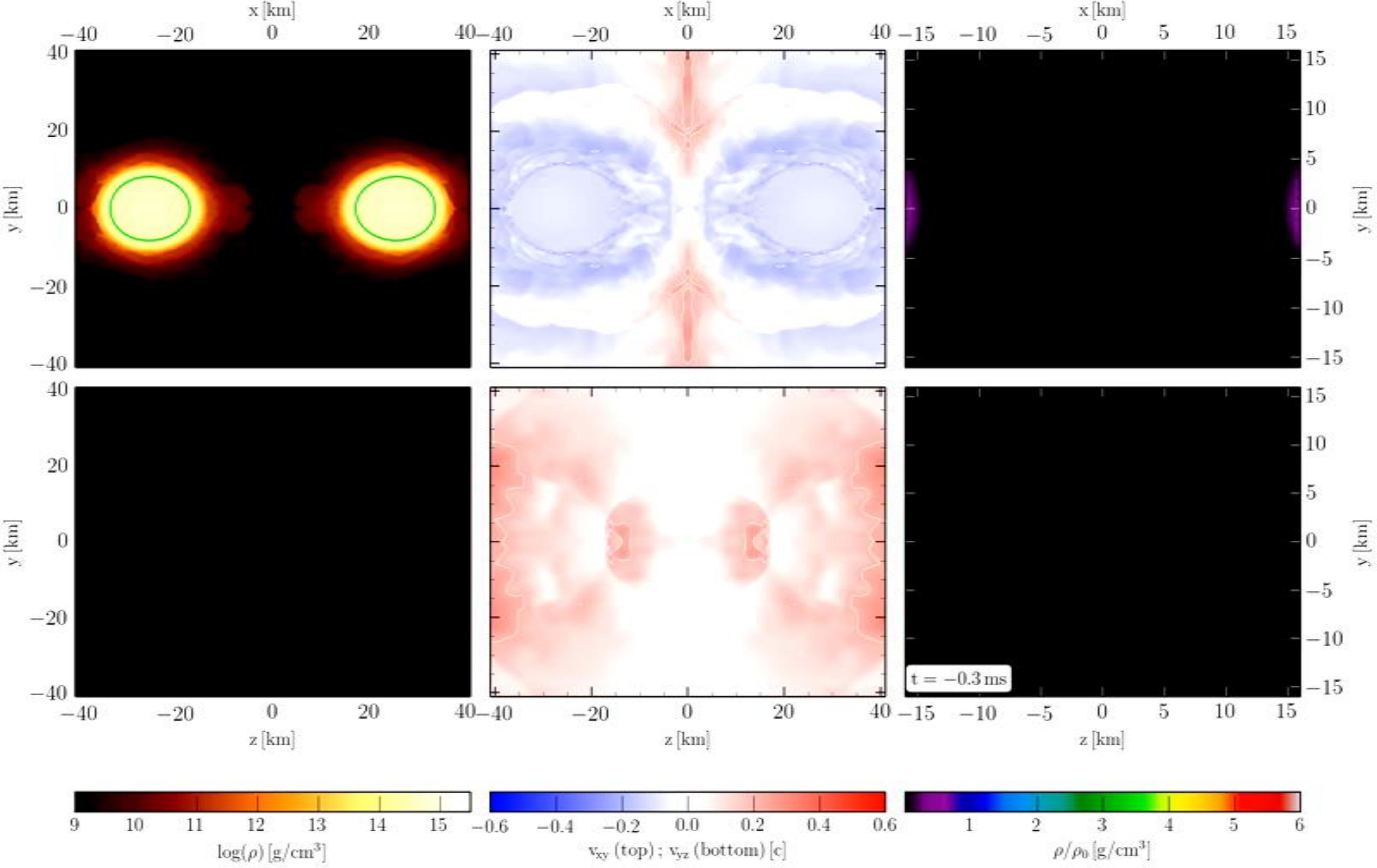

Head-On Collission Comparisson: Neutron Stars - Hybrid Stars

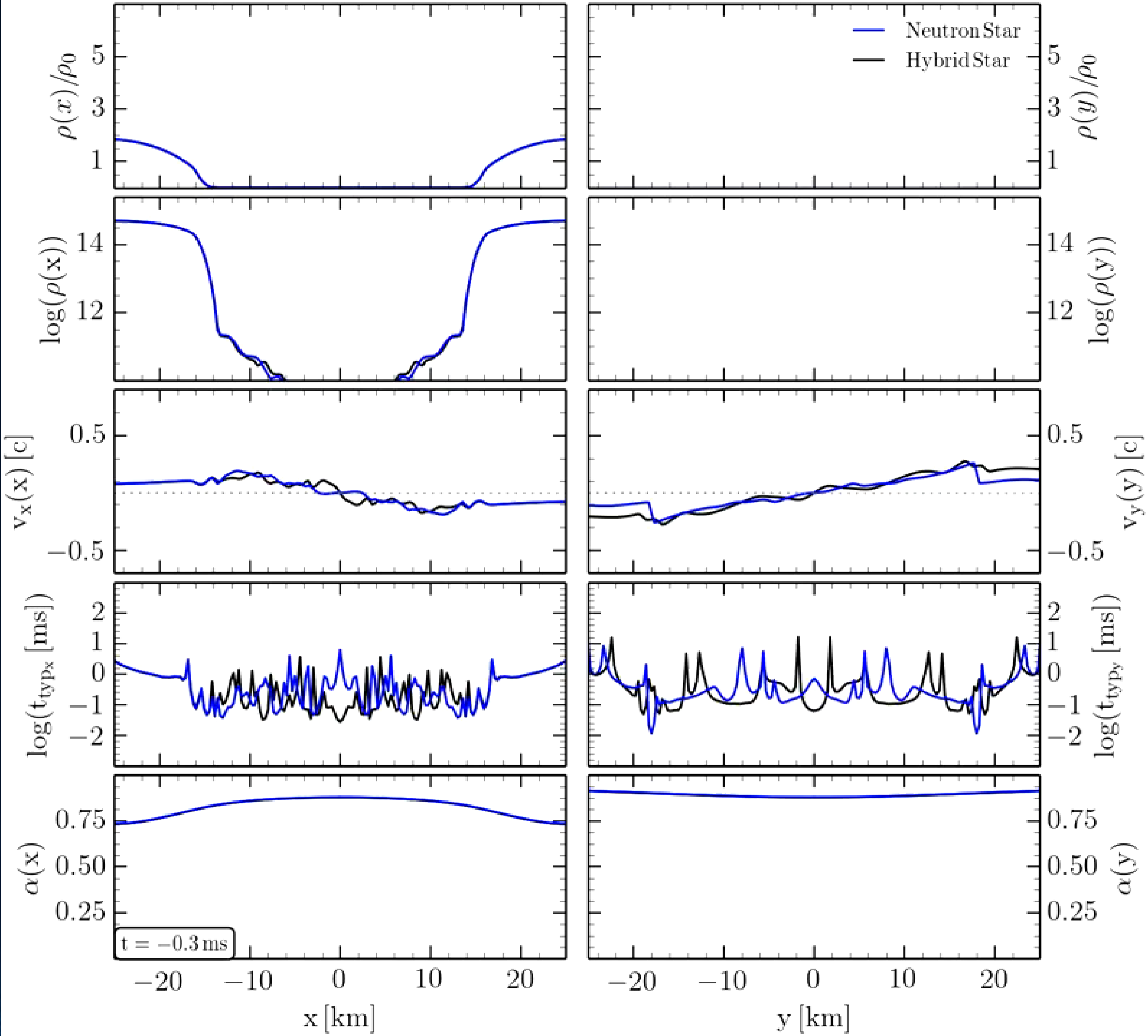

Der Hadron-Quark Phasenübergang

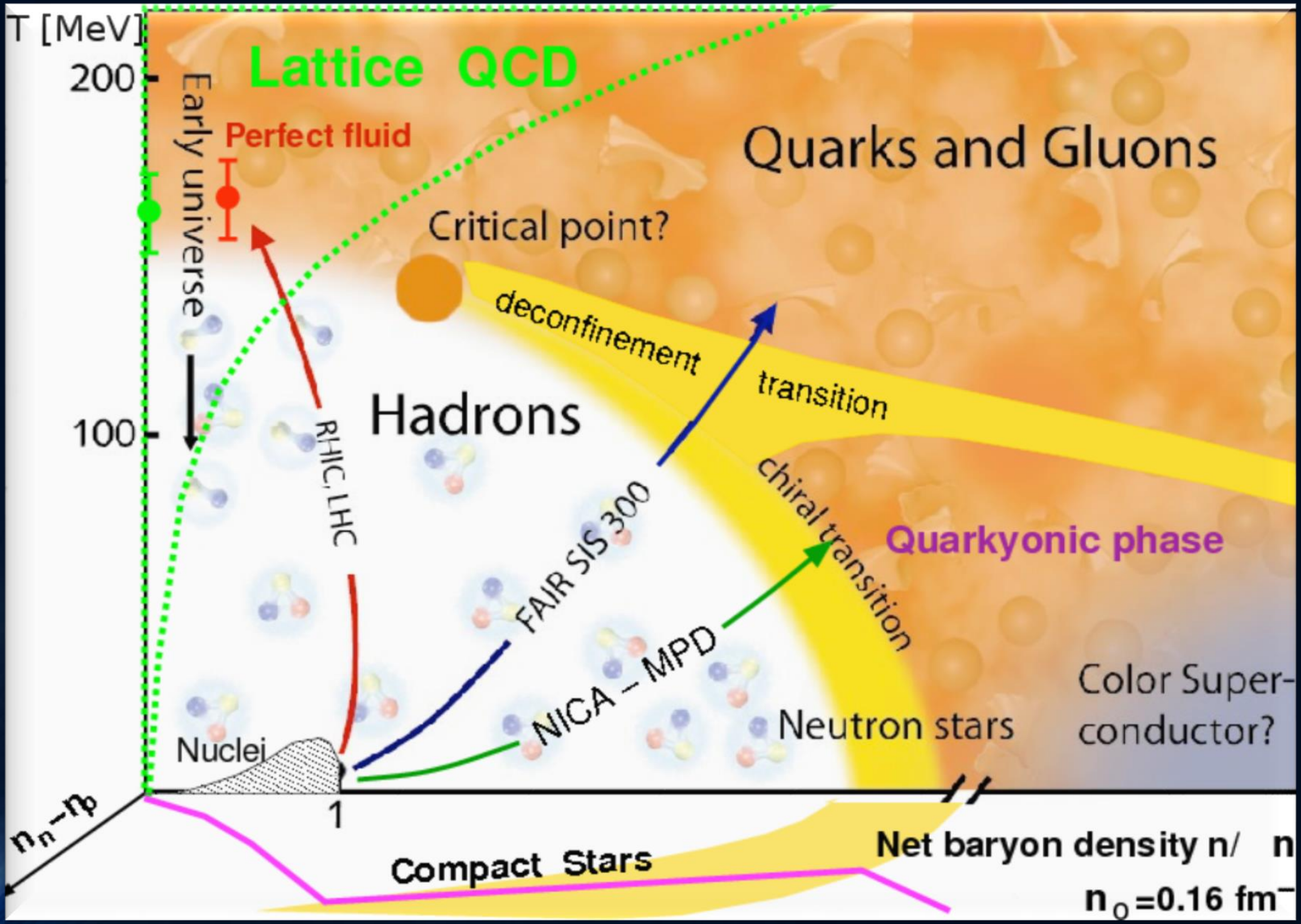

Credits to http://inspirehep.net/record/823172/files/phd_qgp3D_quarkyonic2.png

Neutronensterne, Hybride Sterne, Quarksterne und Schwarze Löcher

Bei welcher Dichte der Phasenübergang zum Quark-Gluon-Plasma einsetzt und welche Eigenschaften dieser Übergang im Detail hat ist weitgehend unbekannt.

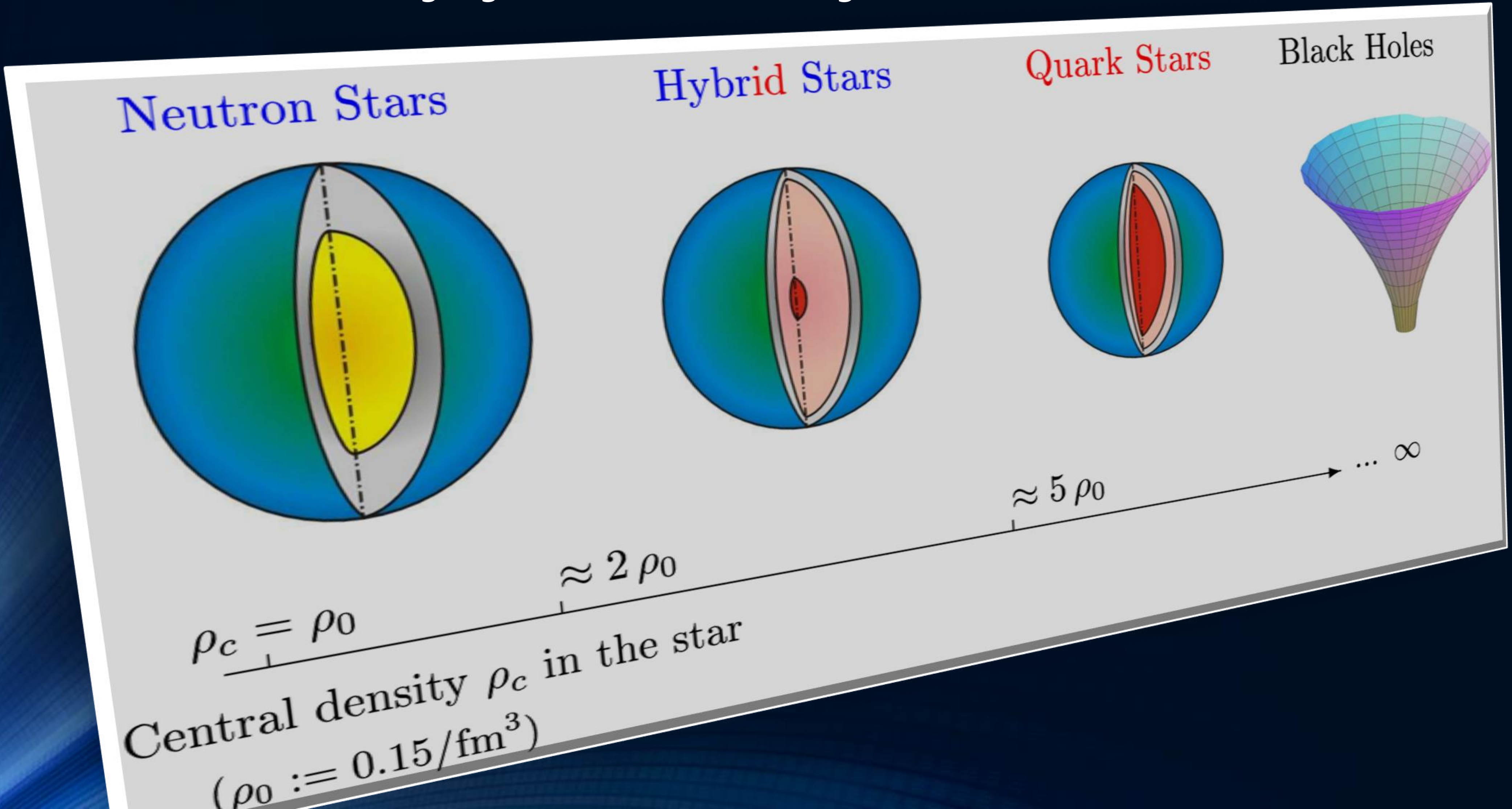

Die Bildung des Ereignishorizontes des Schwarzen Lochs und die Befreiung der elementaren Materie

Die vergessenen Tänze der späten Tango-Phase

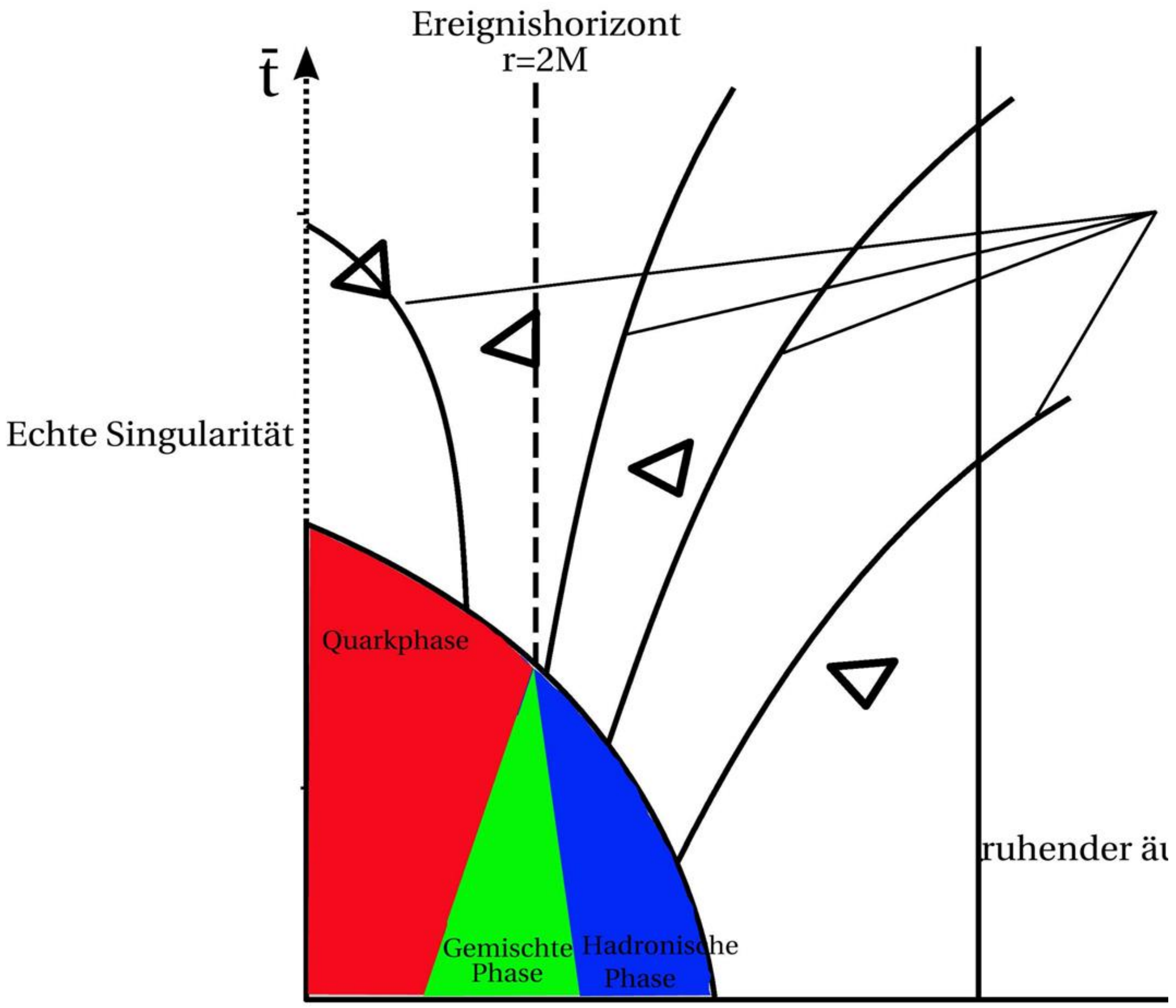

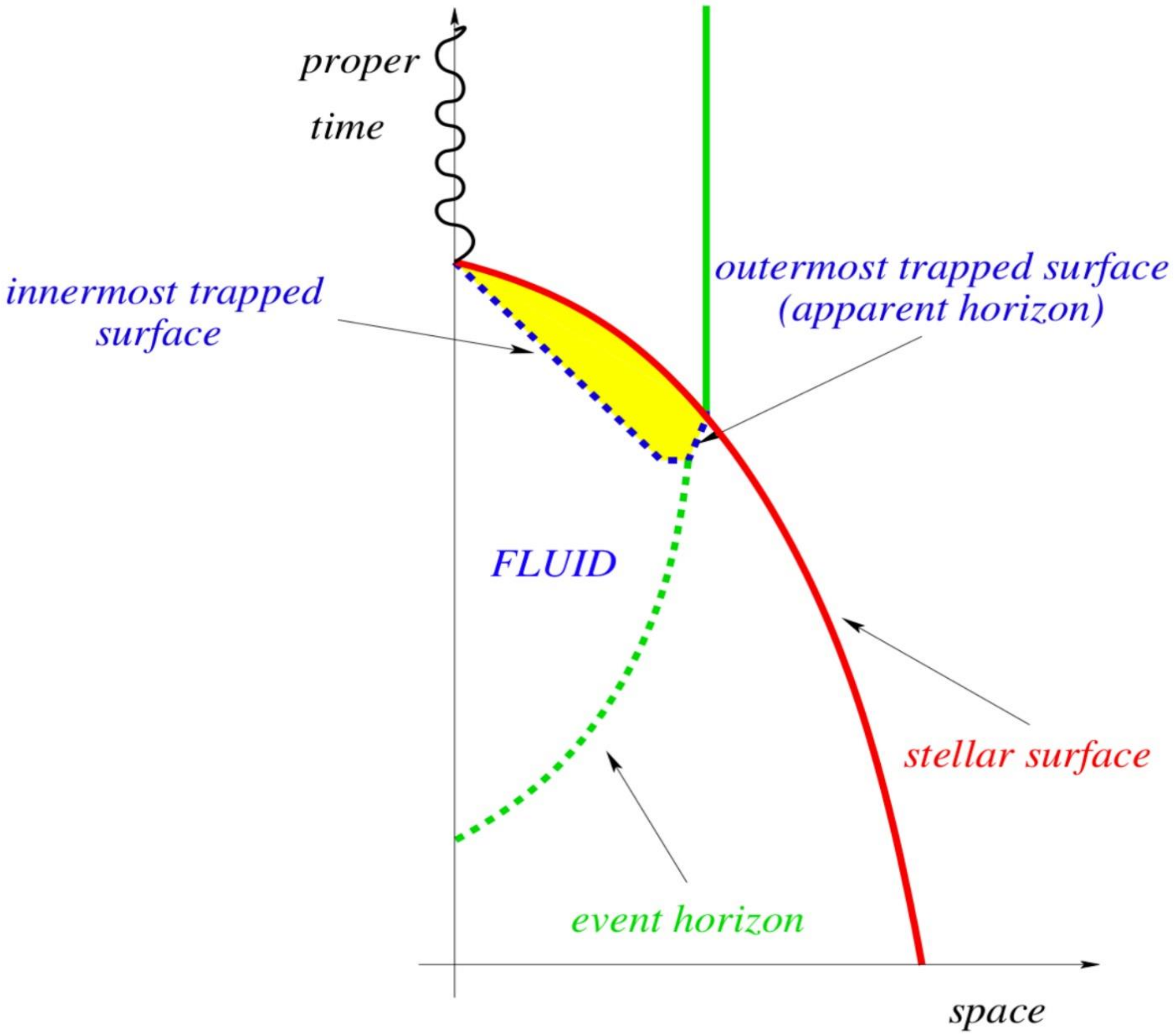

HMNS Evolution for different EoSs

Low mass simulations (M=1.32 Msolar)

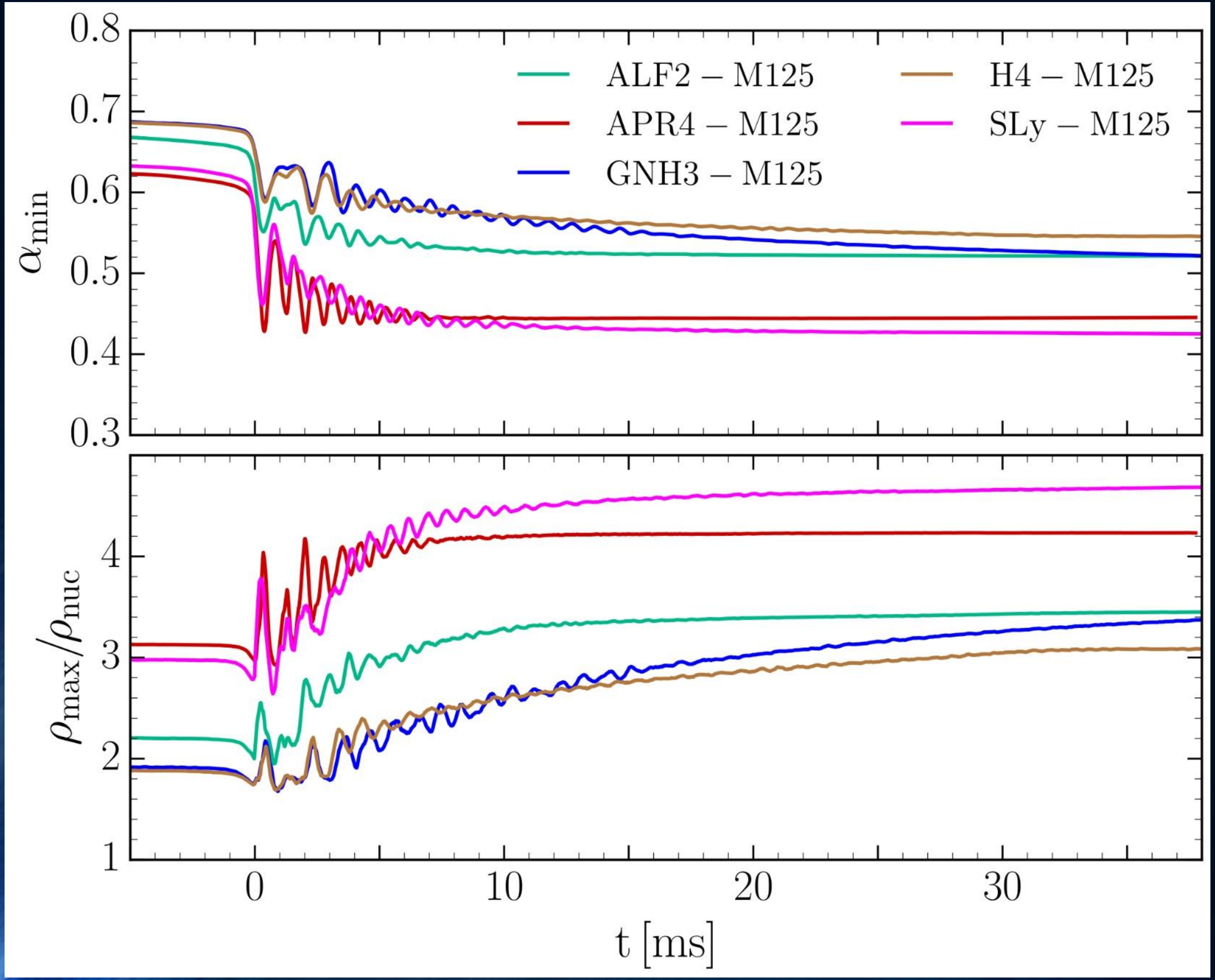

Central value of the lapse function α_c (upper panel) and maximum of the rest mass density ρ_{max} in units of ρ_0 (lower panel) versus time for the low mass simulations.

Time dependence of the Rotation Profile

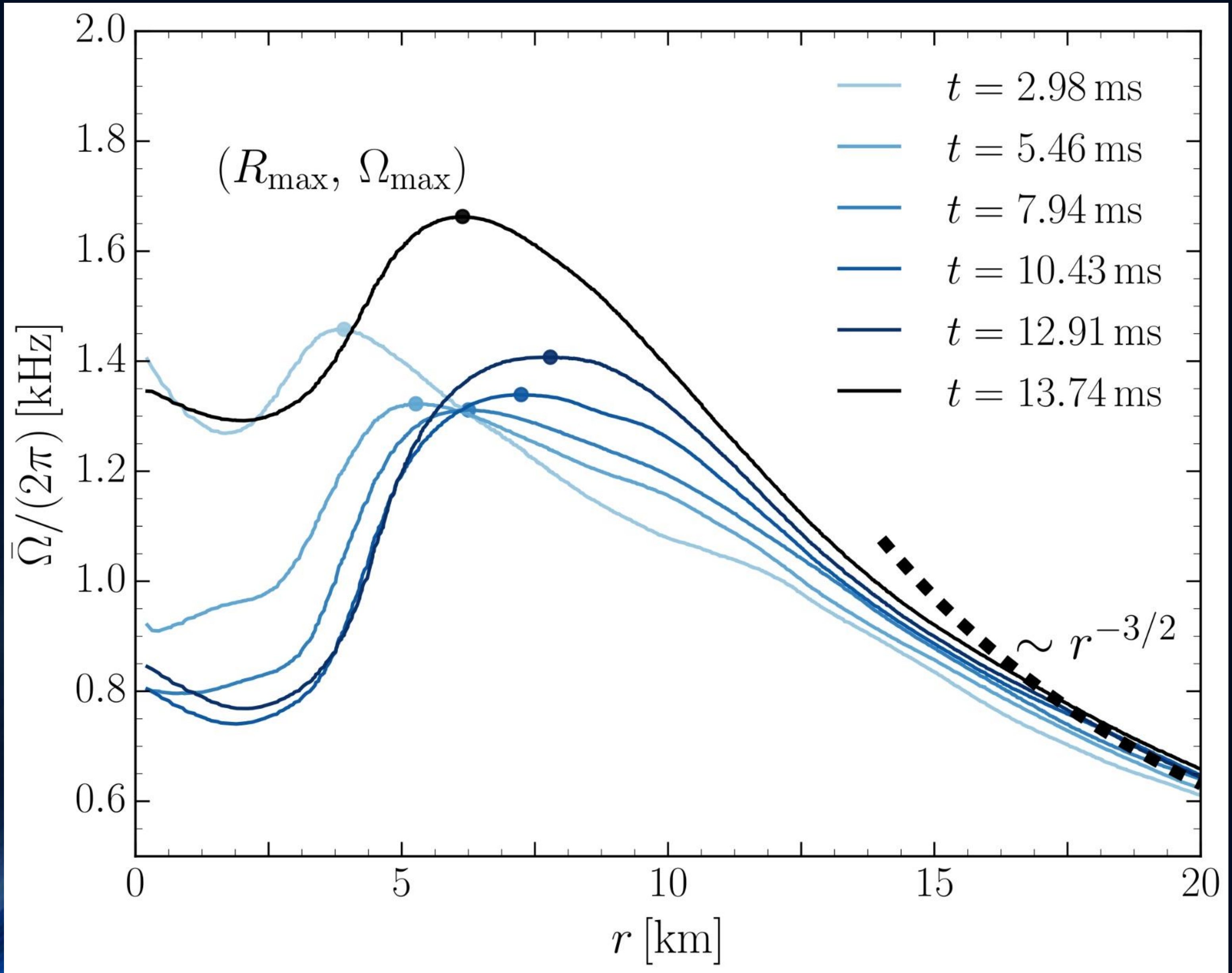

Averaged fluid angular velocity on the equatorial plane for the ALF2-M135 binary as averaged at different times and with intervals of length t = 1 ms.

Spectral Properties of GWs

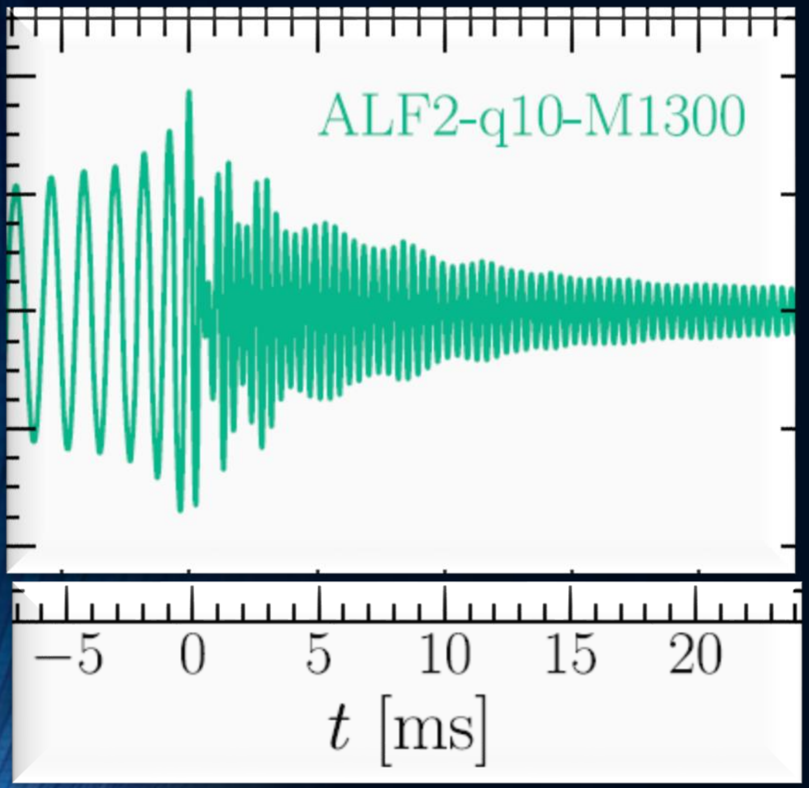

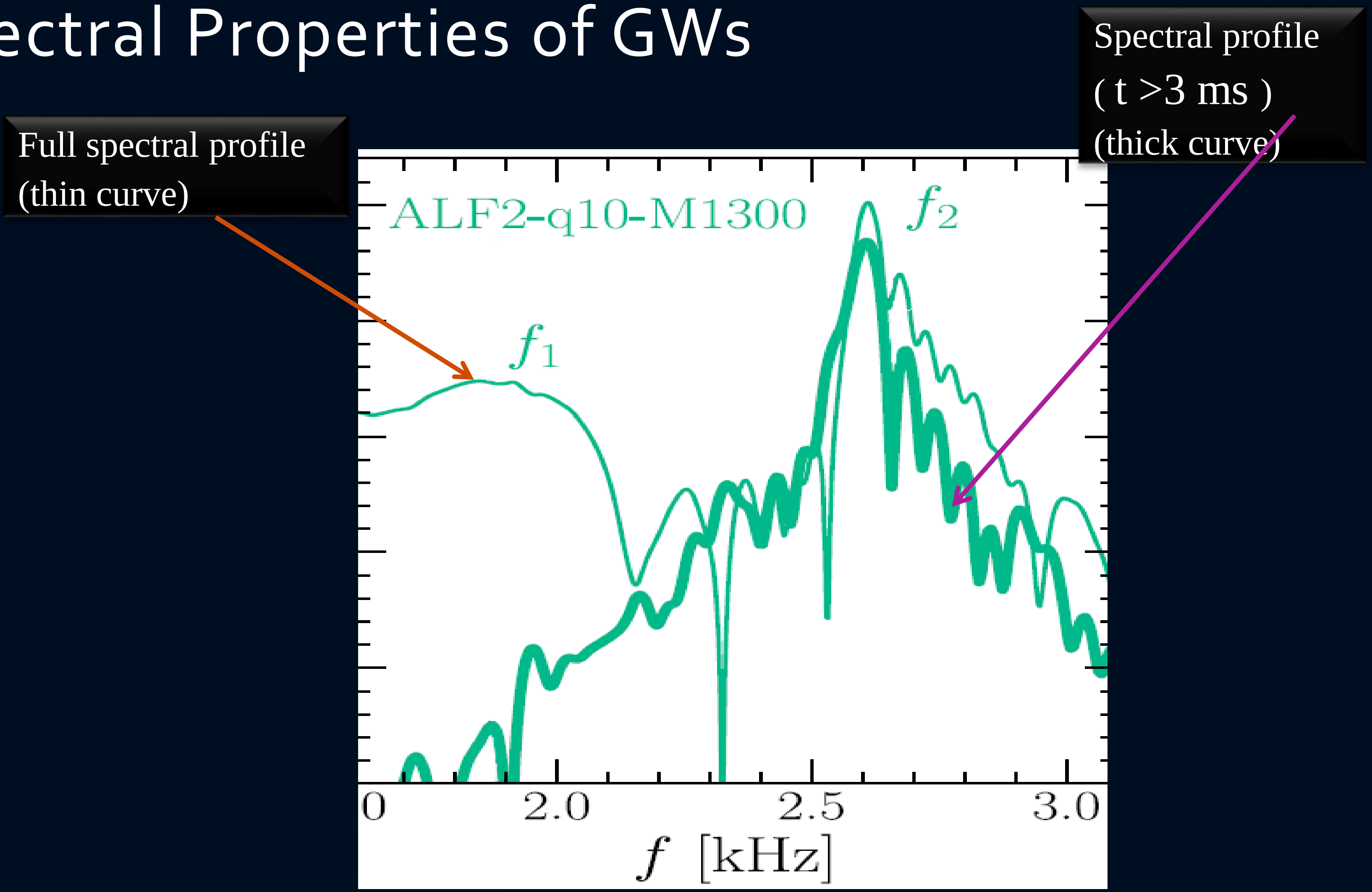

Two characteristic GW frequency peaks (f_1 and f_2);

the origin of f_1 comes from t<3 ms. By measuring M, f_1 and f_2 one can set high constraints on the EoS.

"Spectral properties of the post-merger gravitational-wave signal from binary neutron stars",
Kentaro Takami, Luciano Rezzolla, and Luca Baiotti, PHYSICAL REVIEW D 91, 064001 (2015)

Gravitational Waves and the Maximum of the Rotation Profile

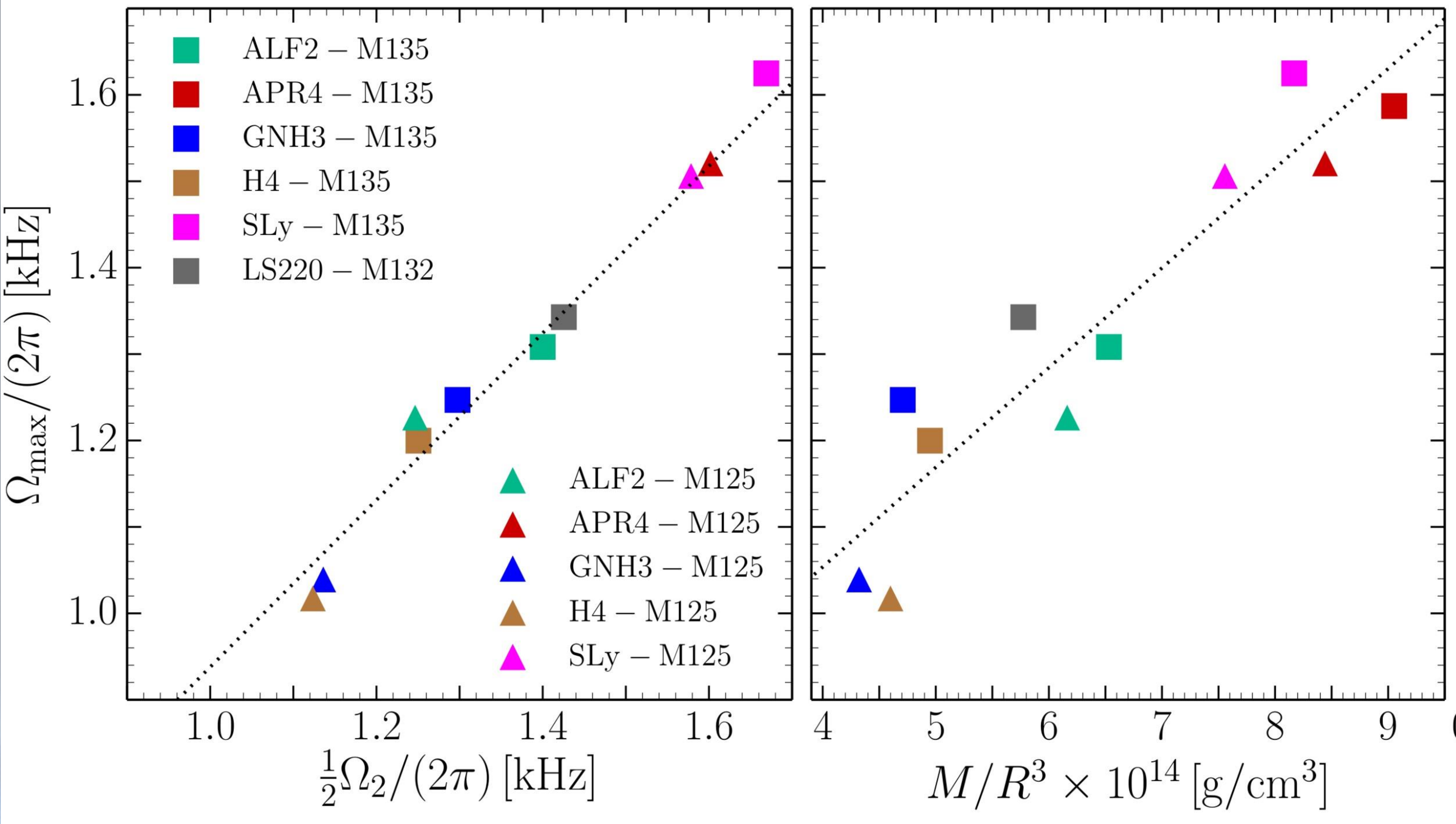

Universal Behavior of f_1 and f_{max}

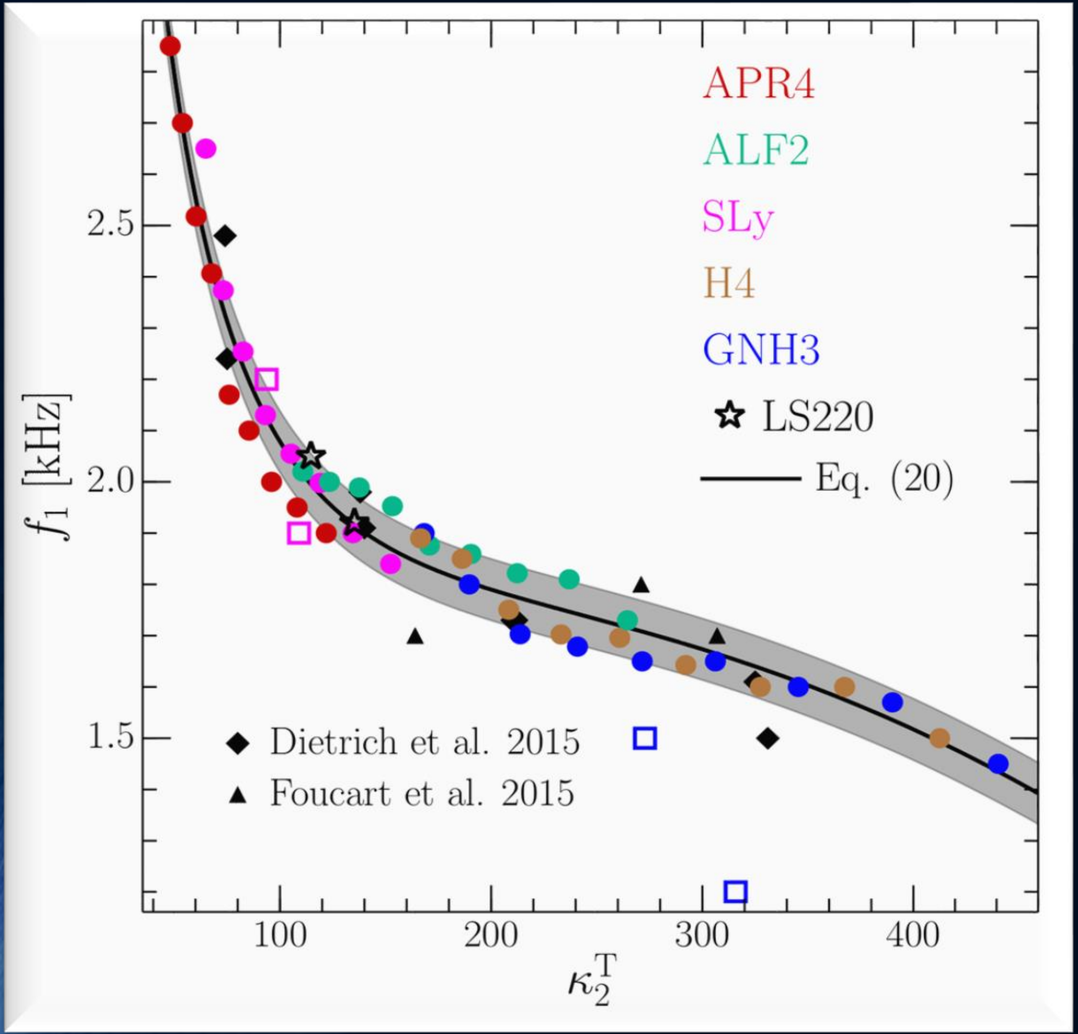

Values of the low-frequency peaks f_1 shown as a function of the tidal deformability parameter κ^T_2.

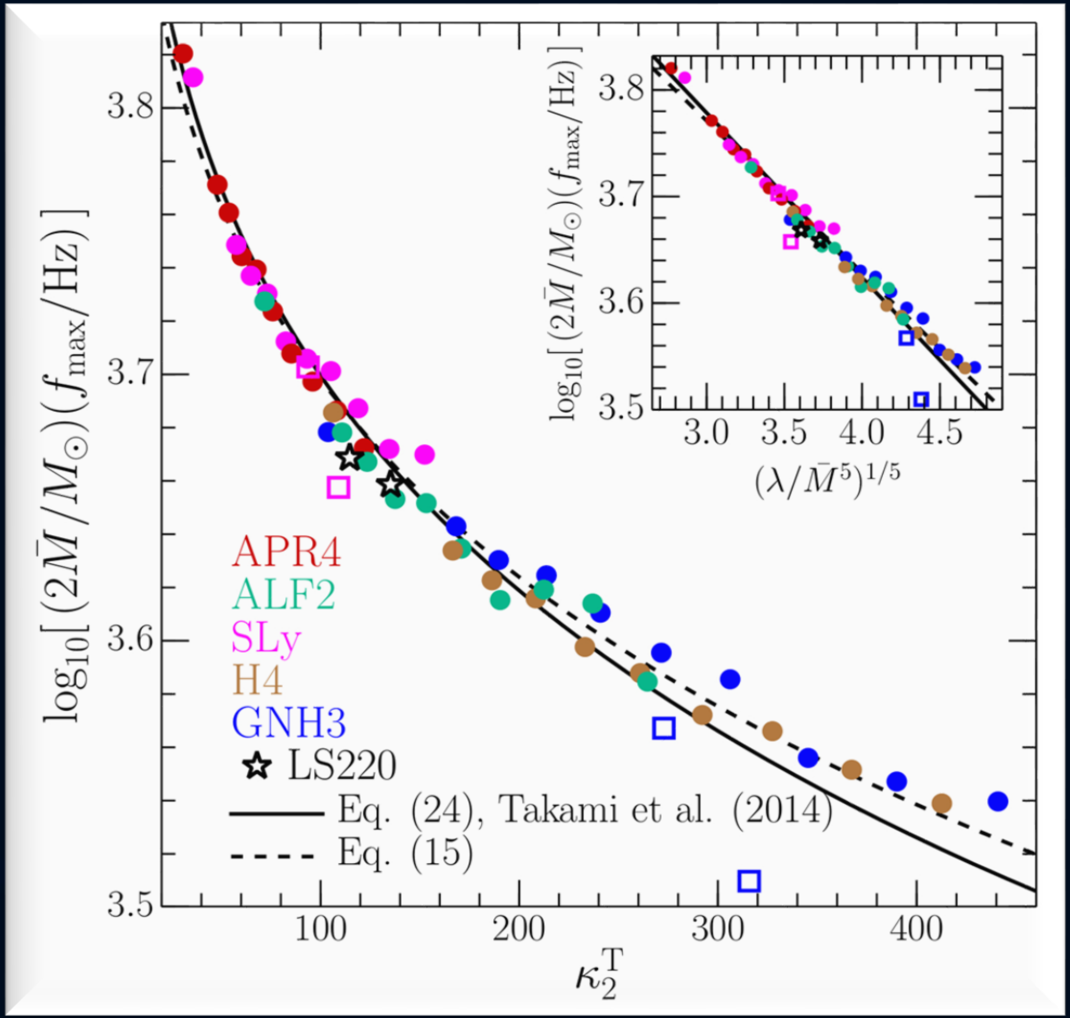

Mass-weighted frequencies at amplitude maximum f_{max} shown as a function of the tidal deformability parameter κ^T_2.

Evolution of the rest-mass density distribution

ALF2, High mass model: Mixed phase region starts at $3\rho_0$,initial NS mass: 1.35 M_{solar}

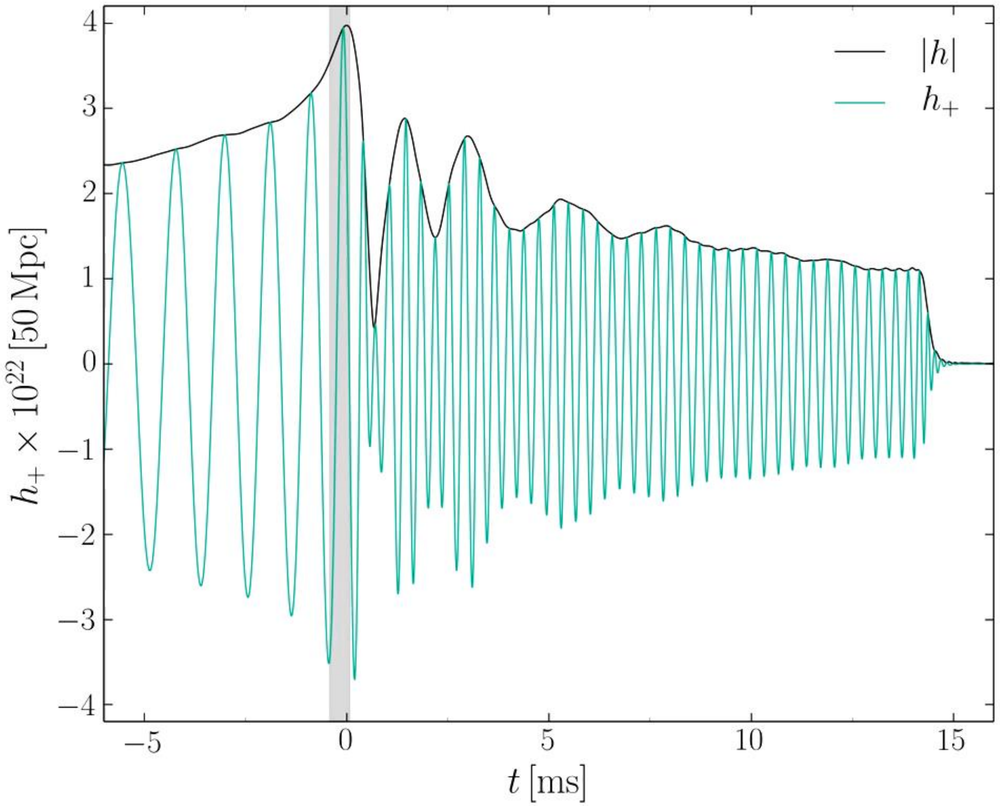

Gravitational wave amplitude
at a distance of 50 Mpc

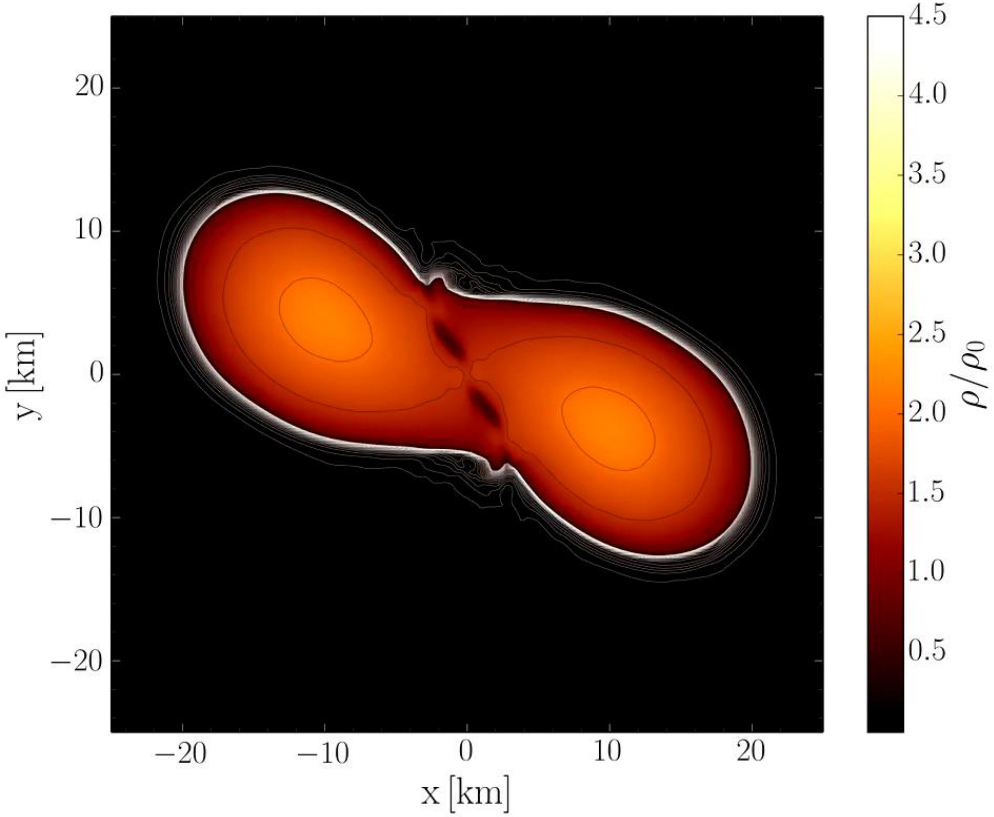

Rest mass density distribution ρ(x,y)
in the equatorial plane
in units of the nuclear matter density ρ_0

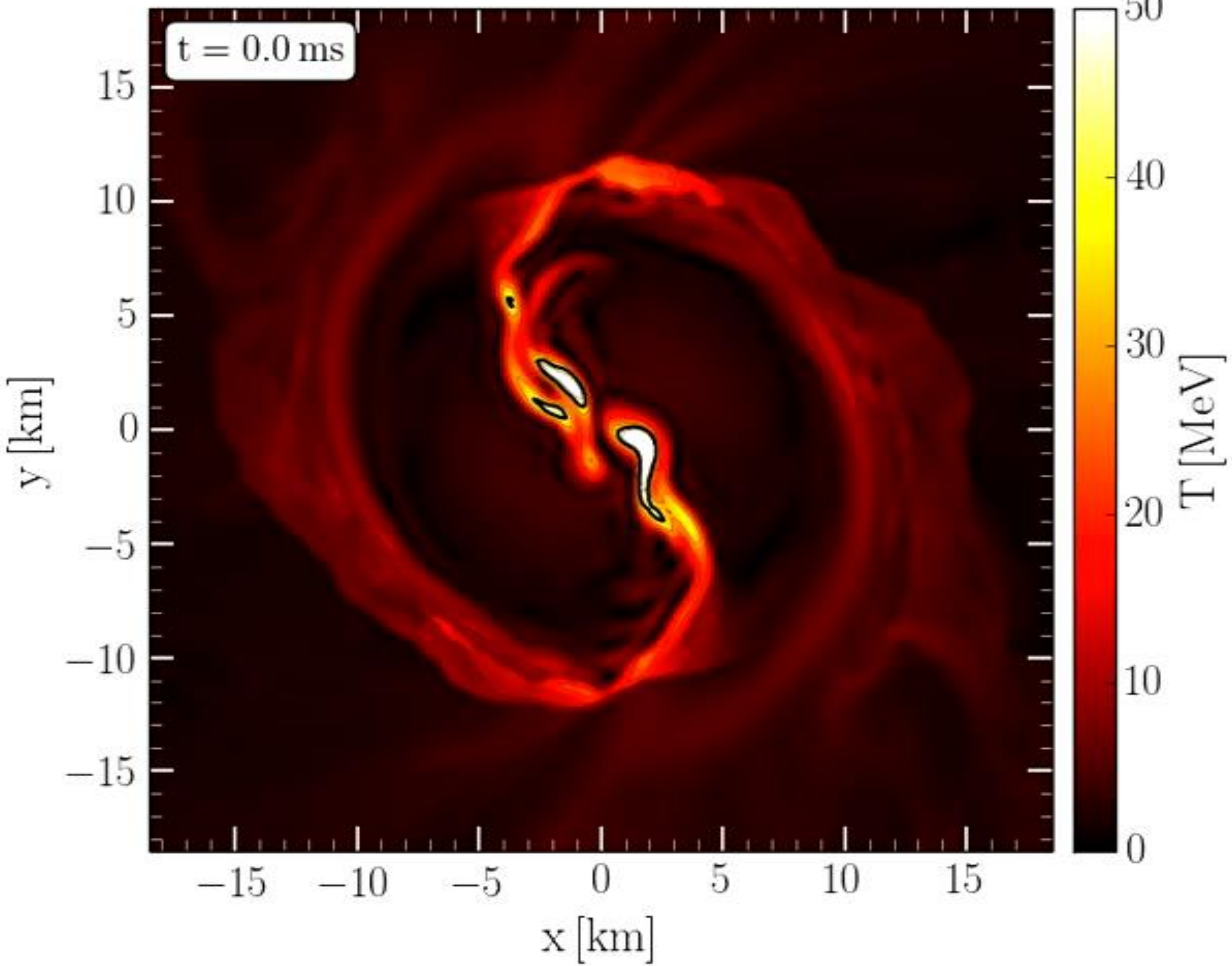
t = 0.0 ms
y [km]
x [km]
T [MeV]
15
10
5
0
−5
−10
−15
50
40
30
20
10

Millisecond and Second Pulsars

PSR B0531+21 (33.5 ms)
Crab Pulsar

PSR B0329+54 (0.715 s)

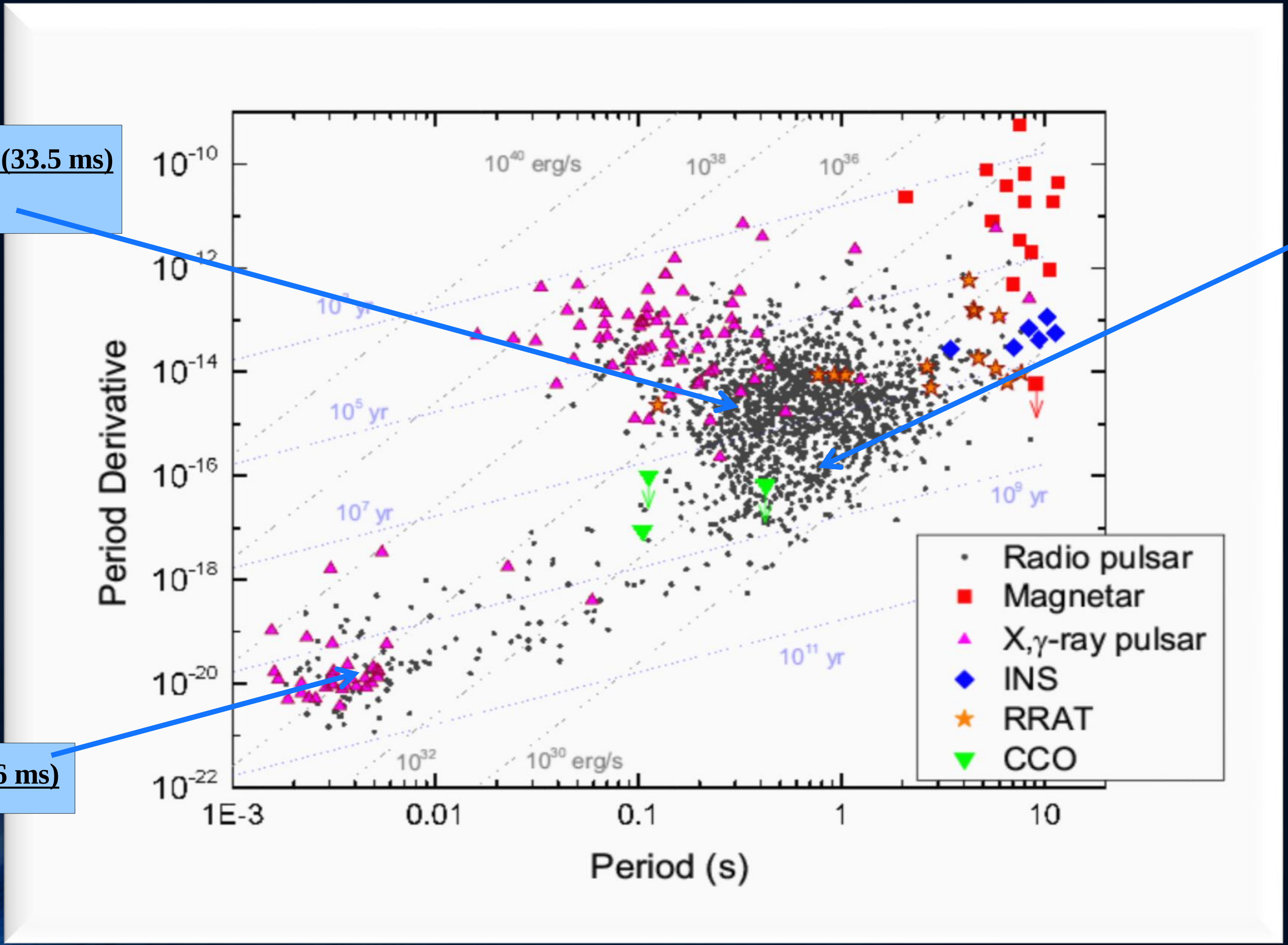

PSR B1937+21 (1.56 ms)

Binary Neutron Star Systems

Kramer, Wex, Class. Quantum Grav. 2009

The **Double Pulsar** (PSR J0737-3039A/B):
Observed in 2003
Eccentricity: 0.088
Pulsar A: P=23 ms, M=1.3381(7)
Pulsar B: P=2.7 s, M=1.2489(7)
Only separated 800,000 km from each other
Orbital period: 147 Minuten
Pulsar A is eclipsed by Pulsar B
(30 s for each orbit)

Distance shrinks
due to Gravitational Wave emission
→ They will collide in 85 Million Years!

McGill NCS Multimedia Services Animation by Daniel Cantin, DarwinDimensions)

GW170817, GRB170817A Localisation and unusual dimness

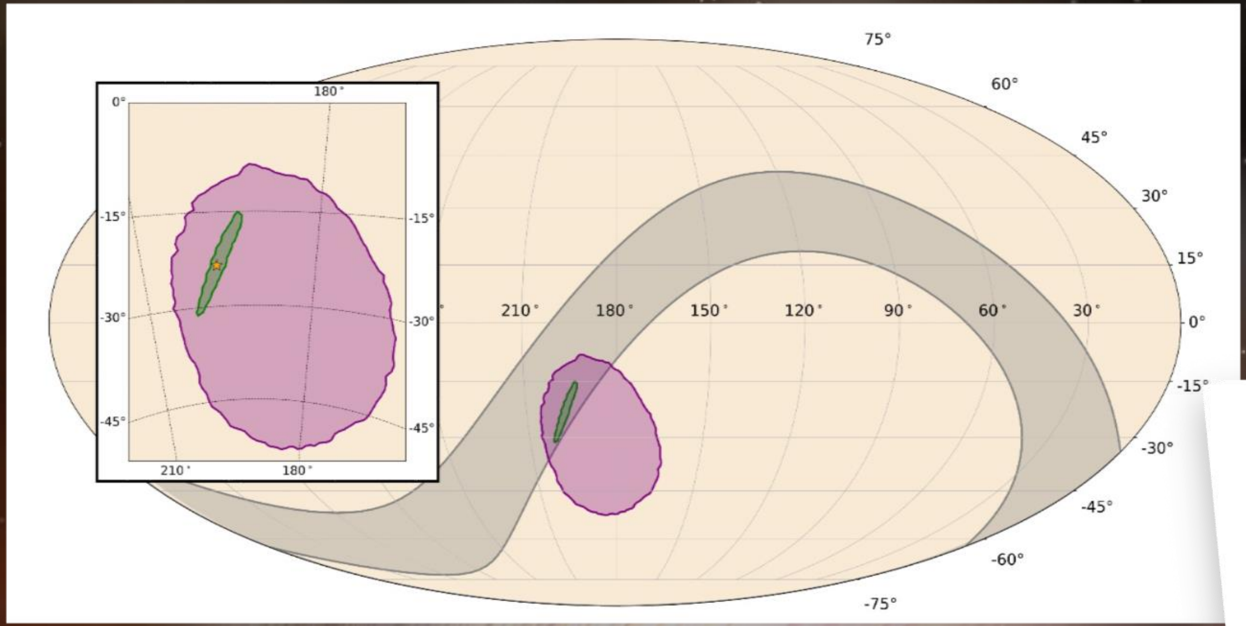

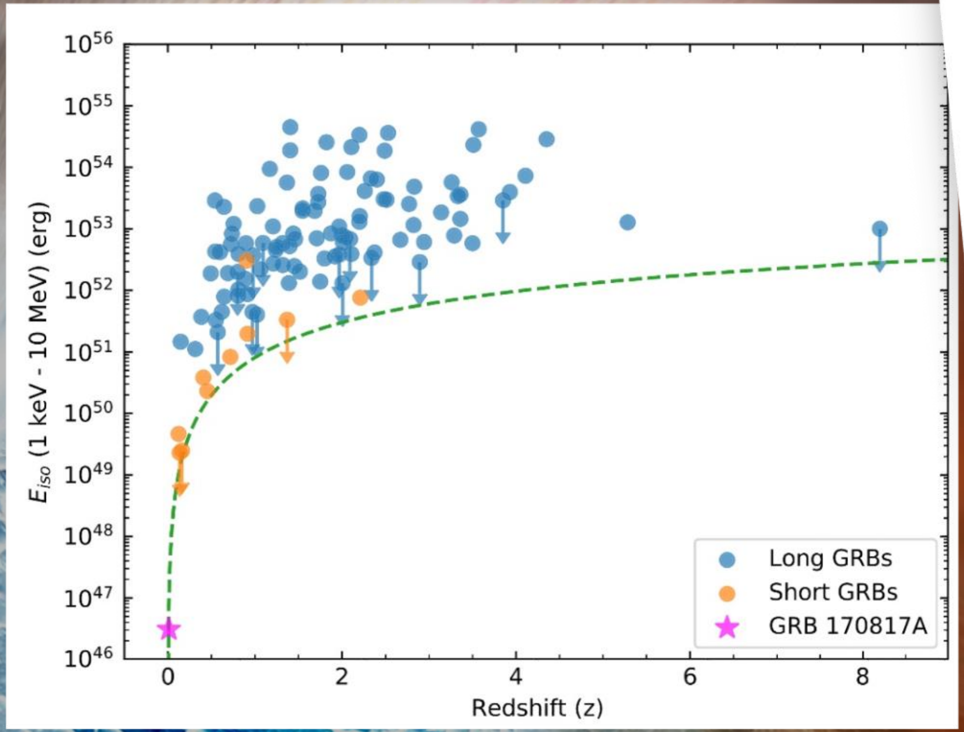

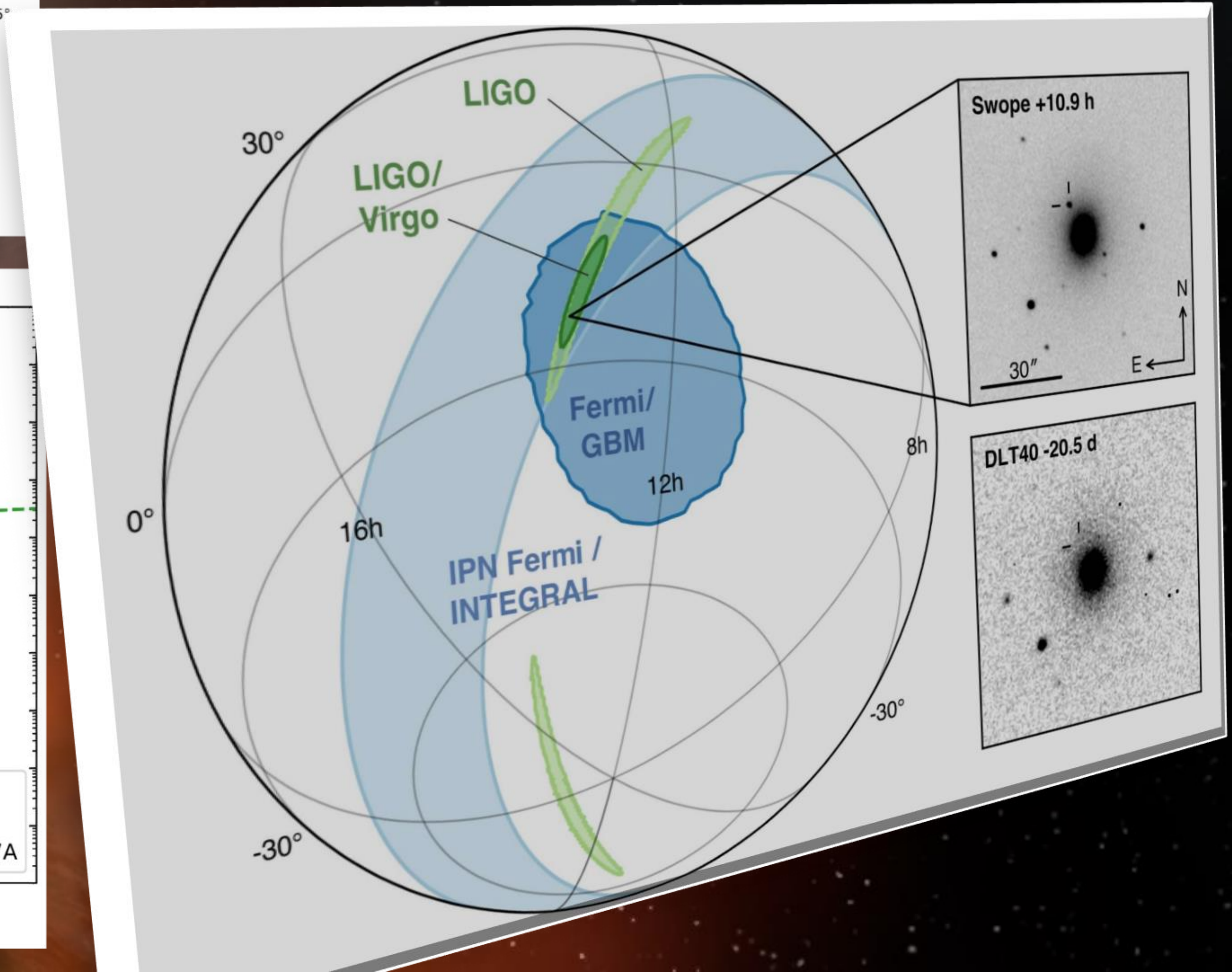

GW170817

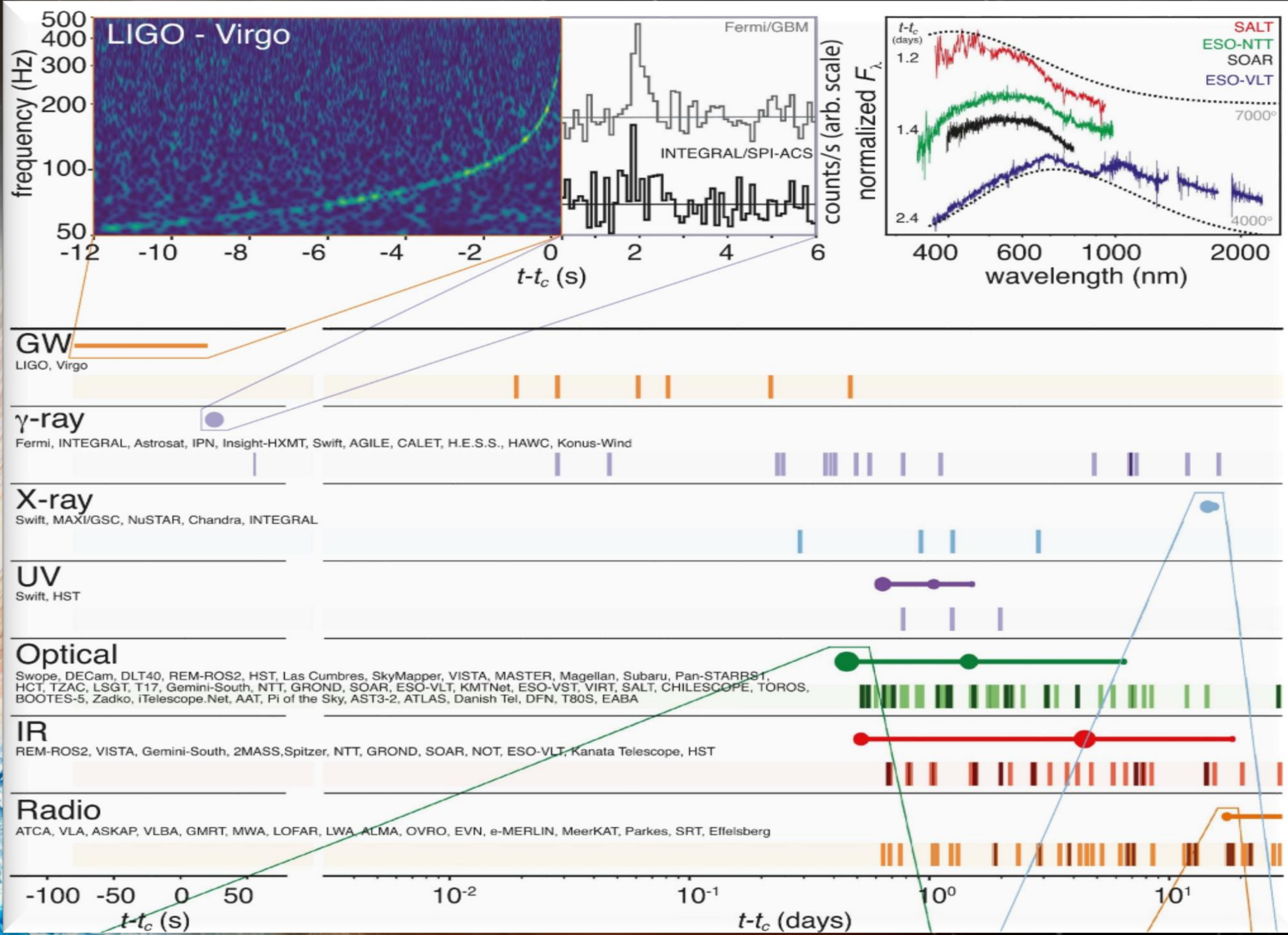
LIGO - Virgo
frequency (Hz)
Fermi/GBM
INTEGRAL/SPI-ACS
counts/s (arb. scale)
t-tc (s)
normalized Fλ
SALT
ESO-NTT
SOAR
ESO-VLT
wavelength (nm)
GW
LIGO, Virgo
γ-ray
Fermi, INTEGRAL, Astrosat, IPN, Insight-HXMT, Swift, AGILE, CALET, H.E.S.S., HAWC, Konus-Wind
X-ray
Swift, MAXI/GSC, NuSTAR, Chandra, INTEGRAL
UV
Swift, HST
Optical
Swope, DECam, DLT40, REM-ROS2, HST, Las Cumbres, SkyMapper, VISTA, MASTER, Magellan, Subaru, Pan-STARRS1, HCT, TZAC, LSGT, T17, Gemini-South, NTT, GROND, SOAR, ESO-VLT, KMTNet, ESO-VST, VIRT, SALT, CHILESCOPE, TOROS, BOOTES-5, Zadko, iTelescope.Net, AAT, Pi of the Sky, AST3-2, ATLAS, Danish Tel, DFN, T80S, EABA
IR
REM-ROS2, VISTA, Gemini-South, 2MASS, Spitzer, NTT, GROND, SOAR, NOT, ESO-VLT, Kanata Telescope, HST
Radio
ATCA, VLA, ASKAP, VLBA, GMRT, MWA, LOFAR, LWA, ALMA, OVRO, EVN, e-MERLIN, MeerKAT, Parkes, SRT, Effelsberg
t-tc (s)
t-tc (days)

EOSs

Several different EOSs : ALF2, APR4, GNH3, H4 and Sly, approximated by piecewise polytopes. Thermal ideal fluid component (Γ=2) added to the nuclear-physics EOSs.

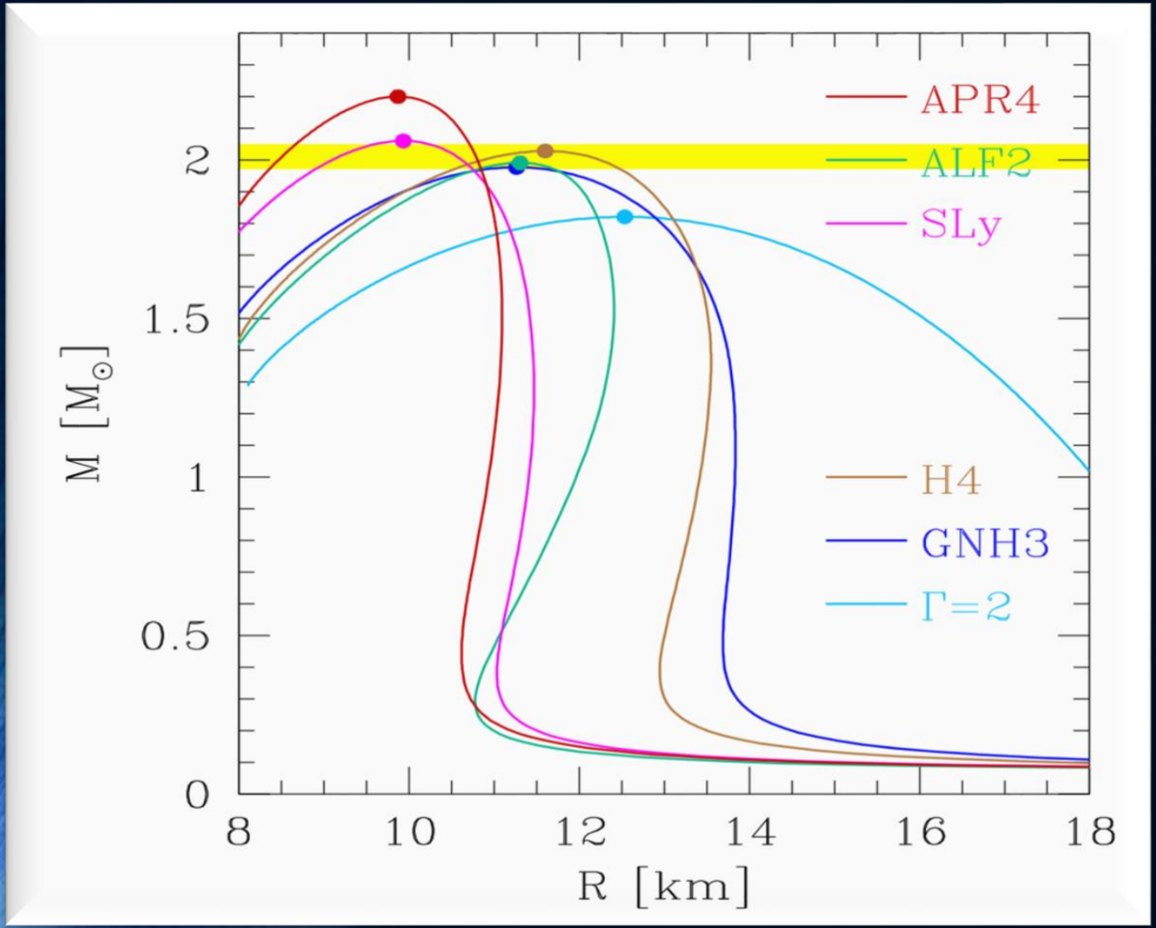

composed of a "cold" nuclear-physics part and of a "thermal" ideal-fluid component[1] [56]

$$p = p_{\rm c} + p_{\rm th}\,, \qquad \epsilon = \epsilon_{\rm c} + \epsilon_{\rm th}\,, \tag{6}$$

where p and ϵ are the pressure and specific internal energy,

The "cold" nuclear-physics contribution to each EOS is obtained after expressing the pressure and specific internal energy $\epsilon_{\rm c}$ in the rest-mass density range $\rho_{i-1} \leq \rho < \rho_i$ as (for details see [36, 64–66])

$$p_{\rm c} = K_i \rho^{\Gamma_i}\,, \qquad \epsilon_{\rm c} = \epsilon_i + K_i \frac{\rho^{\Gamma_i - 1}}{\Gamma_i - 1}\,. \tag{7}$$

($\Gamma_1 = 4.070$ and $\Gamma_2 = 2.411$). Finally, the "thermal" part of the EOS is given by

$$p_{\rm th} = \rho \epsilon_{\rm th} \left(\Gamma_{\rm th} - 1\right)\,, \qquad \epsilon_{\rm th} = \epsilon - \epsilon_{\rm c}\,. \tag{8}$$

where the last equality in (8) is really a definition, since ϵ refers to the computed value of the specific internal energy. In all of the simulations reported hereafter we use $\Gamma_{\rm th} = 2.0$

Additionally LS220-EOS used: Density and Temperature dependent EOS-table (Lattimer-Swesty)

Three (maybe four) GWs from BH-Mergers detected

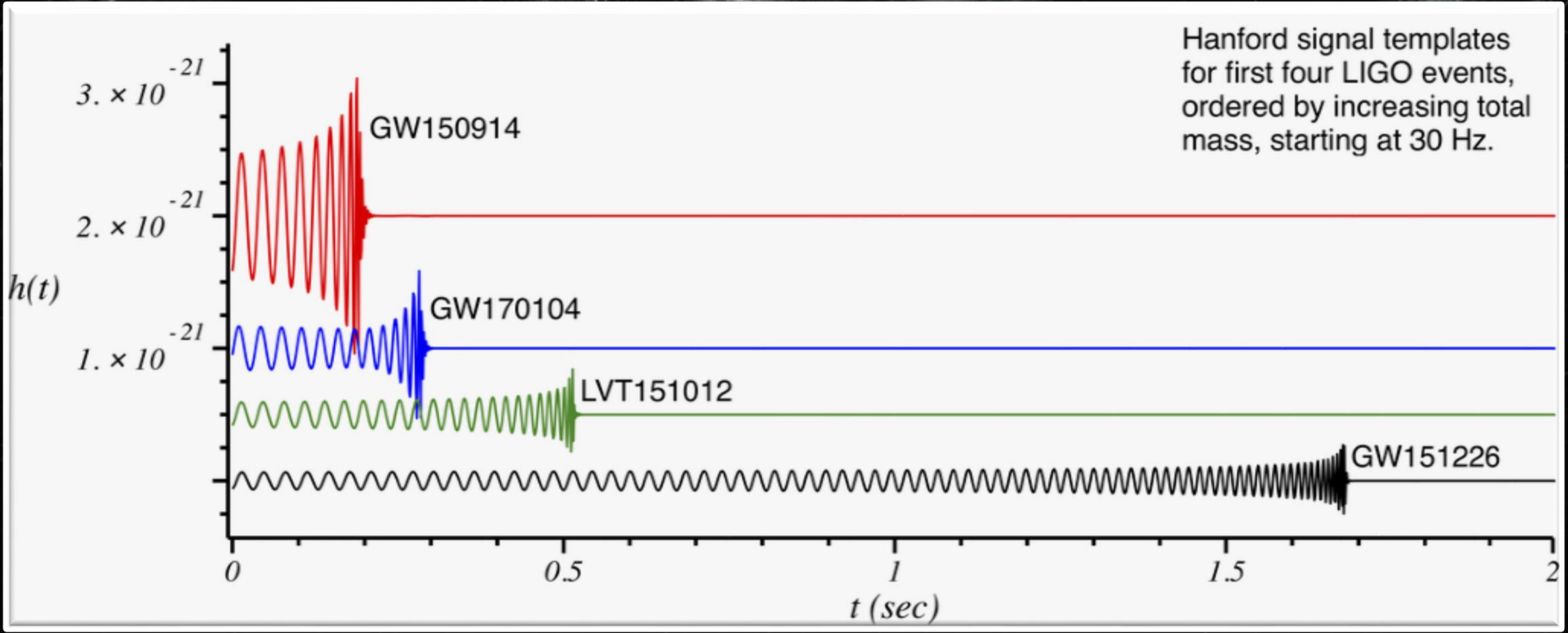

Averaging Procedure for Ω

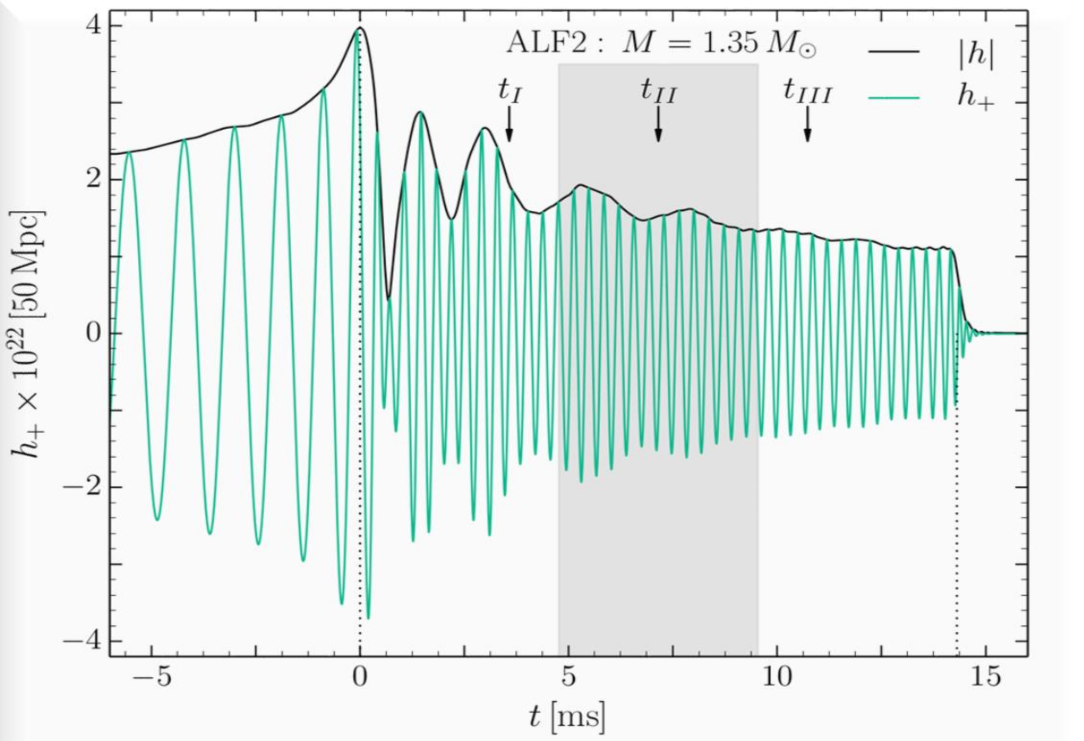

FIG. 2. Gravitational wave amplitude $|h|$ and h_+ at a distance of 50 Mpc for the ALF2-M135 model.

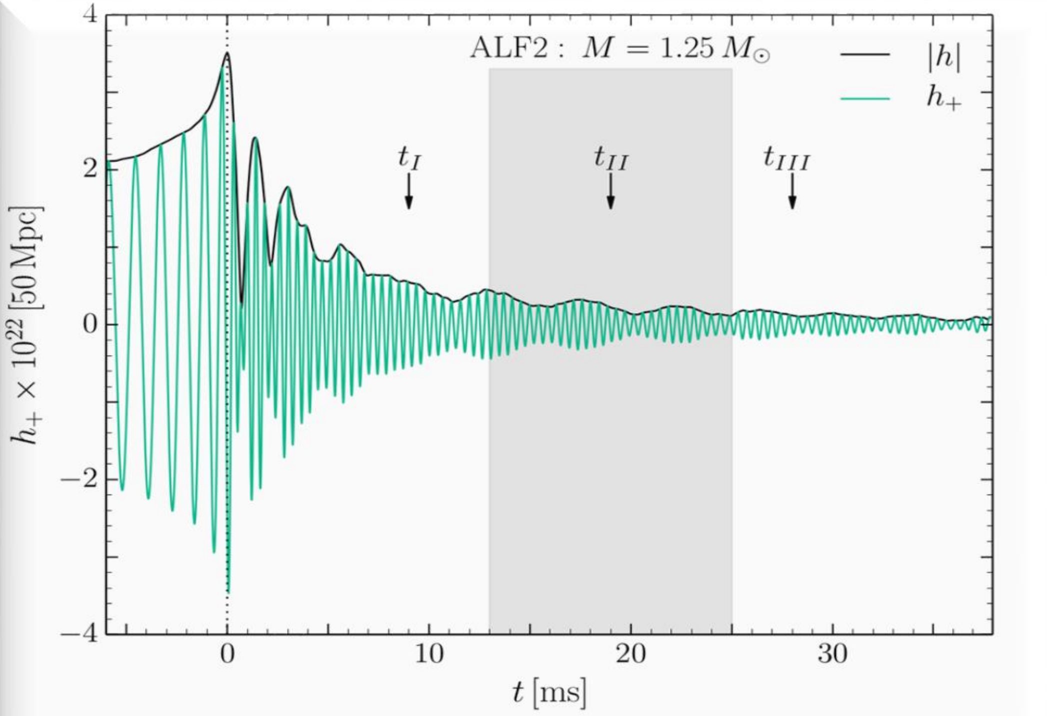

FIG. 10. Gravitational wave amplitude h_+ and $|h|$ at a distance of 50 Mpc for the ALF2-M125 model.

In order to compare the structure of the rotation profiles between the different EOSs, a certain time averaging procedure has been used:

$$\bar{\Omega}(r, t_c) = \int_{t_c-\Delta t/2}^{t_c+\Delta t/2} \int_{-\pi}^{\pi} \Omega(r, \phi, t')\ d\phi\, dt'$$

SEARCH FOR POST-MERGER GRAVITATIONAL WAVES FROM THE REMNANT OF THE BINARYNEUTRON STAR MERGER GW170817 (see arXiv:1710.09320v1)

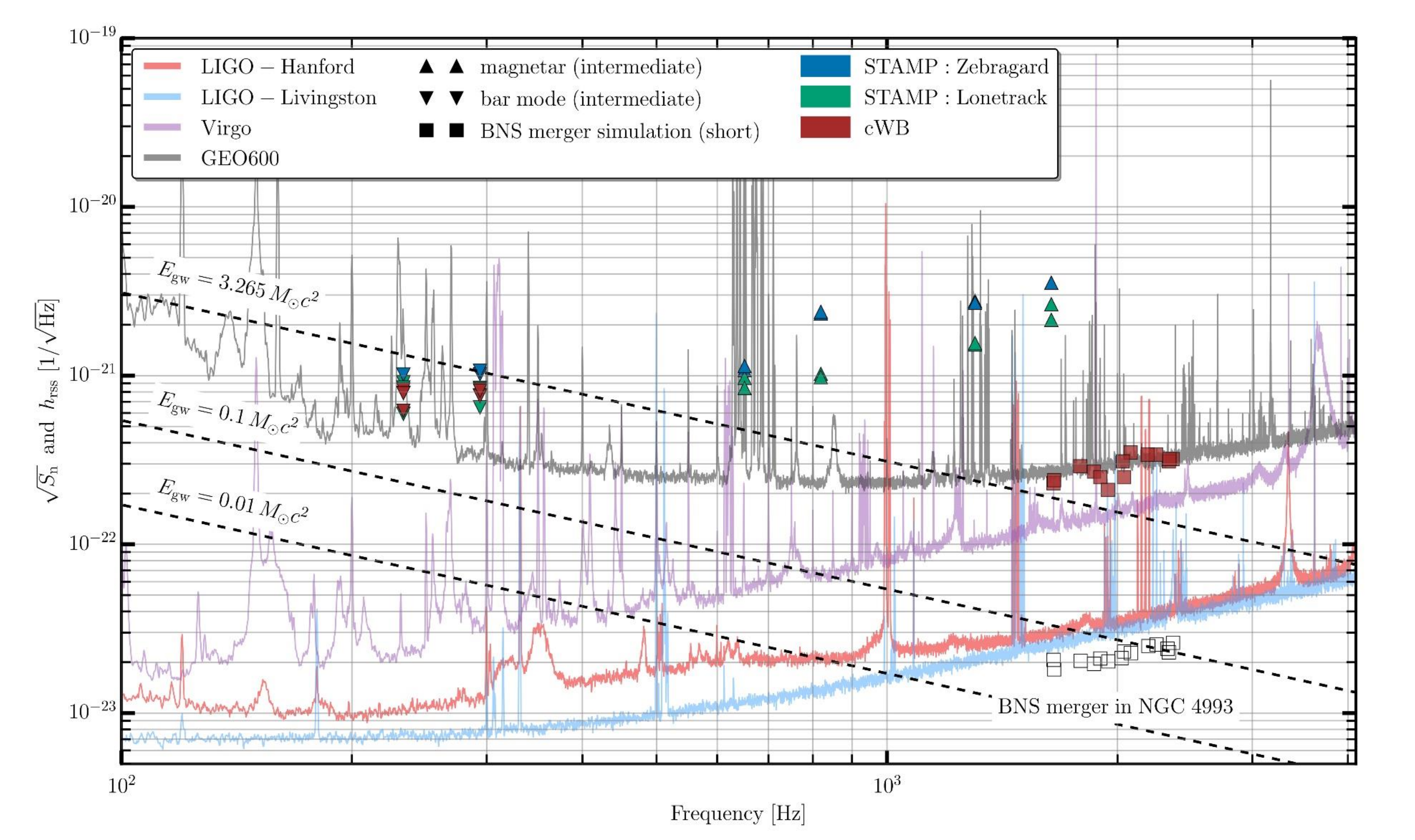

Unfortunately, due to the low sensitivity at high gravitational wave frequencies, no post-merger signal has been found in GW170817.

But, the results indicate that post-merger emission from a similar event may be detectable when advanced detectors reach design sensitivity or with next-generation detectors.